UILU-ENG-74-2006

CIVIL ENGINEERING STUDIES

STRUCTURAL RESEARCH SERIES NO. 407
Illinois Cooperative Highway Research Program
Series No. 149

FATIGUE BEHAVIOR OF WELDED REINFORCEMENT IN REINFORCED CONCRETE BEAMS

By

M. R. BARONE
J. P. CANNON
and
W. H. MUNSE

Project IHR-64

Prepared as a part of an investigation conducted by

THE CIVIL ENGINEERING DEPARTMENT
ENGINEERING EXPERIMENT STATION
UNIVERSITY OF ILLINOIS AT URBANA-CHAMPAIGN

in cooperation with

THE STATE OF ILLINOIS
DEPARTMENT OF TRANSPORTATION
DIVISION OF HIGHWAYS

and

THE U.S. DEPARTMENT OF TRANSPORTATION
FEDERAL WORKS ADMINISTRATION

UNIVERSITY OF ILLINOIS
URBANA-CHAMPAIGN, ILLINOIS
MAY 1974

FATIGUE BEHAVIOR OF WELDED REINFORCEMENT IN REINFORCED CONCRETE BEAMS

by

M. R. Barone
J. P. Cannon
and
W. H. Munse

Department of Civil Engineering
University of Illinois at Urbana-Champaign
Urbana, Illinois

May 1974

TECHNICAL REPORT STANDARD TITLE PAGE

1. Report No.	2. Government Accession No.	3. Recipient's Catalog No.

4. Title and Subtitle	5. Report Date
Fatigue Behavior of Welded Reinforcement in Reinforced Concrete Beams	May 1974
	6. Performing Organization Code
7. Author(s)	8. Performing Organization Report No.
M. R. Barone, J. P. Cannon and W. H. Munse	
9. Performing Organization Name and Address	10. Work Unit No.
Department of Civil Engineering Engineering Experiment Station University of Illinois at Urbana-Champaign Urbana, Illinois 61801	11. Contract or Grant No. IHR-64
	13. Type of Report and Period Covered Final July 1959 to June 1973
12. Sponsoring Agency Name and Address Illinois Department of Transportation 2300 South 31st Street Springfield, Illinois 62764	14. Sponsoring Agency Code

15. Supplementary Notes

Study was conducted in cooperation with the U. S. Department of Transportation, Federal Highway Administration

16. Abstract

Fatigue tests were conducted on reinforcing bars subjected to axial loadings and reinforcing bars embedded in concrete beams. Major emphasis was placed on determining the effect of both welding and type of bar material on the fatigue behavior of the beam reinforcement. To this end a variety of butt and lap-welded joint types were studied. In addition, the relative fatigue behavior of intermediate grade and high strength reinforcing bars was investigated.

17. Key Words	18. Distribution Statement
Reinforced concrete beams, fatigue behavior, welded reinforcement	

19. Security Classif. (of this report)	20. Security Classif. (of this page)	21. No. of Pages	22. Price
unclassified	unclassified	161	

Form DOT F 1700.7 (8-69)

ABSTRACT

Fatigue tests were conducted on reinforcing bars subjected to axial loadings and reinforcing bars embedded in concrete beams. Major emphasis was placed on determining the effect of both welding and type of bar material on the fatigue behavior of the beam reinforcement. To this end a variety of butt and lap-welded joint types were studied. In addition, the relative fatigue behavior of intermediate grade and high strength reinforcing bars was investigated.

ACKNOWLEDGEMENTS

The studies described herein were conducted as part of the research under the Illinois Cooperative Highway Research Program Project IHR-64, "Behavior of Welded Highway Structures." The research was conducted by the Department of Civil Engineering of the University of Illinois in cooperation with the Illinois Department of Transportation and the U. S. Department of Transportation, Federal Highway Administration.

The direct supervision of this study was provided by W. H. Munse, Professor of Civil Engineering. The studies were conducted by a number of former staff members and assistants, including W. W. Sanders, J. C. Walls, A. T. Derecho, J. P. Cannon, H. E. Rutenschroer, M. R. Barone and R. Higashionna. The authors are grateful also to the many laboratory mechanics, secretaries, draftsmen and student assistants who have assisted with the investigation.

The contents of this report reflect the views of the authors who are responsible for the facts and the accuracy of the data presented herein. The contents do not necessarily reflect the official views or policies of the Illinois Department of Transportation or the Federal Highway Administration. This report does not constitute a standard specification or regulation.

TABLE OF CONTENTS

LIST OF TABLES

LIST OF FIGURES

I. INTRODUCTION

Welding of the reinforcement for reinforced concrete beams has generally been prohibited because of the lack of control over the chemistry of most reinforcing bars and the possibility of defective welds being produced if the carbon and manganese content (the carbon equivalent) of the bars is too high. The welds in such bars, because of possible weld defects, could be expected to have a lower fatigue resistance than the bars and thus require design specification restrictions. Because of the obvious advantages of the welding of reinforcement and the lack of information on the behavior of such bars, fatigue studies of welded bars are of considerable interest and importance and were pursued in detail in the investigation to acquire a better understanding of the fatigue behavior of welded reinforcement in reinforced concrete beams. To this end 69 flexural fatigue tests were conducted on reinforced concrete beams and 169 axial fatigue tests on reinforcing bars.

The results from the axial tests have been used to evaluate the fatigue behavior of several types of welded joints and to analyze the results of the beam tests. The bar tests, in contrast to the beam tests, were relatively inexpensive and could be conducted with relative ease. However, the bar tests did not include the interacting effect of the concrete and the reinforcement that occurs in reinforced concrete beams. An attempt was made to overcome this disadvantage in a beam-simulation specimen by encasing axially loaded bars in blocks of concrete and restraining a portion of the concrete with a steel collar. In these specimens some bond and small compressive stresses were developed in the concrete; unfortunately, these modified

axially loaded bar or beam-simulation specimens did not adequately duplicate flexural behavior (see Appendix A).

The influence of the type of joint and the type of reinforcement on the fatigue behavior of the beams was of major concern. However, only single-v (60°) butt-welded joints, and single-lap welded joints were used in the beam tests; several additional joint types were employed in the tests on axially loaded bars. The two types of steel used in the study were intermediate grade (ASTM A15)[1]* and high strength (ASTM A431)[1] reinforcing bars. The 1962 ASTM specifications were in effect at the time the tests were in progress; therefore, both ASTM designations refer to the 1962 specifications.

The majority of the fatigue tests were conducted to provide stress cycles** of C-T (compression to an equal tension) and 2-T (2 ksi to tension). A small number of tests were conducted at a stress cycle of 1/2 T-T (1/2 tension to tension) and 0.73 C-T (0.73 compression to tension).

In the following sections the physical properties and chemical compositions of the materials tested are presented, along with a description of the test specimens and test equipment. In addition, the various test procedures are outlined and the static and fatigue test results for both the axially loaded bars and the reinforced concrete beams are discussed. The effect on the fatigue behavior of the type of bar deformation pattern, type of welded joint, type of material, and type of stress cycle is emphasized in the discussion of the test results for axially loaded bars; the effect of these same variables on the fatigue behavior of the reinforced concrete beams

---

* Small number refer to references presented in the Bibliography.

** The computed stress cycles applied to the reinforcement in the beams differed slightly from the stress cycles noted.

Note: The ASTM A15 and A431 Specifications were replaced in 1968 by the ASTM A615 Specification. The bars used in the investigation would in general correspond to the Grade 40 and Grade 75 respectively in A615.

is also considered. Moreover, the influence of the extent of concrete cracking on the strain in the reinforcement and on the fatigue behavior is analyzed. Finally several appendices are presented to provide more detailed data on the tests and test results.

II. DESCRIPTION OF MATERIALS AND TEST SPECIMENS

2.1 Materials

2.1.1 Reinforcing Bars

The range of required ASTM physical properties and chemical compositions for the reinforcing bars are shown in Table 1a. Here it may be seen that the yield and ultimate strengths specified for the intermediate grade reinforcement (A-15) are significantly lower than those specified for the high strength reinforcement (A431). The range of physical properties and chemical compositions for the test bars, as obtained from the mill reports, is given in Table 1b; this indicates that the bars conformed fully to the requirements of the ASTM specifications. The physical properties and chemical compositions of the reinforcing bars corresponding to the individual static and fatigue test specimens are shown in Tables B1 and B2 (see Appendix B). The physical properties determined by laboratory tests at the University and the mill report data are both listed. In most cases the "Lab" results agree closely with the properties given in the mill reports. Furthermore, the variations in physical properties and chemical compositions of the reinforcing bars were small; it is not uncommon for substantially larger variations to exist in both grades of reinforcing bar steel.

2.1.2 Concrete

Since the physical properties of the concrete were not intended to be a major variable in this study, the same concrete mix was used for all beams. The cement:sand:gravel mix was 1.0:2.7:4.2 by weight and the water

cement ratio was approximately 0.75. High early strength (Type III) Portland cement and Wabash River gravel with a maximum size of one inch were used in the mix.

Although the physical properties of the concrete were not intended to be a major variable in this study, the compressive strength and modulus of rupture of the concrete in most of the reinforced concrete beams were determined both before and after fatigue testing so that their effect could be considered. This was accomplished by conducting static tests on 6 x 12 in. concrete cylinders and 6 x 6 x 24 in. beams cast from the same batch of concrete as that used in the corresponding reinforced concrete beams.

The compressive strengths and moduli of rupture determined before the reinforced concrete beam fatigue tests and the compressive strengths deteremined after the tests are presented in Table B3. The compressive strengths and corresponding ages of the various cylinders are plotted in Fig. 1. The curve shown in Fig. 1 is an approximate best fit curve for the plotted data. The standard deviation[2,3] of these data with respect to the curve is approximately 560 psi, and indicates a significant amount of scatter in compressive strengths. It is evident from Table B3 that the moduli of rupture also exhibited a significant amount of scatter. One fact that may account for this scatter, at least in part, is that the basic concrete mix was not adjusted to compensate for any change in the moisture content of the aggregate. This moisture may have varied considerably over the extended period of time encompassed by the testing program.

Although there were some cases where the strength of the concrete seemed to have some influence on the fatigue strength of the beam reinforcement, there did not appear to be a consistent relation between the properties

of the concrete and the fatigue behavior of the beam reinforcement. The effect of the variations in concrete properties on the fatigue behavior of the beams with butt-welded reinforcement is discussed more fully in Section 7.3.1.

2.2 Test Specimens

2.2.1 Axially Loaded Bars

In all but a few instances the test specimens were fabricated from either No. 7* intermediate grade (A15) or No. 7 high strength (A431) reinforcing bars. Four types of bar deformation patterns were included in the program; the three principal types have been designated as patterns A, B, and C. In addition, a pattern designated as X was included in a limited number of beam tests. Each of these patterns is presented schematically in Fig. 2. Significantly different bar deformation patterns were selected to evaluate the overall effect of the variations in deformations.

It should be pointed out that the study of bar deformations was concerned exclusively with the orientation of the lugs. No attempt was made to determine the extent to which the age of the rolls used in manufacturing the bars affected the local geometry of the individual lugs. It is well-known that the shape of the rolls will be altered by wear which increases with the age of the rolls. Lugs that are formed with rolls that have undergone a substantial amount of wear will have a less severe geometric profile than lugs that are formed with new rolls. Therefore, bars that have lugs formed with

---

* The axially loaded bar specimens were fabricated from No. 7 bars with the exception of nine specimens fabricated from No. 6 bars.

new rolls will tend to have a lower fatigue resistance than bars with lugs formed from old rolls. Fatigue tests of reinforced concrete beams were conducted by Burton[4] to determine the influence of the age of the rolls used in manufacturing bars with pattern C lugs on the fatigue life of the reinforcement. The results of these tests showed that the age of the rolls had only a minor effect on the fatigue life.

A number of welded joint types were tested using both intermediate and high strength reinforcing bars. A detailed sketch of each joint type is shown in Fig. 3. These joints may be categorized into two basic groups:

1. Butt-type joints (groove-welded)
2. Lap-type joints (fillet-welded)

Butt joints were by far the most numerous of the joints tested. Of this group, 60-degree single-v groove-welded joints predominated.

Differences were incorporated in some of the welding procedures for the various joint types in an attempt to produce sound welds (see Table B4). Sound welds are important because of the significant effect that weld flaws can have on fatigue behavior. Radiographs of the specimens, taken before testing, and photographs of the fractured specimens showed that the degree of porosity varied considerably from specimen to specimen of the same type joint.

The axially-loaded butt-welded bars had a total length of approximately 30 in. and a length between grips of nearly 20 in. Since this 20-in. length was unbraced during testing, considerable care was taken in fabrication to minimize warping, misalignment or other distortions that would introduce bending stresses during the tests. In addition, static tests were conducted in both tension and compression to determine the extent to which bending

stresses might develop as a result of eccentricities in the testing machines and fixtures. The bending stresses were found to be relatively small, even for the compressive loadings, but tended to increase with increasing compressive loads. The maximum compressive loads used in the static tests were slightly greater than the highest compressive loads applied in any of the fatigue tests and produced bending stresses which were from 4.5 percent to 5.0 percent of the nominal applied stress. For tensile loads bending stresses were virtually nonexistent.

2.2.2 Reinforced Concrete Beams

The details of the concrete beams are shown in Fig. 4. Four types of specimens were tested (designated as types 1, 2, 3 and 4). However, most of the tests were performed on types 1 and 2. Specimen types 3 and 4 were used mainly to study the effect of steel percentage on fatigue behavior.

As noted earlier, a variety of joint types (not embedded in concrete) were subjected to axial, static and fatigue loadings. These studies rendered considerable information concerning the relative fatigue behavior of each joint type. Therefore, there was little advantage in including all the joint types in the beam study. Only 60-degree single-v butt joints and single lap welds were tested in the beams. These two joint types were selected because:

1. Both joint types were tested extensively under axial static and fatigue loadings.
2. The external geometry of these joint types differed significantly, thereby allowing a more meaningful study of the

effect of joint geometry on the fatigue behavior of the reinforced concrete beams.

3. These are probably the most common types of joints in current use.

To study the effect of concrete cracking on the fatigue behavior of the welded reinforcement contained in the beams, thin aluminum plates or cardboard sheets were used as crack formers at the welds in some of the beams. These preformed cracks insured that at least one concrete crack developed in the region of the weld.

III. TEST EQUIPMENT AND TEST PROCEDURE

3.1 Test Equipment

All tests on the axially loaded bars were carried out in the University of Illinois' 50,000-lb lever-type fatigue machines at a cyclic frequency of approximately 300 cpm (Fig. 5). These machines are equipped with variable-throw eccentrics and turn buckles which can be adjusted to provide the desired test loads. The force provided by the eccentric is transmitted to the specimen by means of a lever or walking beam. This force at the specimen is approximately ten times greater than the force acting at the load measuring dynamometer.

The specimens were held in the pull heads of the machine by means of special tapered gripping devices (Fig. 6). These gripping devices consisted of two thick steel blocks which were machined to form a tapered conical cavity when bolted together. High strength tin-base babitt was cast around the ends of each bar and to the shape of the cavity in the gripping devices. Thus, when gripped in the machine, the shapped babbitt provided a suitable gradual transfer of force from the test fixtures to the test specimen.

The solidified babbitt was rigid enough not to creep excessively when subjected to sizeable loads and therefore was able to provide an effective transfer of force to the bars. On the other hand, the babbitt was ductile enough to minimize the local gripping stresses.

The beam tests were conducted in the University of Illinois' 200,000-lb lever-type fatigue machines at a cyclic frequency of approximately

180 cpm (Fig. 7). These machines transmitted a load to the specimen which was approximately seven times the load at the dynamometer. Basically the machines operate on the same principal as the 50,000-lb machines. In the case of the beam tests, however, the load was applied through a loading strut connected to the walking beam rather than through pull-heads at the end of the machine.

3.2 Test Procedure

3.2.1 Axially Loaded Bars

After welding, some of the bar specimens were radiographed to determine the extent of porosity. Next, the babbitt was cast around the ends of the specimen, the grips being used as casting molds. The grips and the specimen were then bolted into the pull-heads of the fatigue machine.

Before subjecting a specimen to repeated loadings (a stress cycle of C-T, 2-T, or 1/2 T-T), a static tensile load was applied to the specimen and held for approximately thirty minutes. This allowed the babbitt to creep until it reached a state approaching equilibrium in which the rate of creep was, for all practical purposes, reduced to zero. A stress cycle of 2-T (2 ksi to tension) rather than 0-T was selected in order to eliminate the possibility of the minimum stress becoming compressive with increased cycling. If a zero minimum stress were used initially, a compressive stress could arise as a result of a slight creep in the babbitt, slip between the grips and pull heads, or possibly slight changes in the machine.

In the case of specimens subjected to complete reversal, steel plugs which were threaded to fit into the ends of the gripping devices were fastened tightly against the ends of the specimens. The plugs were used to assist the babbitt by applying the compressive loads directly to the specimen and helped to prevent excessive creeping of the babbitt. Once the specimen was placed in the fatigue machine, it was necessary to stabilize the load; however, the stabilization procedure used for the specimens subjected to the 2-T and 1/2 T-T stress cycles was not satisfactory for the reversal tests. Initially, therefore, the desired loads were set and the fatigue machine was allowed to run for a few minutes and then the loads rechecked. Generally the loads were found to have drifted or decreased slightly and were reset to the desired values. This process was repeated at increasing time intervals until the loads had stabilized. The number of cycles required for stabilization was insignificant compared to the number of cycles required to cause failure. However, even after the loads had been stabilized, they were still checked periodically.

When a fatigue failure occurred, the gap between the pull-heads increased enough to actuate a micro-switch (Fig. 5) which in turn shut the machine off. The number of cycles to failure was obtained from an automatic counter. Pieces of the specimen containing the fracture faces were cut out of all the specimens and stored for further study of the degree of weld porosity and the location of points of fatigue failure initiation. Typical photographs of fracture surfaces taken for various joint types are shown in Fig. 8.

3.2.2 Reinforced Concrete Beams

Since the fatigue behavior of the welded reinforcement in the beams and its relationship to the fatigue behavior obtained in the axial bar tests was of basic concern in this investigation, various types of data were obtained in the tests. SR-4 Type A-7 electrical resistance strain gages were mounted at various locations along the welded reinforcement to obtain detailed data on their strain behavior. In some cases radiographs of the weld were taken before the gages were mounted. The gage locations were confined to a region along the middle third of the reinforcement, but varied considerably within this region. The gages were mounted on nearly flat surfaces, approximately 3/16 in. x 3 in. which were formed by grinding off portions of the longitudinal ribs of the reinforcement. Once the surfaces had been properly ground, cleaned and chemically treated, the gages were mounted using Eastman 910 cement and then waterproofed with an Epoxy Cement or petrolastic compound; the petrolastic compound was used for most of the tests. After the gages were mounted and the longitudinal reinforcement and stirrups tied, the cage was placed in a steel form. If the beam was to contain a preformed crack, an aluminum or cardboard crack former was placed at the weld (Fig. 4) prior to the concrete pouring.

In order to gain a detailed understanding of the fatigue behavior of the reinforced concrete beams, strain gage readings were taken in the following sequence.

1. Strain readings on the bars were taken, (a) before pouring the concrete (with the reinforcement resting in the form), (b) after casting the concrete but before installing the beam in the fatigue

machine, and (c) after the beam was placed on the beam supports in the fatigue machine.

2. Strains in the reinforcing steel and, in some cases, deflections at mid span were recorded for various load increments while the first three or four cycles of loading were slowly applied. These loadings were applied manually to obtain an indication of the effect of initial cracking on the reinforcement strains.
3. Strain readings corresponding to the maximum and minimum loads were taken periodically during the fatigue tests to determine the effect of increased concrete cracking on the strains in the reinforcement.

The general testing procedure for the concrete beams was similar to that used for the axially loaded bars in that the loads were periodically checked to maintain the desired loading cycle. The number of cycles required to produce failure were recorded as the time the fatigue crack in the bar had developed to such an extent as to allow a sufficient increase in the deflection of the beam to actuate a microswitch. In the case of the beams this increase in deflection usually occurred suddenly, and was accompanied by complete fracture of the tensile reinforcement. Photographs of the beams were taken after failure in order to provide an accurate record of the concrete cracking patterns.

IV. RESULTS OF STATIC TESTS ON AXIALLY LOADED BARS

Static tests were conducted for both unwelded and welded intermediate grade reinforcing bars. The physical properties obtained from the static tests on unwelded bars (Table B1) were generally in good agreement with the mill report properties.

The test results for welded reinforcing bars (Table 2) show that the yield and ultimate strengths of the bars were virtually unaffected by the inclusion of a 60-degree single-v butt-weld, or angle splice joint. However, the ultimate strength of the bars containing either the single strap or single lap joint was below that of the unwelded bars. This reduction appears to have occurred as a consequence of the eccentricity which resulted directly from the joint geometry, i.e., the unsymmetrical lapping of the bars. The eccentric loading produced bending in the bars which was a maximum at the ends of the joint. It is in this region that the specimens failed (see Fig. 9). The severity of this bending apparently increased with a reduction in lap length; the ultimate strength of the bars with the shorter lap joints was less than that of the bars with the longer lap joints. On the basis of this very limited number of tests it is evident that a lap of at least 5 in. was necessary to develop the minimum specified strength of the A15 bars when spliced with a single lap joint (see Fig. 10).

V. RESULTS OF FATIGUE TESTS ON AXIALLY LOADED REINFORCING BARS

5.1 Introduction

The geometrical details of a structural element are known to be one of the most significant factors to influence its fatigue behavior. A sharp geometric discontinuity can drastically reduce the fatigue resistance of a member. Although the principal objective of the fatigue study of axially loaded reinforcing bars was to investigate the effect of welding and joint details on fatigue behavior, it was recognized that the different types of deformation patterns involved in these tests represented an additional geometrical factor. Consequently, the influence of this factor on fatigue behavior was considered in the tests on unwelded reinforcing bars. Welded bar test results were not used in the study of bar deformation pattern since the results would then be complicated by the presence of the geometrical discontinuities which result from welding.

Several reasons can be advanced for the increased susceptibility of welded reinforcement to fail in fatigue. The two most significant factors are the weld geometry and material properties. The deposition of weld metal may result in both "projecting notches" and "internal defects" which provide sources of stress concentration. A study of stress concentrations in axially loaded plates with projecting notches lends evidence to the importance, in combating fatigue, of gradual geometrical transitions.[5]

5.2 Unwelded Bars*

Most of the unwelded specimens were fabricated from A15 intermediate

---

* See Table 3 for fatigue test results.

grade reinforcement with three types of deformation patterns, patterns A, B, and C (Fig. 2). The results of the tests on these three types of bars were used to obtain the S-N curves (a 2-T stress cycle) shown in Figs. 11, 12, and 13. It should be emphasized that the S-N curves are based on data obtained from only those tests in which fracture did not occur at the grips. In examining the data it is significant to note that these three S-N curves are nearly coincident; that is, when all the data for the intermediate grade unwelded bars (excluding data representing grip failures) were used in constructing the lower S-N curve shown in Fig. 14, little difference in fatigue behavior was observed for the bars of the three different deformation patterns. It appears that the effect on fatigue behavior of the different deformation patterns studied is insignificant, especially when compared to the effect of welding. However, it may be observed that none of the bars with the type A pattern failed in the grips, five out of eight bars with the type B pattern failed in the grip, and ten out of thirteen bars with the type C pattern failed in the grips. Thus, it appears that the type of deformation pattern may have had an effect on the mode of failure obtained in the tests. The gripping device had the greatest effect in the case of patterns B and C.

It should be emphasized that the above conclusions are based on tests of axially loaded bars and do not necessarily apply to unwelded reinforcement contained in concrete beams. In the case of concrete beams, bond stresses will be transmitted to the lugs of the reinforcement which in turn might aggravate local stress conditions and thus amplify the effect of the pattern on the fatigue behavior of the reinforcement. This possibility is

supported by the tests on concrete beams with unwelded reinforcement conducted by Pfister and Hognesad which indicated that the type of deformation had a significant effect on fatigue behavior of the bars.[6] Similarily, two Japanese researchers, Kokubu and Okamura,[7] found that the 2,000,000 cycle fatigue strength of unwelded reinforcement contained in concrete beams was related to the angle which the lugs made with the axis of the reinforcement.* As the angle was increased from 45° to 90° the fatigue strength was reduced approximately 20 percent. However, the effect of the bar pattern on the fatigue behavior of the beam reinforcement is not of principal concern in the study reported herein because all but three of the beams contained welded reinforcement and the fatigue failures almost always occurred at the welds.

One interesting feature of the tests on intermediate grade axially loaded reinforcement was that most of the grip failures occurred with bars having the type C deformation pattern (see Fig. 2). The orientation of the lugs with respect to the direction of axially applied load may account at least in part for this observed behavior. In such bars the ends of the unwelded specimens encased in babbitt will tend to slide or creep along planes parallel to the direction of the lugs; thus, the motion of the ends of the specimen will have two components, one vertical and one horizontal. The vertical displacements at each end will be in the direction of the applied load and the horizontal displacements at the two ends will be of opposite sense, thereby tending to induce bending moments at the ends of the specimen. Under such a combination of bending and axial load, the point of most critical stress would be where the bar enters the grip, since in this region both the induced bending moment and axial load are at their respective maximum values.

---

* Most of the reinforcement conformed to the Japanese Industrial Standard G 3112-Bar Steel for Reinforced Concrete.

However, the fatigue strength of many of the bars with deformation pattern C that failed in the grips was not very different from that of the bars which did not fail in the grips. This suggests that the effect of the gripping or bending was generally of a secondary nature.

The bending phenomenon described in the preceding paragraph would not occur in bars with the type A or B deformations because the type A lugs are not inclined and the type B lugs, although inclined, have lugs which produce opposing effects. The occurrence of grip failures in the case of bars with the deformation pattern B is probably the result of the effective stress concentrations caused by gripping rather than the result of bending stresses.

A few tests were conducted also using high strength steel reinforcement having deformation pattern C; the data obtained from these tests were used in constructing the upper S-N curve (2-T) shown in Fig. 14. In comparing this curve with the lower curve for intermediate grade steel it is evident that the high strength steel has a somewhat greater fatigue resistance than that of the intermediate grade steel.

5.3 Welded Bars*

5.3.1 Intermediate Grade Bars

The welded bar tests were conducted to determine the effect of various types of welded joints on the fatigue behavior of intermediate grade reinforcing bars. Although several types of welded joints were investigated,

---

* See Table 4 for fatigue test results.

most of the fatigue tests were conducted on bars containing 60-degree single-v butt welds. The S-N curves for these bars are shown in Fig. 15 for full reversal, 2-T, and 1/2 T-to-T stress cycles. The data used in establishing the S-N curves corresponding to the C-T and 2-T stress cycles are relatively consistent and provide a good index of the fatigue behavior of the bars. The relatively small amount of available data for the 1/2 T-to-T stress cycles makes it difficult to assign the same degree of confidence to the S-N curve corresponding to this stress cycle. However, the data appear, in general, to be consistent with that obtained from the other stress cycles. The 1/2 T-to-T curve is reasonably well defined in the region of longer lives, but not for the shorter lives (less than 400,000 cycles). Thus, the complete S-N curve cannot be constructed without resorting to excessive extrapolation.

The S-N curves discussed above (Fig. 15) are for bars that contained 60-degree single-v butt-welded joints. These joints were mechanically cut in preparation for welding. Several tests were conducted on 60-degree single-v butt-welded specimens for which modifications were made in the joint fabrication. In some instances the joints were flame cut rather than mechanically cut. In a few cases the bars were subjected to a 400°F preheat; however, the bars reported in Fig. 15 were prepared by the basic procedure, not by the modified procedure or preheated. The results of fatigue tests on specimens having flame cut joints are plotted in Fig. 16 and those for specimen which were preheated to 400°F are plotted in Fig. 17. The curves shown in both of these figures are taken from Fig. 15. Figures 16 and 17 indicate that most of the data for the specimens with flame cut joints and those which were subjected to a preheat of 400°F fall within the scatter band, associated with the data used in establishing the basic S-N curves. Two exceptions are

evident for the preheated joints; in Fig. 17 it may be seen that two of the data points (at a stress cycle of 2-22 ksi) are located considerably below the basic 2-to-T curve.

The data for all of the tests are summarized in Fig. 18 in terms of the total range of stress to which the bars were subjected. The average fatigue strengths for failure at 100,000 and 2,000,000 cycles are presented in Table 5 along with the standard deviation for the data. These data help to provide a basis on which fatigue specifications for welded intermediate grade reinforcing bars can be based.

Although most of the fatigue tests on welded intermediate grade reinforcing bars were conducted on bars with 60-degree single-v butt welds, a number of additional tests were carried out, at a stress cycle of 2-28 ksi, using specimens with other types of weld and joint configurations. Several of these specimens were encased in concrete (Fig. 3). The results of these various tests are shown in Fig. 19. The data points represent the average life for each type of specimen and the number in parentheses indicates the number of tests on which this average life is based. The S-N curve shown in the figure corresponds to the curve for the 2-to-T stress cycle for the 60-degree single-v butt-welded specimens and is presented for purposes of comparison. The results plotted in Fig. 19 clearly show that the 3-1/2 in. single strap fillet-welded lap joints had the lowest fatigue resistance of all the joint types tested (minimum life was 7400 cycles). One of the principal reasons for this reduced fatigue resistance is the bending stress induced in the region of the joint by the eccentrically applied tensile load. Another of the reasons for the reduced fatigue strength of the single-strap lap joints is the stress concentration resulting from the abrupt

geometrical change at the joint. The test results for symmetrical double strap lap joints suggest, however, that the stress concentration was not as significant a factor as the bending stress. The fatigue resistance of the bars with symmetrical double-strap lap joints (no eccentric loading) was not greatly different from that of the bars with 60-degree single-v butt-welded joints.

Some of the single strap lap welds were encased in concrete so that the effect of confinement could be studied. No significant increase in fatigue resistance could be observed for the specimens encased in plain concrete. However, a noticeable increase in fatigue life occurred when the concrete contained circular reinforcement. Apparently the plain concrete did not provide sufficient lateral restraint to reduce the bending effects. This conclusion is borne out by the fact that the plain concrete not only contained cracks transverse to the axis of the bar but also contained longitudinal cracks. The degree of longitudinal cracking in the concrete with circular reinforcement was substantially less than for the plain concrete.

Of the bars which did not contain a single strap lap joint, the specimens containing either an angle splice or a 45-degree single-v butt joint exhibited the greatest reduction in fatigue life. On the other hand, unwelded bars on which No. 3 bars were tack welded in a transverse direction and unwelded bars encased in concrete showed the least susceptibility to fatigue failure. It should be noted that in some cases the lives of the individual specimens deviated considerably from the average lives (see Table 4).

5.3.2 High Strength Bars

Sixty-degree single-v butt-welded high strength reinforcing bars (A431) were tested at stress cycles of C-T and 2-T. The results of these tests were used to construct the two S-N curves shown in Fig. 20. The scatter might be expected since, when a compressive load is applied to a bar any slight misalignment in the bar would result in noticeable bending stresses in addition to the axial stress. Although strain measurements have shown that the magnitude of such bending stresses were not very great with respect to the nominal stress (the misalignment was generally quite small), there was a tendency for the magnitude of the bending stress to be somewhat higher (but probably less than 5.0 percent of the nominal stress*) in the case of high strength bars than for the intermediate grade bars because the high strength bars were subjected to higher compressive loadings.

The fatigue behavior of the 60-degree single-v butt-welded high strength bars may be compared to that of the 60-degree single-v butt-welded intermediate grade bars by considering the superposed curves on the Modified Goodman diagram shown in Fig. 21. The broken lines, representing the results of tests on high strength bars, were constructed using the S-N curves shown in Fig. 20. The solid curves were constructed using the S-N curves shown in Fig. 15 for the intermediate grade bars. The region of the Modified Goodman diagram between C-T and 2-T is believed to be reliable for both types of steel. This observation is based on the consistency of the data used in establishing the S-N curves shown in Figs. 15 and 20. Unfortunately, only a small amount of data are available for the 1/2 T-T stress cycle. Nevertheless,

---

* Tests to determine the magnitude of the bending stresses in axially loaded bars due to bar misalignment are discussed in Section 2.2.1.

the portions of the Modified Goodman diagrams based on these limited data agree well with the areas of the diagrams that are more firmly established.

It is worth noting, in comparing the curves on the Modified Goodman diagram, that the difference in fatigue strengths of the high strength and intermediate grade bars is relatively small in contrast to the difference in static strengths of the two types of bars. This point is brought out even more strongly when the fatigue strengths plotted in Fig. 21 are divided by the ultimate strengths of the respective bar materials (see Fig. 22).

VI. THE CYCLIC STRAIN BEHAVIOR OF REINFORCEMENT IN CONCRETE BEAMS

6.1 First Cycle Behavior

One of the principal objectives of this investigation was to evaluate the fatigue behavior of reinforcing bars that are embedded in concrete beams and also to relate this behavior to that observed for bars not encased in concrete. To make this evaluation it has been necessary to consider in detail the cyclic strain behavior of the bars. As noted in Section 3.2.2, strains were measured at various locations along the bars and during various stages of the tests to define this behavior.

Since the observed cyclic strains in the reinforcement (converted to stresses) are compared to the computed stresses in this and latter sections, the significance and limitations of the computed stresses will be considered before proceeding with the discussion of the observed cyclic strains.

The computed tensile stress in the reinforcement was obtained using the following relationship:

$$f_s = \frac{M}{A_s\,(jd)} \tag{6.1}$$

where:

f_s = the computed stress in the reinforcement (ksi)

M = the moment acting at the test section (kip-in.)

A_s = the area the steel (sq in.) subjected to the stress f_s

(jd) = the moment arm (in.) of the force $(A_s f_s)$ at the test

section as determined by a transformed section analysis in which it is assumed that stresses and strains vary linearly through the depth of the beam. (The tensile strength of the concrete has been ignored in the analysis.)

To compute the stress in the reinforcement in the usual manner, the magnitude of the modular ratio n had to be determined also. Where:

$$n = \left(\frac{\text{modulus of elasticity of the reinforcement}}{\text{modulus of elasticity of the concrete}} \right) \qquad (6.2)$$

Various factors, including the modulus of elasticity of the reinforcement, the density of the concrete, the compressive strength of the concrete and repeated loadings[8] can affect the magnitude of n. The modulus of elasticity of the reinforcement and the density of the concrete remained nearly constant in this study and consequently would cause no change in n. However, the compressive strength of the concrete varied from beam to beam; it tended to increase noticeably during the fatigue tests (see Table B3 and Fig. 1). Nevertheless, calculations showed that the computed stress in the steel was not affected significantly by the change in modular ratio that resulted from this variation in compressive strength.

In the study, by virtue of the way in which n is defined, it has been assumed that the stress-strain curve for the concrete in compression is essentially linear and that the compression stresses vary linearly through the compression region of the beam. This assumption is considered reliable if the maximum compressive stress in the concrete is less than one-half of its maximum compressive strength.[9] For most of the beams tested, the maximum computed compressive stress in the concrete was less than one-half its compressive

strength. There were only a few beam tests for which the maximum computed compressive stress in the concrete was greater than one-half its compressive strength. The distribution of the concrete compressive stresses in these beams would probably not be linear at the maximum load condition. However, since the distance from the centroid of the compression block to the computed neutral axis of these beams, based on a linear analysis, was small in comparison to the total depth of the beam, the distance from the steel force to the resultant of the compressive stress at a cracked section would not be expected to change much as the distribution of compressive stresses became nonlinear at the higher loads.

It should be noted at this point that the computed steel stress was used mainly to analyze the fatigue test results in terms which are familar to the designer. The computed stresses did not necessarily provide an exact indication of the magnitudes and variations of the actual reinforcement stresses along the length of the beams since the assumptions used in arriving at the computed stresses are at best idealized approximations. In using these approximations, the stresses in the reinforcement resulting from the shrinkage of the concrete are ignored.

In order to evaluate better the influence of the stress cycle and a preformed crack on the fatigue behavior of the reinforcement, actual strains on the surface of the reinforcement were measured for the first loading cycle.

The moment versus average measured steel strain curves, as shown in Figs. 23, 24 and 25, represent the results averaged from a number of one-cycle beam tests conducted prior to the repeated fatigue cycling on the same beams.* As noted on the figures these data represent strains obtained either

---

* A detailed explanation of how these average curves were obtained from the strain gage data acquired from the different beam tests is provided in Appendix C.

at cracked or uncracked sections of the beams. These "first-cycle" loading tests were conducted on beam specimens (Type 1)* with intermediate grade reinforcing bars which, with one exception (an unwelded bar), contained 60-degree single-v butt-welds. A number of test results were available for the lower applied moments; therefore, the curves shown in Figs. 23, 24 and 25 have more supporting data at the smaller moments than at the larger moments.

The average strains in Figs. 23, 24 and 25 are those that resulted from the applied loads. The initial zero-load strain gage readings were recorded with the uncracked, unloaded beam resting on simple supports. Calculations show that the dead load strains for the uncracked beam would be negligible (approximately 8 μ in./in.). Therefore, the effect of the dead load on the initial zero-load strain readings was neglected.

Since the locations of the gages were known with respect to visible surface cracks rather than with respect to internal cracks, a certain element of judgment was involved in determining whether or not a gage was truly measuring strains at a "cracked" or "uncracked" section (Fig. 26). If a gage were located within a distance of approximately one inch from where cracking existed, it was considered to be located at a cracked section.

In Figs. 23, 24 and 25, the loading curves for cracked sections always lie below the loading curves for uncracked sections. This result, of course, was expected since the concrete does not carry a tensile load in the cracked regions. For beams with fully preformed cracks (Fig. 25) and beams without preformed cracks (Fig. 23), the stresses (based on measured strains) at the cracked sections tended to approach the computed stresses calculated from Eq. 6.1. However, for the beams with partially preformed cracks (Fig. 24)

---

* See Fig. 4.

the stresses at the cracked sections were generally not as great as the stresses at the cracked sections of the other beams. This difference in behavior is thought to be a result of two factors. First, there was a considerable amount of scatter among the individual gage readings (see Appendix C) and second, there was not a sufficient amount of strain gage data available for "cracked" sections. Approximately eighty percent of the gages were located at "uncracked" sections. In spite of this scatter and lack of data, the results of the "first-cycle" tests were valuable because they showed that the stresses (obtained from measured strains) in the reinforcement at cracked sections probably approach the stresses obtained from Eq. 6.1 and that the stresses in the reinforcement at uncracked sections will be considerably less than the computed stresses.

There is not as much data available for the unloading curves as for the loading curves. However, Figs. 23, 24 and 25 show that there is a tendency for the tensile reinforcement to acquire a permanent strain (or stress) after the first few cycles of loading and that the permanent strain tends to be greater for cracked sections than for uncracked sections.* One possible explanation for this behavior is that after the cracks have developed they are not able to completely close as a result of imperfect remeshing of the concrete because of broken bits of concrete lodged between the surfaces of the fracture. It is reasonable also then to expect that the portions of the reinforcing bar located between cracked sections would exhibit less permanent strain than reinforcement located at cracked sections since the concrete in the uncracked region carries part of the tensile force. This is generally what was observed.

---

* Average permanent stresses (based on measured strains) for individual beams are shown in Table 7.

The permanent strains should not in general be associated with plastic strains, since measured reinforcement strains beyond the elastic limit were encountered only in the case of one beam (BW 4). Of course, it may have been possible for local plastic strains to develop and remain undetected in some of the beams. However, even if permanent set or strain had occurred, a general plastic deformation would not have been responsible for the set because significant permanent strains were observed for beams which were subjected to moments that were substantially less than the calculated yield moment.

6.2 The Cyclic Strain Behavior of Reinforcement in Concrete Beams as Affected by Previous Load Cycles

A discussion of the reinforcement strains during the first loading cycle was presented in Section 6.1. This section is concerned with the measured steel strains as affected by previous cyclic loadings.

For most beams, the maximum steel strains increased with an increasing number of loading cycles (see Table 7). During cycling the stiffness of the section diminished progressively due to propagation of cracking in the concrete. This continual reduction in beam stiffness is borne out by the fact that it was necessary in most cases to periodically increase the beam deflection in order to maintain the desired maximum moment. As the beam stiffness decreased the steel was forced to carry more stress to compensate for the loss of concrete participation. A simplified explanation of this phenomenon can be provided by considering the idealized moment vs. strain diagram shown in Fig. 27. Because of progressive cracking, each loading curve shown in Fig. 27 has an effective slope somewhat less than that of the previous

loading curve. Thus, a slight increase in maximum steel stress is produced by each reloading. The accumulation of the minimum strains is probably due to the propagation of old cracks and the initiation of new cracks which fail to remesh completely upon unloading. A considerable variation in the magnitudes of the steel strains was observed for the various tests. These strains converted to average stress are shown in Table 7. It is readily evident that the average measured stresses generally differed from the computed stresses.

In view of the above discussion, it is conceivable that the reinforcement could experience either beneficial or detrimental strain effects, depending on the extent of cracking and how well the cracks remesh when the load is removed. For example, as the cracking becomes more severe, the maximum stress tends to increase; however, there may be a reduction in stress range if there is a greater increase in the minimum stress than in the maximum stress.

loading curve. Thus, a slight increase in maximum steel stress is produced by each reloading. The accumulation of the minimum strains is probably due to the propagation of old cracks and the initiation of new cracks which fail to remesh completely upon unloading. A considerable variation in the magnitudes of the steel strains was observed for the various tests. These strains converted to average stress are shown in Table 7. It is readily evident that the average measured stresses generally differed from the computed stresses.

In view of the above discussion, it is conceivable that the reinforcement could experience either beneficial or detrimental strain effects, depending on the extent of cracking and how well the cracks remesh when the load is removed. For example, as the cracking becomes more severe, the maximum stress tends to increase; however, there may be a reduction in stress range if there is a greater increase in the minimum stress than in the maximum stress.

are presented in terms of the computed stress cycle acting on the reinforcement. For this reason the reader should be fully aware of the significance and limitations of the computed stress discussed in Section 6.1 and bear in mind that the minimum and maximum computed stresses in the beam reinforcement, as calculated from Eq. 6.1, were based on a representative value of modular ratio, n = 7.* Moreover, it is important to note that the magnitudes of the minimum and maximum applied moments** were maintained essentially constant throughout each beam fatigue test. Since the magnitudes of these moments were known, the resulting maximum theoretical stresses could be computed.

Finally, it should be mentioned that for the doubly reinforced beams (Type 2)*** subjected to alternating positive and negative deflections, two values of moment arm, jd, were used, depending on whether the deflection was positive or negative. In computing each of the "jd" values a transformed section analysis was used in which the transformed compression steel area was determined by multiplying the actual area of the compression steel by the factor (2n - 1). The computed stress in the compression steel was determined by multiplying the stress acting on the transformed area of compression steel by the factor 2n. This factor is introduced in working stress design to account for the difference in the creep behavior of the reinforcement and concrete. In other words, when a reinforced concrete beam is subjected to sustained loading, the concrete will creep much more than the steel. Therefore,

---

* The modular ratio was determined in conformity with the ACI code recommendations.

** The minimum and maximum moments included the dead weight of the beam which amounted to $0.676^{k\text{-}ft}$, a relatively small value.

*** See Fig. 4.

the compression stress in the reinforcement will increase with time. Under such conditions it is possible for the compression stress in the reinforcement to increase by a factor of two with respect to the compressive stress predicted by a transformed section analysis which ignores creep.[10]

The use of the factor 2n to account for creep cannot be justified in the case of beams subjected to relatively short term fatigue loadings since creep in the concrete is not likely to be significant enough to noticeably affect the compressive stresses in the reinforcement. On the other hand, strain gage data and fatigue tests results* suggest that it is quite possible for the compression stress in the reinforcement to approach the computed compressive stress based on the factor 2n. In view of the above observations, the use of the factor 2n does not appear unreasonable.

7.2 Unwelded Reinforcement**

The data available for concrete beams reinforced with unwelded bars are limited but do indicate that beams with unwelded reinforcement are not as susceptible to fatigue failures as beams with welded reinforcement. For example, the only beam tested that contained unwelded intermediate grade reinforcement (SBC1, no preformed crack) was subjected to a computed stress cycle of 3.2 to 32.3 ksi and had not failed after 4,884,600 cycles of loading. However, beam BW2 (no preformed crack) with intermediate grade 60-degree single-v butt-welded reinforcement was subjected to a stress cycle of 3.5 to 26.4 ksi and failed after 3,320,000 cycles of loading.

The same general behavior was observed for beams that contained high

---

* These strain data and fatigue test results are discussed in Section 7.3.

** See Table 6 for fatigue test results.

strength reinforcement. Beams BT1 and BT2 (with partial preformed cracks)--the only beams that contained high strength unwelded reinforcement--were tested at stress cycles of 4 to 40.5, and 2.3 and 52.3 ksi and had not failed after 2,570,000 and 3,690,000 cycles respectively. Every beam that contained welded high strength reinforcement and was subjected to stress cycles similar to those imposed on the reinforcement contained in beams BT1 and BT2 failed at lives considerably shorter than 3,690,000 cycles (see Table 7).

7.3 Welded Reinforcement

7.3.1 Intermediate Grade Reinforcement

Thirty-two beams (Types 1 and 2) with intermediate grade reinforcement joined by a 60-degree single-v butt-weld were tested. All of the specimens which were tested to failure fractured at the weld. The fatigue test results for beams without preformed cracks as well as for beams with partially and fully preformed cracks were used in obtaining the S-N curves shown in Fig. 28. The stress cycles represented are 0.93C-T, 4-T and 0.47T-T. Each of these stress cycles is actually an average stress cycle for the series of tests to which they refer. For example, in the case of the fifteen beams subjected to the average stress cycle 4-T, the minimum computed stress varies from 2.1 to 6.1 ksi and the average minimum stress was 4 ksi.

The test results for the beams with welded reinforcement subjected to the 0.93 C-T stress cycle are reasonably consistent in that the data exhibit a relatively small amount of scatter, although a sizeable variation existed in the concrete compressive strengths and moduli of rupture for the different beam specimens (see Table B3). Apparently these variations in the

physical properties were not great enough to significantly affect the fatigue test results for the beams.

There is a more noticeable amount of scatter among the data for the beams tested at a stress cycle of 4-T. Again, however, there does not seem to be a consistent correlation between fatigue life and concrete properties for beams with the same preformed crack type. Insofar as the bulk of this scatter is concerned, it may be more significant to note that beams without preformed cracks tended to have longer fatigue lives than beams which contained preformed cracks. Moreover, the beams with fully preformed cracks generally had the least resistance to fatigue failure.

It is important at this point to recall from the discussions in Section 6 that there was a tendency for the stresses in the reinforcement at uncracked sections to be somewhat smaller than the stresses in the reinforcement at cracked sections. Based on this observation it seems reasonable to assume that the internal tensile stress acting at the weld would tend to be smaller for a beam without a preformed crack than for a beam with a preformed crack at this weld. Therefore, one would expect that the beams without preformed cracks would tend to have a longer fatigue lives than the beams with preformed cracks, provided large natural cracks did not develop at the weld for beams without the preformed cracks. A natural crack in the concrete developed at the weld in only one of the bemas (BW4) which did not contain a preformed crack. Beam BW4 was tested at a computed stress cycle of 5.1 to 51.4 ksi and failed after 342,800 cycles. The only other beam without a preformed crack (BW3) subjected to a similar stress cycle (6.1 to 52.9 ksi) failed after 684,100 cycles, a higher fatigue resistance than that of BW4.

None of the beams tested at a stress cycle of 0.47 T-T failed, even though the maximum computed stresses were as high as 65.4 ksi. It was not possible to test these beams to failure because of the limited deflection capacity of the fatigue machine. Since none of these beams failed, it is difficult to determine the fatigue strength or to consider, in detail, the effect of the 0.47 T-T stress cycle on the fatigue behavior of the concrete beams with welded reinforcement. Nevertheless, comparing the beam fatigue test results for the 0.47 T-T computed stress cycle with the fatigue test results for the axially loaded bars subjected to a 1/2 T-T stress cycle, one finds that the beam reinforcement possessed a much greater fatigue resistance than the unembedded bars (see Figs. 15 and 28). It must be realized, however, that this comparison is based on the computed stress cycle and that the actual stress cycles acting on the beam reinforcement as determined from measured strains (see Table 7) may have been substantially less severe than the computed reinforcement stress cycle of 0.47 T-T. Most of the strain gages used in obtaining the average stresses were located at uncracked sections, approximately two inches away from the weld. However, some of the gages were mounted on the weld reinforcement in beams with preformed cracks. The strain readings from these gages did not deviate significantly from the readings of the gages at uncracked sections. When the fatigue behavior of the beams provided by the measured strains is compared with the fatigue resistance of the unembedded bars, a fairly good correlation is obtained. Thus, it appears that the concrete provides an improvement in the fatigue resistance of the welded bars in the beams.

A Modified Goodman fatigue diagram representing the S-N curves for

both the beams and axially loaded intermediate reinforcing bars is shown in Fig. 29. The diagram clearly verifies that the reinforcement in the beams, based on the computed stresses, had longer fatigue lives than the corresponding axially loaded bars. This finding agrees with results published by Soretz[11] who showed that reinforcement* contained in concrete beams had a greater fatigue strength than the same type of reinforcement tested under axial fatigue loading. In tests conducted by Rehm[12] on quality III concrete rib steel, the opposite behavior was observed. In addition, Mayer[13] reported unpublished data which was in general agreement with Rehm's results. The differences in the above observations may have been to some extent the result of differences between the loading conditions encountered in these various studies. In the studies reported herein, as well as in Soretz's work, the critical region of the beam was under a constant moment. However, in Rehm's tests and in the tests reported by Mayer, a single concentrated load was applied at the center of the beam and, therefore, the moments varied linearly over the entire length of the beam. Mayer also presented results which indicated that the shape of the moment diagram had a significant effect on the fatigue life of the beam reinforcement and that the fatigue strength of reinforcement increased as the shear at the critical section decreased. This may also be a factor in the tests reported herein.

The observed fatigue behavior of reinforcement embedded in the concrete beams as opposed to the behavior of identical "unembedded" reinforcement (tested under axial load) may be explained further, insofar as this study is concerned, by noting that,

---

* Ribbed TOR steel.

1. The stress cycles (based on measured strains) in the beam reinforcement at both cracked and uncracked sections were generally less severe than the computed stress cycles;* whereas the stress cycles (based on measured strains) and the computed stress cycles in the axially loaded bars were for all practical purposes identical.
2. The magnitudes of the maximum stresses (based on measured strains) were generally less than the magnitudes of the maximum computed stresses in the beam reinforcement.

It is significant also, that the fatigue strength of the concrete beam reinforcement is in better agreement with that of the axially loaded bars for the 0.93 C-T computed stress cycle than for the 4-T or 0.47 T-T computed stress cycles.

Most of the beams with welded reinforcement and subjected to the 0.93 C-T stress cycle contained partially preformed cracks at the weld location. Natural cracks initiated in the vicinity of these partially preformed cracks as well as at other locations in the beams and were often very pronounced because of the severe stress cycling. Perhaps of even greater significance was the fact that the cracks developed at both the top and bottom of the beams that were subjected to reversal loadings. After these beams had been subjected to a substantial number of loading cycles, the magnitudes of the maximum average stress (based on measured strains) sometimes exceeded the magnitudes of the computed stresses (see Table 7). These high stresses probably occurred because of a lack of remeshing of the cracked concrete at the top and bottom faces of the beams. Such a lack of remeshing may have been caused

---

* This was observed for the individual strain gage readings as well as for the average of the various gage readings (see Appendix C and Table 7).

by chips of concrete lodging between the cracks and may have led to a shifting of the neutral axis in the beams and a resulting increase in the net tensile force in the reinforcement. The action described for tensile force may also explain, at least in part, the changes observed in the compressive stresses in the reinforcement with an increase in number of cycles. Because of these increasing strains the reinforcement in the beams subjected to the 0.93 C-T stress cycle could be expected to have a fatigue strength in better agreement with that of the axially loaded bars than the reinforcement in the beams subjected to the 4-T and 0.47 T-T stress cycles. This is further verified by the fact that the observed stress ranges for the beam reinforcement subjected to the 0.93 C-T stress cycle tended to approach the computed stress ranges more closely than the observed stress ranges in the beam reinforcement subjected to the 4-T and 0.47 T-T stress cycles.

In addition to the tests of beams containing a single No. 7 reinforcing bar, tests of beams containing either two No. 10 bars or four No. 7 bars were conducted. The results of these tests, presented in Table 8, suggest that the beams with higher percentages of steel may behave more favorably under fatigue loadings. However, the apparent increase in fatigue resistance is only slight and the amount of available data is not sufficient to justify a firm conclusion on this point.

Most of the beam tests were conducted on specimens that contained butt-welded reinforcing bars; however, tests were also conducted on beams with single-lap-welded reinforcement.* The primary reason for testing the lap-welded reinforcement was to gain a more complete understanding of the

---

* The beams with lap-welded reinforcement conformed to the beam Type 1 designation (see Fig. 4).

effect of joint type on the fatigue behavior of reinforcement embedded in concrete beams. It will be recalled from earlier discussions that the relative fatigue behavior of "unbedded" bars, as affected by the various joint types shown in Fig. 3, was determined from tests in which the welded reinforcing bars were subjected to axial fatigue loadings (see Fig. 19). For this reason it was necessary to pursue a costly concrete beam study involving each of these joint types. By comparing the fatigue strengths of the lap-welded reinforcement and the 60-degree single-v butt-welded reinforcement contained in the beams with the fatigue strengths of the axially loaded welded reinforcing bars shown in Fig. 19, it would be possible to estimate the relative effect of the various joint types* on the fatigue behavior of the beam reinforcement.

If the (3.6-T) S-N curve for beams containing the lap joints is compared to the (4-T) S-N curve for beams containing 60-degree single-v butt-welded reinforcement it will be noted that the fatigue strengths are similar for the longer lives but for shorter lives the fatigue strength of the lap-welded reinforcement becomes significantly smaller than that of the butt-welded reinforcement (see Figs. 28 and 30). This behavior could be expected since for the shorter lives the average observed steel strains in the vicinity of the lap-joints tended to be greater than the observed steel strains for 60-degree single-v butt-welded reinforcement (see Table 7). This difference in observed strains is not unreasonable since the cracks which developed in the concrete beams with lap-welded reinforcement were more severe than the cracks contained in the beams with 60-degree single-v butt-welded reinforcement.

---

* Those joint types other than 60-degree single-v butt-welded or single lap-welded joints (see Figs. 3 and 19).

Longitudinal as well as vertical cracks developed in the beams with lap-welded reinforcement (see Fig. 31), while the beams with the butt-welded reinforcement contained only vertical cracks. The longitudinal cracks are believed to be a direct consequence of the abrupt change in geometry of the lap-welded joint and the tendency of the lap-welded reinforcement to deflect laterally when subjected to an axial tensile force. Because of the restraining effect of the concrete, the lateral deflection of the reinforcement was not very great. However, this lateral deflection may have been great enough to allow significant bending stresses to occur at the ends of the single lap joints. The lateral deflections and consequently the bending stresses at the lap joints would be more pronounced in the beams subjected to the larger maximum loads. This would explain the observed differences between fatigue strengths of the beams with butt-welded joints and the beams with single strap lap-welded joints noted above for the shorter lives.

7.3.2 High Strength Reinforcement

The beams with high strength reinforcement all contained partial preformed cracks. In addition, all of the high strength reinforcing bars were joined with 60-degree single-v butt welds. The S-N curves for these beams (Types 1 and 2) are shown in Fig. 32 and can be compared to those for high strength axially loaded reinforcing bars (see Fig. 20) and to those for beams with intermediate grade reinforcement (see Fig. 28). A comparison of these figures shows that the high strength reinforcing bars contained in the beams are not as prone to fatigue failures as the axially loaded reinforcement for the (1.6-to-T) stress cycle. However, under the (0.73C-to-T) stress cycle,

the fatigue resistance of the bars in the beams and those tested axially were not greatly different if examined on the basis of the stress range to which the bars were subjected. This is similar to the behavior observed for the intermediate grade bars. Some of the reasons for this behavior were discussed in the preceeding section which dealt with the beams that contained intermediate grade reinforcement. It should be noted that the attempt which was made to obtain a complete S-N curve for a C-T stress cycle had to be abandoned because the deflection capacity of the fatigue machine was not great enough to provide the necessary load range. As an alternative a (0.73 C to T) stress cycle was adopted. Although the S-N curve for this stress cycle is based on only three tests, it is strengthened by the presence of the data obtained from the reversal tests. These reversal data are also shown in Fig. 32, adjusted to the (0.73 C to T) stress cycle on the basis of stress range. This adjustment is not considered to introduce any great error.

A Modified Goodman diagram representing the S-N curves for both the beams and the axially loaded high strength bars is shown in Fig. 33. One interesting feature of the diagram is the convergence of the curves near the C to T stress cycle. This may be accounted for by the fact that the steel stresses (based on measured strains) in beams tested at a stress cycle of 0.73 C to T were found to compare very closely to the computed stresses, and in some cases were found to be slightly greater (see Table 7). The extensive damage produced in the concrete as a result of severe stress cycling is believed to be responsible for the high steel strain readings and consequently lower fatigue strengths.

Comparing the beam data of Fig. 32 with that of Fig. 28 for the

intermediate grade bars, on the basis of range of stress, one finds that the fatigue resistance of the high strength bars was slightly greater than that of the intermediate grade bars. However, the difference was not great. Thus, the type of welded reinforcement, whether intermediate or high strength grade, would not appear to affect to any great extent the fatigue resistance of the welded bars.

In the working stress design approach the compressive stresses acting in the welded reinforcement are assumed to increase by a factor of two with respect to the computed compressive stresses based on an elastic analysis in which the tensile strength of the concrete is ignored. This factor of two was introduced to account for creep in the concrete. Because of the short term loading conditions which prevailed in the 0.73 C to T tests the amount of concrete creep was probably insignificant and yet, as mentioned above, the compressive stresses based on measured strains were in some cases slightly greater than the computed compressive stresses based on the working stress design approach. It appears that the ability of the concrete to transmit compressive loads through the cracked regions of the concrete was impaired because of the severity of the cracks, and the welded reinforcement was forced to carry any additional compressive load not carried by the cracked concrete.

VIII. CONCLUSIONS

The following conclusions are based on the tests of this study:

1. Only three tests were conducted on concrete beams reinforced with unwelded bars. Nevertheless, the results indicate that these beams are not as susceptible to fatigue failures as comparable beams with welded reinforcement. However, further study on beams with unwelded bars should be conducted to provide a better quantitative evaluation of the fatigue resistance of such members.
2. In contrast to the effect of welding, the type of reinforcing bar deformation pattern had an insignificant effect on the fatigue behavior of the axially loaded bars. Although, strictly speaking, this conclusion is valid only for the types of bar deformations studied in this study, it probably applies to most of the more common types of patterns currently in use since the type of patterns considered were fairly representative of those in use.
3. The advantage in using high strength welded reinforcing bars rather than intermediate grade welded reinforcing bars is reduced substantially when the reinforcement is subjected to fatigue loadings.
4. Butt joints, angle splice joints and double strap lap joints have a greater resistance to fatigue failure than single strap lap and single lap joints.

The single lap joints had a great affect on the fatigue life of the welded reinforcing bars (See Fig. 19) and reduced the life of a bar from approximately 2,000,000 cycles to approximately 12,000 cycles under a stress cycle of 2 to 28 ksi tension.

5. The axial fatigue tests of the 60-degree single-V butt welded joints (See Figs. 15 and 16) indicate that the method of edge preparation, mechanically or flame cut, had no significant effect on the fatigue resistance of the joints. Nor did preheating of the bars to 400° F affect the fatigue resistance of the joints significantly.
6. Fatigue design of welded reinforcement contained in concrete beams by the direct application of data from axially loaded welded bars is recommended, provided the designer can conservatively, if not accurately, determine the magnitude of the stresses in the reinforcement. In this study the method used to calculate the reinforcement stresses generally tended to be conservative.
7. The full-penetration 60-degree single-V butt welded joints and the angle-splice joints statically developed both the yield and ultimate strengths of the A15 reinforcement. Unless relatively long splices were provided, the lap joints introduced significant bending and caused a significant reduction in the ultimate strength of the bars (See Fig. 10).

BIBLIOGRAPHY

1. ASTM Standards, "Structural and Boiler Steel; Forgings; Ferro-Alloys; Filler Metal," Part 4, pp. 43-7 and pp. 488-92, 1964.

2. Selby, S. M., Brian, Girling, *Standard Mathematical Tables*, The Chemical Rubber Co., Cleveland, Ohio, 1964.

3. Simon, L. E., *An Engineers' Manual of Statistical Methods*, Wiley and Sons, Inc., New York, 1941.

4. Burton, K. T., "Fatigue Tests of Reinforcing Bars," *Journal of the Portland Cement Association*, Vol. 7, No. 3, pp. 13-23, September 1965.

5. Derecho, A. T., and Munse, W. H., "Stress Concentrations at External Notches in Members Subjected to Axial Loadings," University of Illinois, Engineering Experiment Station Bulletin No. 494, January 1968.

6. Pfister, J. F. and Hognestad, E., "High Strength Bars as Concrete Reinforcement," *Journal of the Portland Cement Association*, Vol. 6, No. 1, pp. 65-84, January 1964.

7. Kokubu, M., Okamura, H., "Fatigue Behavior of High Strength Deformed Bars in Reinforced Concrete Bridges," Private Publication, University of Tokyo, 1967.

8. Sinha, B. P., Gerstle, K. H., and Tulin, L. G., "Stress Strain Relations for Concrete Under Cyclic Loading," *Journal of the American Concrete Institute*, Vol. 61, No. 2, pp. 195-210, 1964.

9. Winter, G., O'Rourke, C. E., Nilson, A. H., *Design of Concrete Structures*, McGraw-Hill Book Co., New York, 1964.

10. Commentary on Building Code Requirements for Reinforced Concrete (ACI 318-63) Publication SP-10, p. 36.

11. Soretz, S., "Fatigue Behavior of High Yield Reinforcement," *Concrete and Constructional Engineering*, Vol. 9, No. 7, July 1965.

12. Rehm, G., "Contribution to the Problem of the Fatigue Strength of Steel Bars for Concrete Reinforcement," Paper 1a2, Sixth Congress IABSE, Stockholm, 1960, pp. 35-46.

13. Mayer, M., "Fatigue Strength of Prestressed Concrete Structures," *Proceedings*, Deutscher Ausschuss fuer Stahlbeton, Vol. 176, Berlin, 1966.

The following are related references that may be of interest to the readers.

A1. Agrawal, G. L., Tulin, L. G. and Gerstle, K. H., "Response of Doubly Reinforced Concrete Beams to Cyclic Loading," *Journal of the American Concrete Institute*, Vol. 62, No. 7, July 1965, pp. 823-34.

A2. Bannister, J. L., "The Behavior of Reinforcing Bars under Fluctuating Stress," *Concrete*, Concrete and Cement Association--London, Vol. 3, No. 10, October 1969, pp. 405-09.

A3. Bethlehem Steel Company, "The Welding of Concrete Reinforcing Bars," Bethlehem Steel Company, 1960.

A4. Bresler, B. and Bertero, V., "Behavior of Reinforced Concrete under Repeated Loads, *Proceedings*, ASCE, Journal of the Structural Division, Vol. 94, No. ST6, June 1968, pp. 1567-89.

A5. Brown, R. H. and Jersa, J. O., "Reinforced Concrete Beams Under Load Reversals," *Journal of the American Concrete Institute*, Vol. 68, No. 5, May 1971, pp. 380-90.

A6. Burton, K. T. and Hognestad, E., "Fatigue Tests of Reinforcing Bars--Tack Welding of Stirrups," *Journal of the American Concrete Institute*, Vol. 64, No. 5, May 1967, pp. 244-52.

A7. Ekberg, C. E., Walther, R. E. and Slutter, R. G., "Fatigue Resistance of Prestressed Concrete Beams in Bending, *Proceedings*, ASCE, Journal of the Structural Division, Vol. 83, No. ST4, July 1957, pp. 1304-1 to 1304-17.

A8. Fisher, I. W. and Viest, I. M., "Fatigue Tests of Bridge Materials of the AASHO Road Test," Special Report 66, Highway Research Board, 1961, pp. 132-47.

A9. Hanson, J. M., Burton, K. T. and Hognestad, E., "Fatigue Tests of Reinforcing Bars--Effect of Deformation Pattern," *Journal of the Portland Cement Association*, Vol. 10, No. 3, September 1968, pp. 2-13.

A10. Henson, J. M., Somes, N. F., Helgason, T., Corley, W. G. and Hognestad, E., "Fatigue Strength of High Yield Reinforcing Bars," interim report of the Portland Cement Association for National Cooperative Highway Research Program Project No. 4-7, February 1970.

A11. Ivey, D. L., "Fatigue of Grouted Sleeve Reinforcing Bar Splices," *Proceedings*, ASCE, Journal of the Structural Division, Vol. 94, No. ST1, January 1968, pp. 199-210.

A12. Jertic, D., "Relaxation, Creep, Fatigue Tests and Tests of the Behavior at High Temperatures of Cold-Drawn Wire in Prestressed Concrete," *Rilem*, Bulletin No. 4, October 1959, pp. 66-75.

A13. Kripanarayanan, K. M. and Branson, D. E., "Short-Time Deflections of Beams under Single and Repeated Load Cycles," *Journal of the American Concrete Institute*, Vol. 69, No. 2, February 1972, pp. 110-17.

A14. Lloyd, J. P., Lott J. L. and Kesler, C. E., "Fatigue of Concrete," University of Illinois, Engineering Experiment Station Bulletin, No. 499, November 1968.

A15. MacGregor, J. G., Jhamb, I. C. and Nuttal, N., "Fatigue Strength of Hot Rolled Deformed Reinforcing Bars," *Journal of the American Concrete Institute*, Vol. 68, No. 3, March 1971, pp. 169-79.

A16. Mattock, A. H., "Rotational Capacity of Hinging Regions in Reinforced Concrete Beams," Portland Cement Association, Bulletin D101, Reprint from Proceedings of the International Symposium, Flexural Mechanics of Reinforced Concrete, ASCE, 1965.

A17. Pauw, A., "Static Modulus of Elasticity of Concrete as Effected by Density," *Proceedings*, ACI Journal, Vol. 57, No. 6, December 1960, pp. 679-88.

A18. Monnier, T., "The Moment-Curvature Relation of Reinforced Concrete," *Heron*, Technological University, Delft, Netherlands, Vol. 17, No. 2, 1970.

A19. Price, K. M. and Edwards, A. D., "Fatigue Strength in Shear of Prestressed Concrete I-Beams," *Journal of the American Concrete Institute*, Vol. 69, No. 4, April 1971, pp. 282-92.

A20. Ross, W. M. and Winter, G., "Reinforced Concrete Beams under Repeated Loads," *Proceedings*, ASCE, Journal of the Structural Division, Vol. 95, No. ST6, June 1969, pp. 1189-1211.

A21. Rudy, J. F., Suyama, F. and Schwartzbart, H., "Welding of Reinforcing Bars for Concrete Construction," *Welding Journal*, Vol. 38, No. 8, August 1959, pp. 335a-344s.

A22. Sanders, W. W. and Munse, W. H., Discussion of "Welding of Reinforcing Bars for Concrete Construction," *Welding Journal*, Vol. 38, No. 8, August 1959, pp. 3405-25.

A23. Sanders, W. W., Jr. and Siess, C. P., "Tension Tests of Large-Size Deformed Concrete Reinforcing Bars," *Proceedings*, ASTM, Vol. 65, 1965, pp. 654-60.

A24. Sanders, W. W., Jr., Hoadley, P. G. and Munse, W. H., "Fatigue Behavior of Welded Joints in Reinforcing Bars for Concrete," *Welding Journal*, Vol. 40, No. 12, December 1961, pp. 5295-5355.

A25. Shah, S. P. and Chandra, S., "Fracture of Concrete Subjected to Cyclic and Sustained Loading," *Journal of the American Concrete Institute*, Vol. 67, No. 10, October 1970, pp. 816-25.

A26. Singh, A., Gerstle, K. H. and Tulin, L. G., "The Behavior of Reinforcing Steel Under Reversed Loading," ASTM, *Materials Research and Standards*, Vol. 5, No. 1, January 1965, pp. 12-17.

A27. Soete, W. and Vancrombrugge, R., "The Resistance to Fatigue of Wires in Prestressed Concrete," *Annales des Travaux Publics de Belgique*, No. 5, October 1949.

A28. Taylor, R., "Some Fatigue Tests on Reinforced Concrete Beams," *Magazine of Concrete Research*, Vol. 16, No. 46, March 1964, pp. 31-38.

A29. Wallo, E. M. and Kesler, C. E., "Prediction of Creep in Structural Concrete," University of Illinois, Engineering Experiment Station Bulletin, No. 498, November 1968.

A30. Walls, J. C., Sanders, W. W., Jr. and Munse, W. H., "Fatigue Behavior of Butt-Welded Reinforcing Bars in Reinforced Concrete Beams," *Journal of the American Concrete Institute*, Vol. 62, No. 2, pp. 169-90, February 1965.

TABLE 1

PHYSICAL PROPERTIES AND CHEMICAL COMPOSITIONS OF REINFORCING BARS

(a) ASTM Specification Requirements

(1) Tensile Requirements

Specification	Yield Strength, σ_y, psi	Ultimate Strength, σ_{ult}, psi	Elongation in 8", Percent
A15-62T[1]	40,000 (min)	70,000 - 90,000	12.0 (min)
A431-62T[1]	75,000 (min)	100,000 (min)	7-1/2 (min)(No. 6 bars) 7 (min)(No. 7 Bats)

(2) Chemical Requirements

Specification	Phosphorus, Max, percent
A15-62T	open hearth, basic oxygen, or electric furnace (Basic--0.05) (Acid---0.08)
	Acid bessemer and open-hearth, basic oxygen, or electric furnace rephosphorized----------0.12
A431-62T	----------0.05

(b) Range of Physical properties and Chemical compositions of reinforcing bars used in tests, as given by mill reports.

(1) Physical Properties

Specification	Yield Strength, σ_y, psi	Ultimate Strength, σ_{ult}, psi	Elongation in 8", percent
A15	49,800 - 53,000	77,300 - 84,600	18 - 22
A431	89,800 - 93,300	123,700 -149,200	7.7 - 11

(2) Chemical Compositions, percent

Specification	C	Mn	P	S	Si
A15	0.35 - 0.45	0.39 - 0.64	0.013 -0.019	0.030 -0.045	0.14 - 0.15
A431	0.40 - 0.45	0.81 - 0.89	0.010 -0.022	0.016 -0.030	0.25 -0.35

Note: The ASTM A15 and A431 Specifications were replaced in 1968 by the ASTM A615 Specification. The bars used in the investigation would in general correspond to the Grade 40 and Grade 75 respectively in A615.

TABLE 2

SUMMARY OF STATIC TESTS ON A15
INTERMEDIATE GRADE WELDED REINFORCING BARS

Specimen Number	Joint Type	Yield Strength* (ksi)	Ultimate Strength (ksi)	Point of Failure
SW-1	60-degree single-v	50.8	79.2	In weld
SW-2	60-degree single-v	51.0	79.4	In weld
SW-3	60-degree single-v	50.3	80.3	Outside weld
SW-41	Angle splice	50.8	78.8	About 6 in. from joint
SL-1	5 in. single lap	51.0	70.0	At end of joint (see Fig. 10)
SL-2	5 in. single lap	49.6	70.4	At end of joint
SL-3	2 in. single lap	50.0	55.2	At end of joint
SL-4	2 in. single lap	50.0	59.0	At end of joint
SL-5	3 in. single lap	51.0	64.9	At end of joint
SL-6	4 in. single lap	51.0	69.5	At end of joint
SL-7	6 in. single lap	50.7	74.4	At end of joint
SL-8	7 in. single lap	50.7	76.8	At end of joint
SLL-1	5 in. single strap lap	--	68.4	At end of joint
SLL-2	5 in. single strap lap	--	68.2	At end of joint
SLL-3	2 in. single strap lap	50.7	58.8	At end of joint
SL-4	7 in. single strap lap	51.0	75.0	At end of joint

* Yield strength as determined by drop of beam

TABLE 3

RESULTS OF FATIGUE TESTS ON UNWELDED REINFORCING BARS

Specimen Number	Bar Pattern	Stress Cycle (ksi)	Cycles to Failure	Remarks
	(a) Reinforcing Bar Material Specification: (A15)			
10	C	-22 to +22	225,100	Failed at lower grip
11	C	-22 to +22	171,900	Failed at lower grip
12	C	-17 to +17	689,400	Failed at lower grip
13	C	-17 to +17	633,000	Failed at upper grip
14	C	-15 to +15	1,047,500	Failed at lower grip
15	C	-14 to +15	2,884,300	No failure
16	C	-25 to +25	46,400	Failed near lower grip Considerable lateral deflection of the specimen was noted.
17	C	-14.5 to +14.5	2,940,100	Failed at lower grip
A-9	A	+2 to +38	464,900	Failed midway between grips
A-10	A	+2 to +38	386,400	Failed midway between grips
A-11	A	+2 to +45	171,200	Failed midway between grips
A-12	A	+2 to +32	1,233,100	Failed midway between grips
B1-9	B	+2 to +38	491,800	Failed midway between grips
B1-10	B	+2 to +32	470,900	Failed at upper grip
B1-11	B	+2 to +42	262,900	Failed one in. from lower grip
B1-12	B	+2 to +32	1,199,200	Failed midway between grips
WDO-1*	B	+2 to +28	839,300	Failed at lower grip
WDO-2	B	+2 to +28	217,900	Failed at lower grip

* Specimens WDO-1 to WDO-4 were fabricated from No. 6 bars, all other bars were No. 7.

TABLE 3 (continued)

Specimen Number	Bar Pattern	Stress Cycle (ksi)		Cycles to Failure	Remarks
WDO-3	B	+2	to +28	>354,600** <797,400	Failed at lower grip
WDO-4	B	+2	to +38	249,800	Failed at lower grip
01	C	+2	to +42	276,100	Failed midway between grips
02	C	+2	to +32	588,900	Failed at lower grip
04	C	+2	to +28.5	1,647,100	Failed at upper grip
1	C	+2	to +38	272,900	Failed one in. from upper grip
2*	C	+0	to +35	84,900	Failed at edge of reduced section
3	C	+2	to +38.4	213,800	Failed at lower grip
4	C	+2	to +30	581,100	Failed at upper grip
5	C	+2	to +30	501,600	Failed at lower grip
6	C	+2	to +41.5	242,700	Failed at lower grip
7	C	0	to +28	4,208,700	No failure
8	C	+2	to +29	867,400	Failed at lower grip
9	C	+2	to +28	1,336,500	Failed at upper grip
18	C	+1	to +43	182,300	Failed at lower grip
19	C	+2	to +42	187,000	Failed in grip

* This specimen was used for load eccentricity measurements and therefore had to be machined smooth so that strain gages could be mounted on the bar.

** The inequality symbols indicate that the automatic cut-off switch on the fatigue machine did not function properly. The last recorded number of cycles before failure was 354,600 cycles and the number of cycles recorded at some time after failure was 797,400 cycles. The life to failure was taken as the average of these two numbers, i.e., 516,000 cycles.

TABLE 3 (Continued)

Specimen Number	Bar Pattern	Stress Cycle (ksi)	Cycles to Failure	Remarks
		(unwelded bars encased in concrete)*		
C-1	C	+2 to +35	584,600	Failed at upper grip
C-2	C	+2 to +28	2,985,000	Failed at upper grip
C-3	C	+2 to +28	2,280,900	No failure (partial crack in conc.)
C-4	C	+2 to +28	1,786,400	Failed at upper grip (partial crack in conc.)
C-5	C	+2 to +35	318,200	Failed at partial crack
		(b) Reinforcing Bar Material Specification: (A431)		
WHO-1**	B	+2 to +38	349,100	Failed at lower grip
WHO-2	B	+2 to +38	416,500	Failed at upper grip
HB-9	C	+2 to +28	2,480,600	No failure
HB-10	C	+2 to +38	3,061,700	No failure
HB-11	C	+2 to +45	648,000	Failed midway between grips
HB-12	C	+2 to +50	303,600	Failed midway between grips

* See Fig. 3

** Specimens WHO-1 and WHO-2 were fabricated from No. 6 bars.

TABLE 4

RESULTS OF FATIGUE TESTS ON WELDED REINFORCING BARS

Specimen Number	Bar Pattern	Stress Cycle (ksi)		Cycles to Failure*	Remarks
		Reinforcing Bar Material Specification: (A15) (a) Joint Type: 60-degree single-v			
A-5	A	-25	to +25	>165,100 <240,000	Failed at weld
A-6	A	-20	to +20	>548,300 <947,000	Failed at weld
A-7	A	-20	to +20	359,200	Failed
A-8	A	-18	to +18	>1,086,100 <1,610,000	Failed
B1-5	B	-25	to +25	>155,000 <394,800	Failed near weld
B1-6	B	-18	to +18	>114,200 <509,400	Failed
W-12	C	-15	to +15	2,095,600	Failed at lower grip
W-13	C	-18	to +18	510,000	Failed at weld
W-14	C	-15	to +15	815,400	Failed in heat affected zone
W-15	C	-15.5	to +13.5	4,300,000	No failure
W-18	C	-20	to +20	234,500	Failed in heat affected zone
W-19	C	-14	to +14	3,734,000	No failure
W-20	C	-15.5	to +15.5	1,040,000	Failed in heat affected zone
W-21	C	-24	to +24	50,000	Failed at weld
A-1	A	+2	to +38	148,700	Failed at top of weld
A-2	A	+2	to +38	172,000	Failed at weld
A-3	A	+2	to +28	565,500	Failed at top of weld
A-4	A	+2	to +28	516,000	Failed near weld

* The inequality symbols indicate that the automatic cut-off switch on the fatigue machine did not function properly. The smaller number indicates the last recorded number of cycles before failure and the large number indicates the number of cycles recorded some time after failure. The life to failure was taken as the average of these two numbers.

TABLE 4 (Continued)

Specimen Number	Bar Pattern	Stress Cycle (ksi)	Cycles to Failure	Remarks
B1-1	B	+2 to +38	155,700	Failed near weld
B1-2	B	+2 to +38	107,300	Failed near weld
B1-3	B	+2 to +28	702,000	Failed near weld
B1-4	B	+2 to +28	513,000	Failed near weld
B1-7	B	+2 to +32	343,500	Failed at weld
B1-8	B	+2 to +20	2,951,200	No failure
W-1	C	+2 to +38	242,100	Failed at edge of weld
W-2	C	+2 to +28	287,100	Failed at edge of weld near heat affected zone
W-3	C	+2 to +28	522,400	Failed at edge of weld near heat affected zone
W-4	C	+2 to +28	853,100	Failed at weld
W-5	C	+2 to +38	232,800	Failed in heat affected zone
W-6	C	+2 to +26	823,600	Failed at weld
W-7	C	+2 to +24	944,400	Failed at weld
W-8	C	+2 to +22	4,937,400	No failure
W-9	C	+2 to +23	2,660,000	No failure
W-10	C	+2 to +23	950,500	Failed at weld
W-11	C	+3 to +48	38,500	Failed at weld
W-54A	C	+2 to +45	81,800	Failed at weld
W-47A	C	+2 to +35	264,400	Failed

TABLE 4 (Continued)

Specimen Number	Bar Pattern	Stress Cycle (ksi)	Cycles to Failure	Remarks
W-16	C	+21 to +42	970,000	Failed at weld
W-17	C	+21 to +42.5	900,500	Failed in heat affected zone
W52A	C	+18 to +36	2,239,900	Failed at weld
W53	C	+23 to +46	683,000	Failed at top of weld
W42A	C	+19 to +38	1,287,400	Failed
W43A	C	+19.5 to +39	397,000	Failed at weld
W44A	C	+18 to +36	4,147,000	No failure
W45	C	+17 to +34	2,327,000	No failure
W46A	C	+19.5 to +39	404,100	Failed at weld
		(b) Joint type: Flame cut 60-degree single-v		
FC9	C	-18 to +18	315,700	Failed near weld
FC10	C	-18 to +18	>109,200 <336,400	Failed at top of weld
FC1	C	+2 to +28	503,300	Failed near weld
FC2	C	+2 to +22	1,258,600	Failed at weld
FC3	C	+2 to +22	2,015,400	Failed at grip
FC4	C	+2 to +38	181,000	Failed at weld
FC5	C	+2 to +38	167,300	Failed near weld
FC6	C	+2 to +20	2,232,900	No failure
FC7	C	+2 to +45	43,500	Failed at weld

Table 4 (Continued)

Specimen Number	Bar Pattern	Stress Cycle (ksi)		Cycles to Failure	Remarks
FC8	C	+2	to +28	501,000	Failed at undercut edge of weld
FC13	C	+2	to +40	184,800	Failed
FC14	C	+2	to +25	664,800	Failed at root of weld
FC15	C	+2	to +22	428,300	Failed at weld
FC16	C	+2	to +22	526,900	Failed at weld
FC17	C	+2	to +22	1,708,100	Failed
FC18	C	+2	to +45	30,400	Failed at notch in root of weld
FC11	C	+21	to +42	448,200	Failed at toe of the weld
FC12	C	+21	to +42	490,700	Failed
FC19	C	+21	to +42	596,600	Failed at weld
FC20	C	+21	to +42	730,600	Failed at weld
FC21	C	+20	to +40	775,900	Failed at toe of weld
		(c)	Joint Type:	60-degree single-v preheated to 400°F	
W-68	-	-20	to +20	278,900	Failed
W-69	C	-20	to +20	192,100	Failed near weld
W-58	-	+2	to +28	691,500	Failed
W-59	-	+2	to +38	176,300	Failed

TABLE 4 (Continued)

Specimen Number	Bar Pattern	Stress Cycle (ksi)	Cycles to Failure	Remarks
W-60	-	+2 to +24	2,710,500	No failure
W-61	C	+2 to +45	129,100	Failed at toe of weld
W-62	-	+2 to +24	1,005,900	Failed
W-66	-	+2 to +28	604,400	Failed
W-63	-	+20 to +40	893,700	Failed
W-64	-	+17.5 to +35	1,284,800	Failed
W-65	C	+17.5 to +35	575,500	Failed at weld
W-67		+17.5 to +35	1,129,200	Failed
		(d) Joint Type: Single strap lap		
W-31	C	+2 to +28	16,800	Failed through bar at the end of fillet
W-32	C	+2 to +28	7,400	Failed through bar at the end of fillet
		(e) Joint Type: Single strap lap encased in concrete		
W-33	C	+2 to +28	16,000	Failed through bar at the end of fillet weld
W-35	C	+2 to +28	41,000	Failed through bar at the end of fillet weld. (With circular rein. spaced @ 3")
		(f) Joint Type: Angle splice		
W-28	C	+2 to +28	165,800	Failed through weld at point where bars butt
W-29	C	+2 to +28	189,100	Failed through weld at point where bars butt
W-30	C	+2 to +28	188,000	Failed through weld at point where bars butt

TABLE 4 (Continued)

Specimen Number	Bar Pattern	Stress Cycle (ksi)	Cycles to Failure	Remarks
		(g) Joint Type: 45-degree single-v		
W-22	C	+2 to +28	78,000	Failed at edge of weld
W-23	C	+2 to +28	276,400	Failed at edge of weld
W-24	C	+2 to +28	570,000	Failed at weld
		(h) Joint Type: Double strap-lap		
WL-1	C	+2 to +28	>211,400 <481,800	Failed at end of joint
WL-2	C	+2 to +28	284,100	Failed at end of joint
WL-3	C	+2 to +28	374,000	Failed at end of joint
		(i) Joint Type: 60-degree double-v		
W-25	C	+2 to +28	478,000	Failed in base material
W-26	C	+2 to +28	332,000	Failed at edge of weld
W-27	C	+2 to +28	367,000	Failed in heat affected area
		(j) Joint Type: 60-degree single-v with pipe back-up		
WP-1	C	+2 to +28	460,600	Failed at edge of weld
WP-2	C	+2 to +28	589,200	Failed at toe of weld
WP-3	C	+2 to +28	> 70,900 <365,100	Failed at toe of weld
		(k) Joint Type: 60-degree single-v encased in concrete		
W-37	C	+2 to +28	2,870,000	Did not fail
W-38	C	+2 to +28	1,848,300	Failed at weld (no preformed crack)
W-39	C	+2 to +28	866,400	Failed at weld (Partial crack in conc.)

TABLE 4 (Continued)

Specimen Number	Bar Pattern	Stress Cycle (ksi)	Cycles to Failure	Remarks
		(k)	Joint Type:	60-degree single-v encased in concrete
W-40	C	+2 to +28	1,751,400	Failed at weld (partial crack in conc.)
W-48	C	+2 to +38	157,000	Failed at weld (partial crack in conc.)
W-49	C	+2 to +38	191,000	Failed at weld (partial crack in conc.)
W-50	C	+2 to +35	117,700	Failed at weld (full crack in conc.)
W-51	C	+2 to +28	1,031,600	Failed at weld (partial crack in conc.)
W-55	C	+2 to +28	557,400	Failed (partial crack in conc.)
W-56	C	+2 to +28	809,900	Failed (partial crack in conc.)
W-57	C	+2 to +28	636,100	Failed at grip (partial crack in conc.)
		(l)	Joint Type:	Bars with tack welded stirrups
WT-1	C	+2 to +28	1,052,800	Failed through #7 bar at the edge of tack weld
WT-2	C	+2 to +28	>531,600 <891,400	Failed at edge of tack weld
WT-3	C	+2 to +28	2,986,300	No failure

TABLE 4 (Continued)

Specimen Number	Bar Pattern	Stress Cycle (ksi)	Cycles to Failure	Remarks
Reinforcing Bar Material Specification: (A431)				
(a) Joint Type: 60-degree single-v				
HB-5	X	-18 to +18	1,104,000	Failed through weld
HB-6	X	-33 to +33	221,900	Failed near weld
HB-7	C	-25 to +25	651,700	Failed at lower grip
HB-8	C	-16.5 to +16.5	3,047,100	No failure
HB-13	C	-35 to +35	142,400	Failed through weld
HB-14	C	-20 to +20	278,600	Failed through the weld
HB-15	C	-20 to +20	572,400	Failed at the toe of weld
HB-17	C	-35 to +35	78,500	Failed through the weld
HB-18	C	-18 to +18	1,983,300	Failed through weld
H-20	X	-33 to +33	88,700	Failed through weld
H-21	X	-16.5 to +16.5	1,209,600	Failed at the toe of weld
H-22	X	-18 to +18	>461,400 <562,100	Failed through weld
H-23	X	-18 to +18	721,500	Failed near the weld
H-24	X	-33 to +33	147,700	Failed through weld
WH-1*	B	+2 to +38	281,300	Failed through weld
WH-2*	B	+2 to +38	235,100	Failed near weld
WH-3*	B	+2 to +28	860,200	Failed through the weld
HB-1	C	+2 to +38	361,500	Failed through weld
HB-2	C	+2 to +38	363,600	Failed through weld
HB-3	C	+2 to +28	3,040,000	No failure
HB-4	C	+2 to +28	1,204,100	Failed through weld
HB-16	C	+21 to +42	2,266,600	No failure

* Specimens WH-1 to WH-3 were fabricated from No. 6 bars

TABLE 5

SUMMARY OF FATIGUE STRENGTHS OF WELDED A15 REINFORCING BARS WITH 60-DEGREE SINGLE-V BUTT JOINTS

Stress Cycle	$F_{100,000}$		$F_{2,000,000}$	
	Max. Stress (ksi)	Std. Dev. (±ksi)	Max. Stress (ksi)	Std. Dev. (±ksi)
C-T	±25.0	±3.5	±14.0	±2.5
2-T	+40.0	±5.0	+20.0	±3.0
1/2T-T	--		+32.0	±2.5

TABLE 6

RESULTS OF FATIGUE TESTS ON CONCRETE BEAMS WITH UNWELDED REINFORCEMENT

Specimen Number	Type of Preformed Crack	Computed Stress Cycles	Ave. Stress in Reinf. After First Few Loading Cycles[1] (ksi)		Ave. Stress in Reinf. After a Substantial Number of Loading Cycles[1] (ksi)			Cycles to Failure	Remarks
			Min.	Max.	Min.	Max.	Cycles		
(a) Reinforcing Bar Material Specification: A15 (Beam Specimen Type 1)[2]									
SBC1	None	+3.2 to +32.3	+9.4	+34.1	+12.5	+28.7	4,214,00	4,884,000	No failure
(b) Reinforcing Bar Material Specification: A431 (Beam Specimen Type 1)[2]									
BT 1	Partial	4.0 to 40.5	14.7	32.1	20.6	39.3	1,314,200	2,570,000	No failure
BT 2	Partial	2.3 to 52.3	22.2	49.7	29.7	--	--	3,690,000	No failure

[1] This stress was obtained by multiplying the average measured strain (based on strain gage readings at cracked and uncracked sections) by 30×10^6 psi.

[2] See Fig. 4

TABLE 7

RESULTS OF FATIGUE TESTS ON CONCRETE BEAMS WITH WELDED REINFORCEMENT

Specimen Number	Type of Preformed Crack	Computed Stress Cycles	Ave. Stress in Reinf. After First Few Loading Cycles[1] (ksi)		Ave. Stress in Reinf. After a Substantial Number of Loading Cycles[1] (ksi)			Cycles to Failure	Remarks
			Min.	Max.	Min.	Max.	Cycles		
(a) Reinforcing Bar Material Specification: A15 (Beam Specimen Type 2)[2] Joint Type: 60 degree single-v									
BR 4	None	-14.4 to +14.8	-2.2	+8.6	-10.4	+24.6	2,173,000	2,883,000	No failure
BR 1	Partial	-23.1 to +25.1	--	--	--	--	--	400,000	Failed at weld
BR 2	Partial	-18.8 to +20.1	-2.0	+14.8	-3.0	+26.5		600,000	Failed at weld
BR 3	Partial	-23.1 to +25.1	--	--	--	--	--	231,400	Failed at weld
BR 5	Partial	-18.9 to +20.4	-10.3	+17.3	-14.4	+20.4	479,900	1,262,600	Failed outside of loading block
BR 6	Partial	-13.7 to +15.6	-8.2	+29.4	-6.9	+32.6	2,245,700	2,496,400	Failed 2 in. from weld
BR 8	Partial	-18.7 to +20.7	--	--	--	--	--	680,000	Failed at toe of weld
BR 9	Partial	-28.0 to +30.7	-8.3	+29.8	-12.4	+27.3	65,300	186,500	Failed 2 in. from weld
BR 10	Partial	-15.8 to +17.0	-6.2	+8.3	-6.3	+14.2	1,559,400	2,223,400	No failure
BR 11	Partial	-30.9 to +32.5	--	--	--	--	--	33,700	Failed at weld
BR 12	Partial	-15.6 to +16.7	-4.6	+3.0	-4.2	+17.7	898,100	1,343,600	Failed at toe of weld
BR 7	Full	-27.8 to +29.1	-8.4	+29.1	-13.5	+39.2	16,300	92,700	Failed at weld

[1] These stresses were obtained by multiplying the average measured strain based on strain gage readings at cracked and uncracked sections by 30 x 10^6 psi. These are the stresses for the maximum and minimum loads applied to the beams. The values are based on the original zero-load stress for the various gages.

[2] See Fig. 4

TABLE 7 (Continued)

Specimen Number	Type of Preformed Crack	Computed Stress Cycles	Ave. Stress in Reinf. After First Few Loading Cycles (ksi)		Ave. Stress in Reinf. After a Substantial Number of Loading Cycles (ksi)			Cycles to Failure	Remarks
			Min.	Max.	Min.	Max.	Cycles		
(a) Reinforcing Bar Material Specification: A15 (Beam Specimen Type 1) Joint Type: 60-degree single-v									
BW 1	None	+2.1 to +31.5	12.5	25.5	21.1	39.6	3,747,500	3,747,500	No failure
BW 2	None	+3.5 to +26.4	10.5	21.5	12.9	25.0	3,098,300	3,320,300	Failed at weld
BW 3	None	+6.1 to +52.9	15.0	39.5	18.4	44.2	657,200	684,100	Failed at weld
BW 4	None	+5.1 to +51.4	17.0	44.0	--	--	--	342,800	Failed at weld
BE 11A	None	+4.3 to +35.9	--	--	--	--	--	1,943,600	Failed at weld
BW 7A	Partial	+3.9 to +32.0	5.5	16.0	14.9	28.7	2,614,900	2,614,900	No failure
BW 10A	Partial	+2.4 to +53.8	9.5	39.5	15.0	44.3	189,400	267,700	Failed at toe of weld (bar placed upside down)
BW 15	Partial	+3.9 to +32.9	5.5	18.0	9.3	25.4	958,700	2,005,600	Failed at weld (bar placed upside down)
BW 17	Partial	+3.9 to +55.0	9.5	35.0	--	--	--	171,800	Failed at weld (bar placed upside down)
BW 6	Full	+3.1 to +26.8	2.0	10.0	18.3	28.7	2,664,700	2,627,000	No failure
BW 8A	Full	+3.9 to +46.1	5.5	32.0	11.2	38.4	71,348	210,748	Failed at weld
BW 9	Full	+3.5 to +30.5	7.2	23.4	--	--	--	513,000	Failed at weld

TABLE 7 (Continued)

Specimen Number	Type of Preformed Crack	Computed Stress Cycles	Ave. Stress in Reinf. After First Few Loading Cycles (ksi)		Ave. Stress in Reinf. After a Substantial Number of Loading Cycles (ksi)			Cycles to Failure	Remarks
			Min.	Max.	Min.	Max.	Cycles		
(a) Reinforcing Bar Material Specification: A15 (Beam Specimen Type 1) Joint Type: 60-degree single-v									
BW 12	Full	+3.0 to +31.3	6.8	22.5	13.0	32.0	213,300	468,000	Failed at weld
BW 13A	Full	+3.9 to +46.1	6.0	30.0	--	--	--	254,000	Failed at weld
BW 14	Full	+3.7 to +28.6	2.0	15.0	4.9	16.6	1,720,000	1,933,400	Failed at weld
BW 18	None	+24.7 to 56.0	26.2	35.7	24.0	31.2	2,193,000	2,193,000	No failure
BW 19	Partial	+26.4 to 54.1	26.8	36.8	--	--	--	2,131,300	No failure
BW 23	Partial	+31.3 to +65.4	31.0	41.0	22.9	32.6	1,422,200	2,494,000	No failure
BW 20	Full	+25.3 to +53.5	36.0	52.5	--	--	--	2,053,000	No failure
BW 22	Full	+29.9 to +61.4	23.7	36.9	--	--	--	2,403,300	No failure

TABLE 7 (Continued)

Specimen Number	Type of Preformed Crack	Computed Stress Cycles	Ave. Stress in Reinf. After First Few Loading Cycles (ksi)		Ave. Stress in Reinf. After a Substantial Number of Loading Cycles (ksi)			Cycles to Failure	Remarks
			Min.	Max.	Min.	Max.	Cycles		
(a) Reinforcing Bar Material Specification: A15 (Beam Specimen Type 1) Joint Type: 3-1/2" single-lap									
BL 1	None	+4.3 to +26.8	6.5	17.4	--	--	--	3,567,900	No failure
BL 2	None	+2.8 to +31.1	7.0	21.3	11.1	25.4	180,867	221,000	Failed at end of joint
BL 3	None	+1.8 to +29.5	8.0	24.3	10.2	25.0		944,100	Failed at end of joint
BL 4	None	+3.6 to +31.6	9.0	25.4	--	--	--	2,008,800	Failed at end of joint
BL 5	None	+3.3 to +45.0	12.0	46.0	--	--	--	38,900	Failed at end of joint
BL 6	None	+3.1 to +38.1	8.0	29.0	--	--	--	163,000	Failed at end of joint
BL 7	None	+3.1 to +38.1	12.5	36.3	--	--	--	27,600	Failed at end of joint
BL 8	None	+3.6 to +41.2	10.0	38.5	--	--	--	127,200	Failed at end of joint
BL 9	Full	+6.3 to +45.1	7.5	35.0	8.6	26.2	130,400	215,000	Failed at end of joint
BL 10	Full	+27.5 to +53.9	17.5	24.0	23.4	33.5	751,000	769,700	Failed at end of joint
BL 11	Full	+3.9 to +44.1	7.0	26.0	6.5	24.9	197,400	277,400	Failed at end of joint

TABLE 7 (Continued)

Specimen Number	Type of Preformed Crack	Computed Stress Cycles	Ave. Stress in Reinf. After First Few Loading Cycles (ksi) Min.	Ave. Stress in Reinf. After First Few Loading Cycles (ksi) Max.	Ave. Stress in Reinf. After a Substantial Number of Loading Cycles (ksi) Min.	Ave. Stress in Reinf. After a Substantial Number of Loading Cycles (ksi) Max.	Ave. Stress in Reinf. After a Substantial Number of Loading Cycles Cycles	Cycles to Failure	Remarks
(a) Reinforcing Bar Material Specification: A15									
(Beam Specimen Type 3)									
Joint Type: 45-degree single-v									
$\overline{BT}$ 1	Full	+2.1 to +31.1	5.1	27.4	--	--	--	713,900	Failed at weld
$\overline{BT}$ 2	Full	+2.0 to +31.0	3.1	24.7	--	--	--	574,900	Failed at weld
(Beam Specimen Type 4)									
Joint Type: 60-degree single-v									
BF 1	Full	+2.6 to +29.9	3.8	17.5	6.6	20.6	861,600	861,600	Failed at weld
BF 2	Full	+2.6 to +30.8	5.4	20.9	7.5	26.14	746,000	746,000	Failed at weld

TABLE 7 (Continued)

Specimen Number	Type of Preformed Crack	Computed Stress Cycles	Ave. Stress in Reinf. After First Few Loading Cycles (ksi) Min.	Ave. Stress in Reinf. After First Few Loading Cycles (ksi) Max.	Ave. Stress in Reinf. After a Substantial Number of Loading Cycles (ksi) Min.	Ave. Stress in Reinf. After a Substantial Number of Loading Cycles (ksi) Max.	Ave. Stress in Reinf. After a Substantial Number of Loading Cycles Cycles	Cycles to Failure	Remarks
(b) Reinforcing Bar Material Specification: A431 (Beam Specimen Type 1) Joint Type: 60-degree single-v									
BT 3	Partial	+1.7 to +52.6	6.9	33.7	8.7	39.5	264,300	355,300	Failed at toe of weld
BT 4	Partial	+1.6 to +52.5	13.5	42.8	14.4	42.5	210,000	225,300	Failed at toe of weld
BT 5	Partial	+1.6 to +52.8	--	--	--	--	--	628,600	Failed at toe of weld
BT 6	Partial	+1.6 to +31.3	18.6	33.4	23.1	36.2	2,466,600	3,097,500	No failure
BT 7	Partial	+1.6 to +43.5	10.4	35.7	12.1	41.5	427,900	454,400	Failed at weld
BT 8	Partial	+1.6 to +37.7	20.4	33.7	30.5	43.3	1,893,200	2,111,500	No failure
BT 9	Partial	+1.6 to +37.9	--	--	--	--	--	3,270,400	No failure
BT 10	Partial	+1.6 to +44.1	22.4	41.0	29.5	47.3	2,252,000	2,432,300	Failed at toe of weld
BT 11	Partial	+1.6 to +45.6	16.0	34.9	26.5	44.7	448,600	453,800	Failed at weld
BT 12	Partial	+1.6 to +42.7	11.7	29.9	12.0	31.3	1,158,200	1,555,400	Failed at weld
BT 13*	Partial	+28.0 to +43.0	20.1	47.5	17.1	45.8	55,000	213,400	Failed near weld

* Loading for BT 13 consisted of two loads at midspan spaced 12 in. apart.

TABLE 7 (Continued)

Specimen Number	Type of Preformed Crack	Computed Stress Cycles	Ave. Stress in Reinf. After First Few Loading Cycles (ksi) Min.	Max.	Ave. Stress in Reinf. After a Substantial Number of Loading Cycles (ksi) Min.	Max.	Cycles	Cycles to Failure	Remarks
(b) Reinforcing Bar Material Specification: A431 (Beam Specimen Type 2) Joint Type: 60-degree single-v									
BR 13	Partial	-23.8 to +24.8	-4.8	+21.1	-7.9	+26.1	619,600	716,100	Failed at weld
BR 14	Partial	-23.8 to +24.3	--	--	--	--	--	246,400	Failed at weld
BR 15	Partial	-23.6 to +25.7	-4.4	+23.6	-5.7	+29.1	654,200	719,900	Failed at end of weld
BR 16	Partial	-23.5 to +25.0	-12.2	+12.6	-14.2	+19.4		754,600	Failed at weld
BR 18	Partial	-18.6 to +23.4	-17.7	+21.5	-18.6	+22.1	376,900	413,900	Failed at weld
BR 20	Partial	-26.2 to +35.5	-32.0	+35.8	-33.6	+32.7	108,900	120,000	Failed at weld
BR 21	Partial	-23.5 to +35.1	-25.4	+32.7	-27.9	+27.9	73,200	160,000	Failed at weld

TABLE 8

RESULTS OF FATIGUE TESTS ON CONCRETE BEAMS WITH VARIOUS PERCENTAGES OF INTERMEDIATE GRADE REINFORCEMENT

Specimen Number	Type of Beam Specimen*	Joint Type	Percentage of Reinforcement	Total Reinf. Perimeter, in.	Type of Preformed Crack	Computed Stress Cycle	Cycles to Failure
BW 9	Type 1	60-degree single-v	1.0	2.7	Full	+3.5 to +30.5	513,00
BW 12	Type 1	60-degree single-v	1.0	2.7	Full	+3.0 to +31.3	468,000
$\overline{BT}$ 1	Type 3	45-degree single-v	4.3	8.0	Full	+2.1 to +31.1	713,900
$\overline{BT}$ 2	Type 3	45-degree single-v	4.3	8.0	Full	+2.0 to +31.0	574,900
BF 1	Type 4	60-degree single-v	4.2	11.0	Full	+2.6 to +29.9	861,600
BF 2	Type 4	60-degree single-v	4.2	11.0	Full	+2.6 to +30.8	746,000

* See Fig. 4.

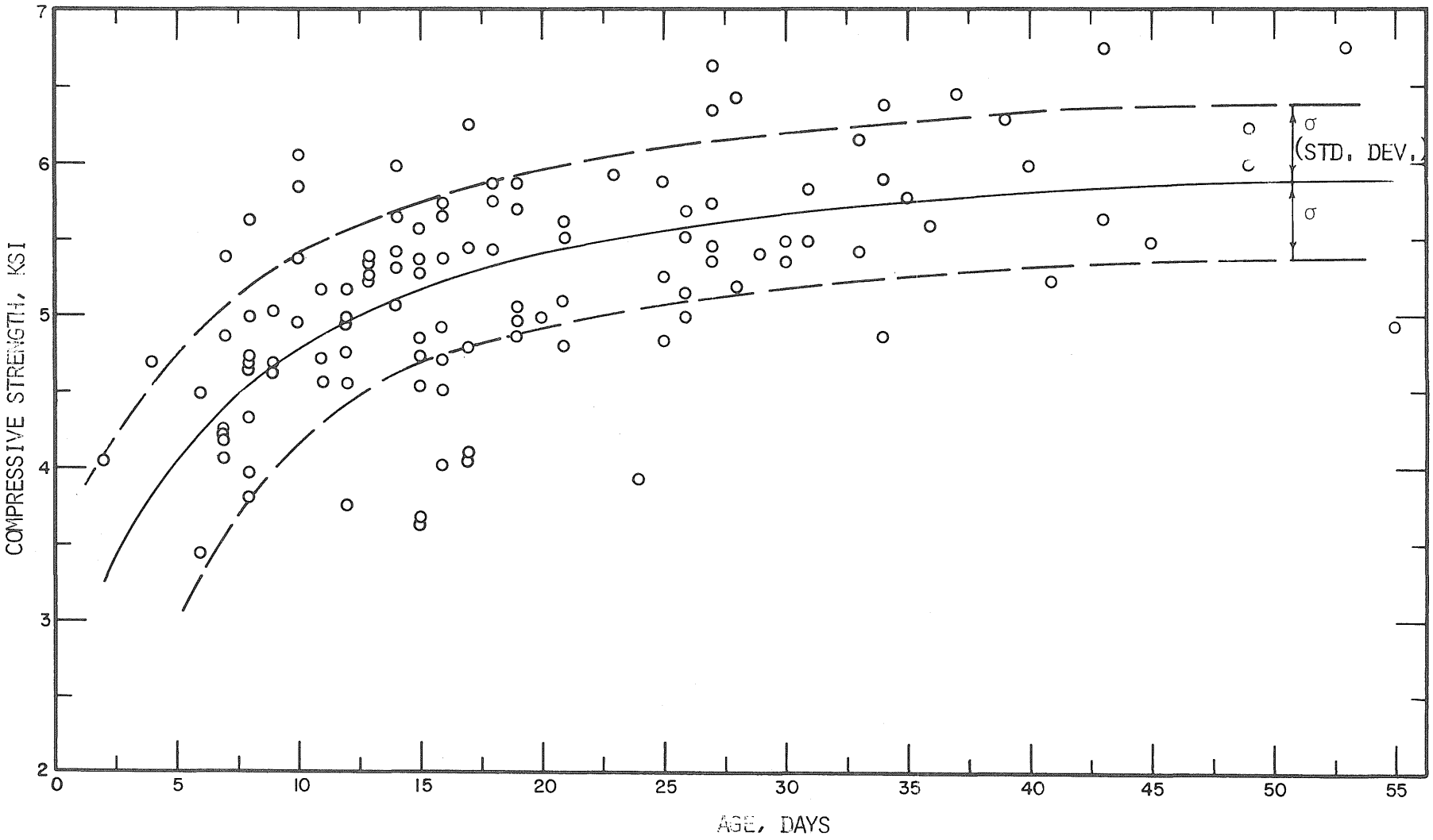

FIG. 1 CONCRETE CYLINDER COMPRESSIVE STRENGTH VS. CURING TIME

FIG. 2 REINFORCING BAR DEFORMATION PATTERNS

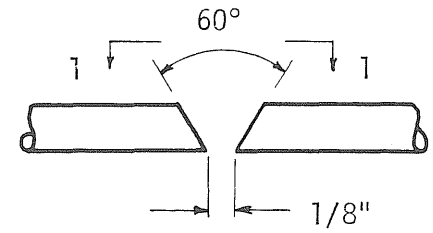

(A) 60° SINGLE-V BUTT JOINT

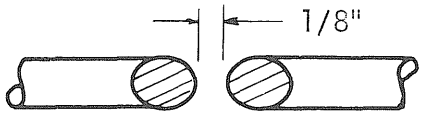

SECTION 1-1

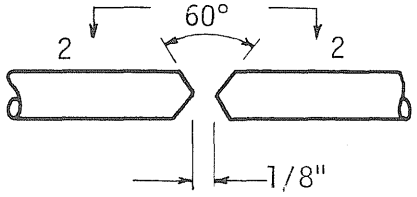

(B) 60° DOUBLE-V BUTT JOINT

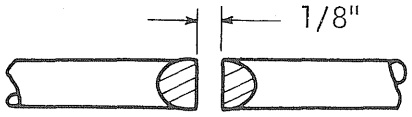

SECTION 2-2

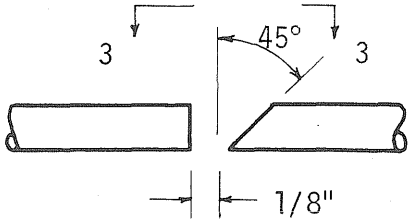

(C) 45° SINGLE-V BUTT JOINT

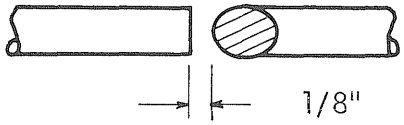

SECTION 3-3

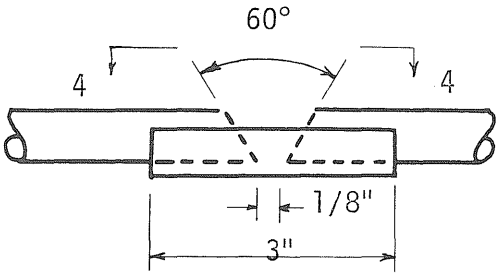

(D) 60° SINGLE-V BUTT JOINT WITH PIPE BACK-UP

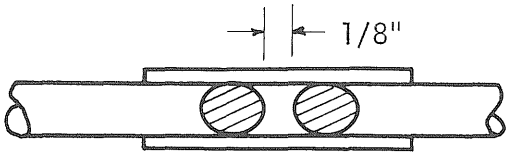

SECTION 4-4

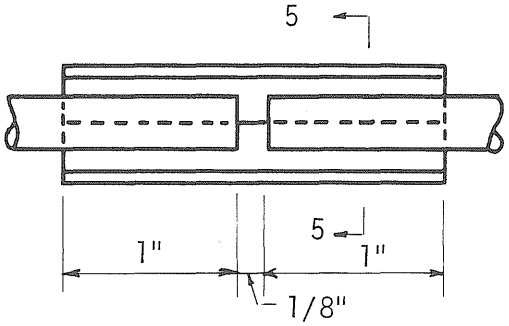

(E) ANGLE SPLICE

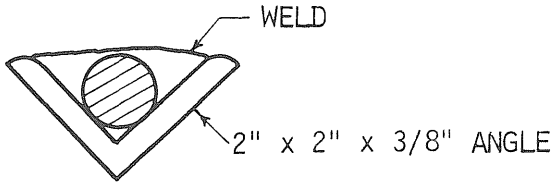

SECTION 5-5

FIG. 3 DETAILS OF JOINT TYPES

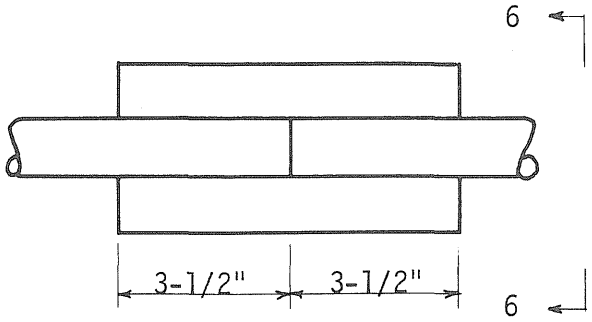

(F) DOUBLE STRAP LAP JOINT

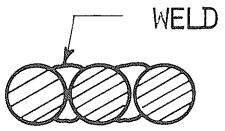

SECTION 6-6

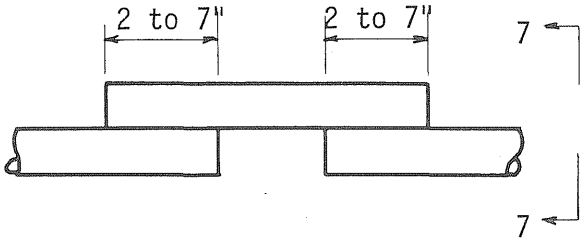

(G) SINGLE STRAP LAP JOINT

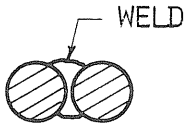

SECTION 7-7

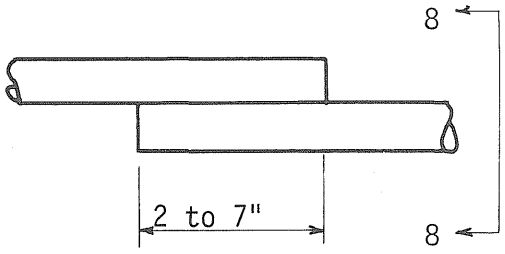

(H) SINGLE LAP JOINT

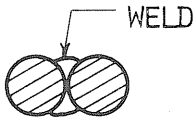

SECTION 8-8

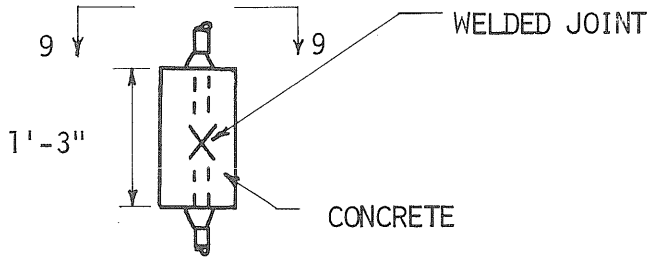

(I) REINFORCING BARS ENCASED IN CONCRETE

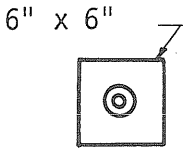

SECTION 9-9

FIG. 3 DETAILS OF JOINT TYPES (CONTINUED)

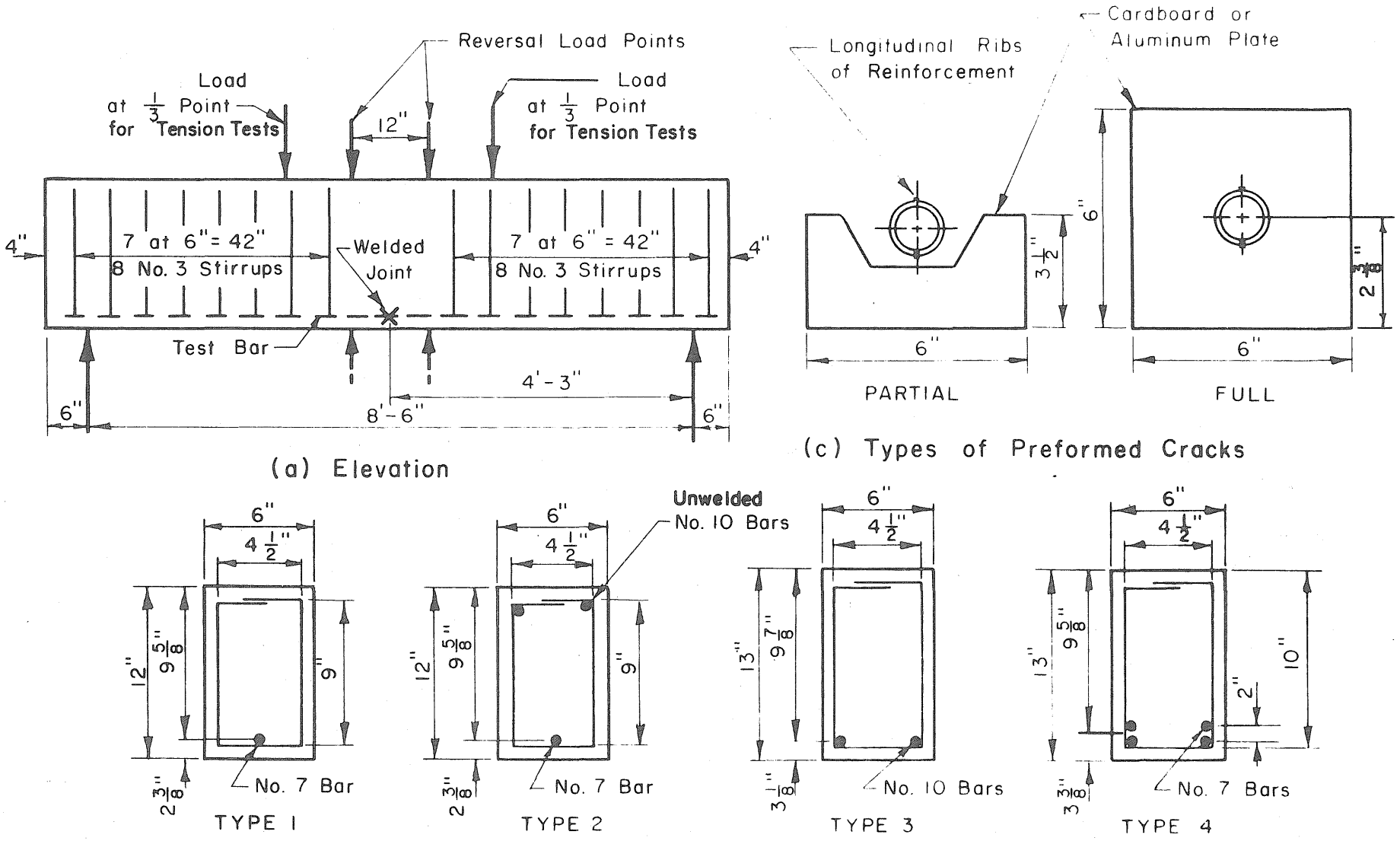

FIG. 4 DETAILS OF REINFORCED CONCRETE BEAMS

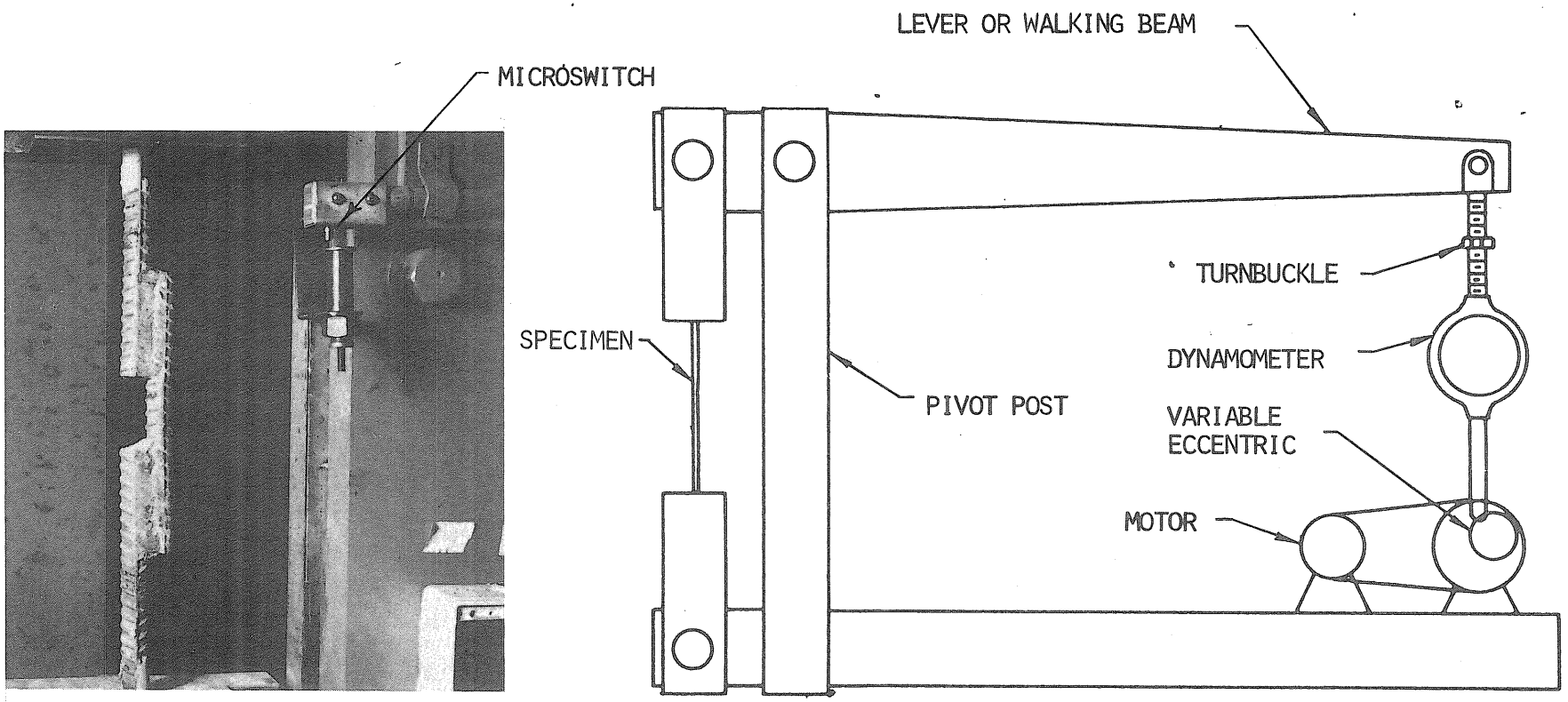

FIG. 5 50,000 LB. UNIVERSITY OF ILLINOIS' FATIGUE MACHINE

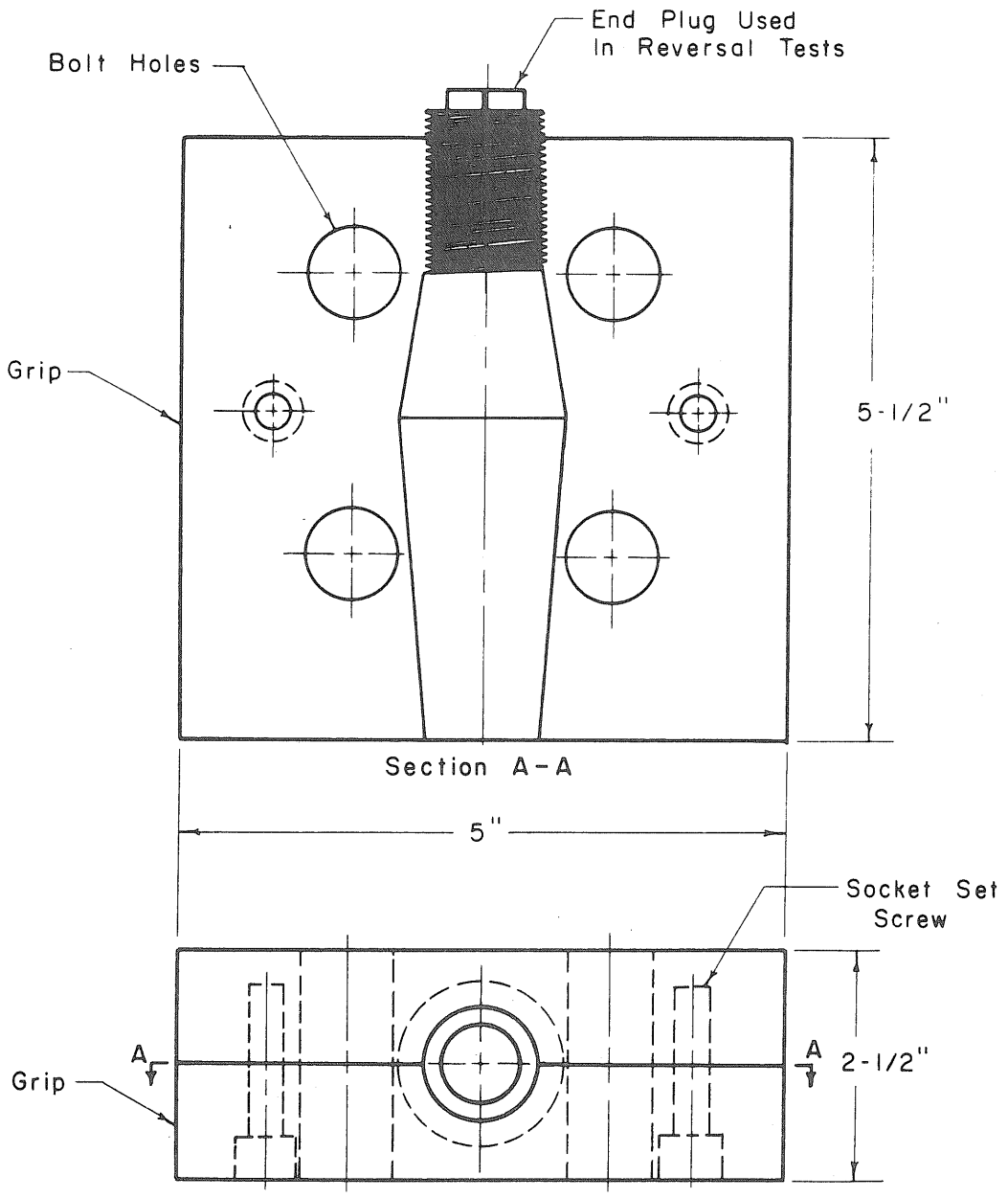

FIG. 6 SPECIAL GRIP DEVICE USED IN 50,000 POUND FATIGUE MACHINE

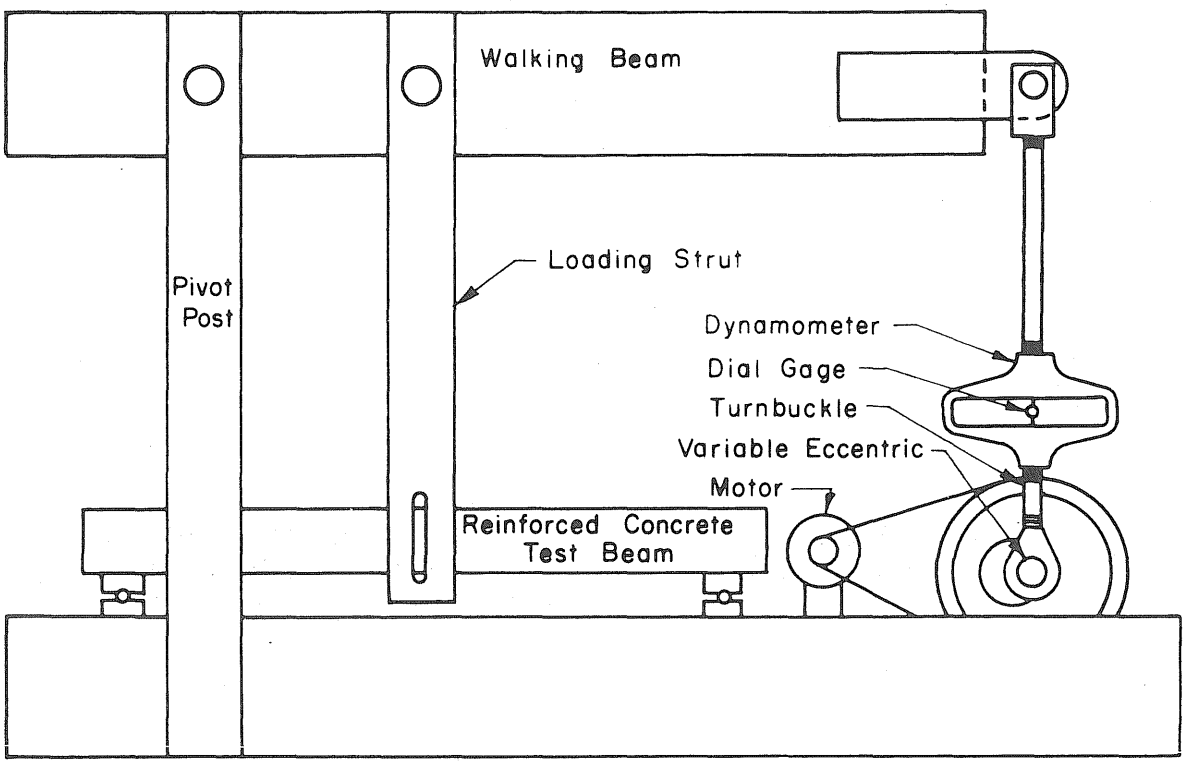

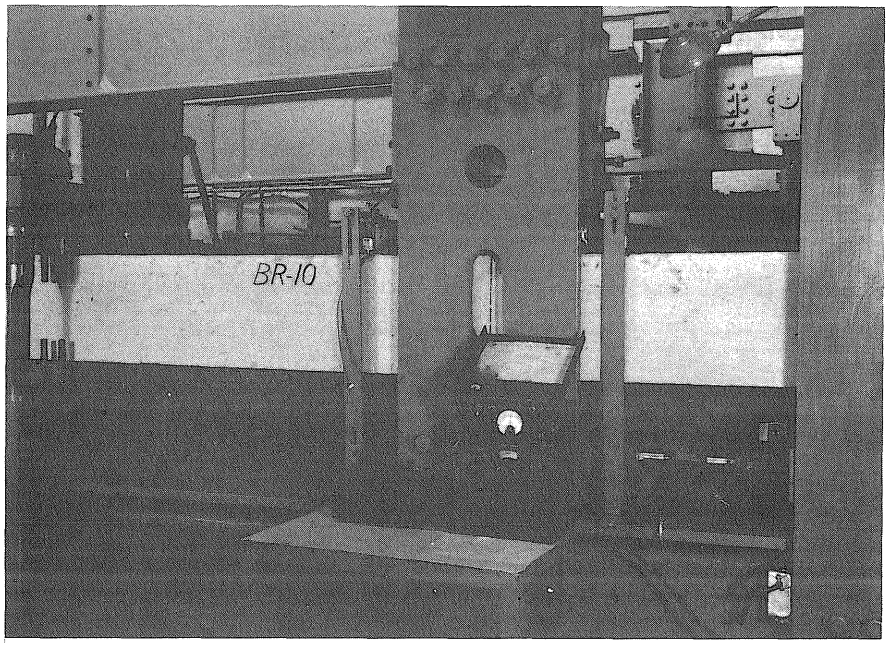

FIG. 7 200,000 LB. UNIVERSITY OF ILLINOIS' FATIGUE MACHINE

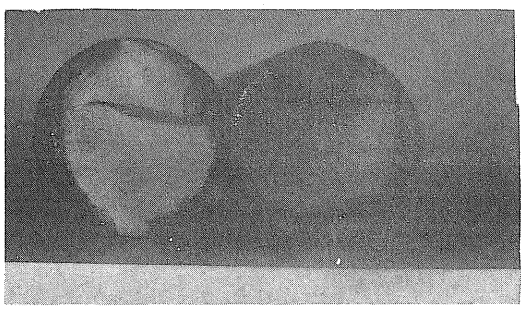

A. UNWELDED BAR
(SPEC. WDO-1)

B. 60° SINGLE-V
BUTT JOINT
(SPEC. W3)

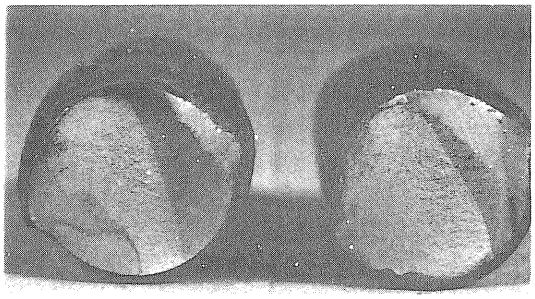

C. 60° DOUBLE-V
BUTT JOINT
(SPEC. W26)

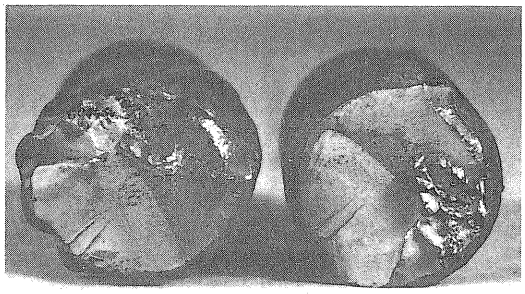

D. 45° SINGLE-V
BUTT JOINT
(SPEC. W23)

FIG. 8 TYPICAL FATIGUE FAILURES

E. 60° SINGLE-V BUTT WELDED JOINT
WITH PIPE BACK-UP (SPEC WP2)

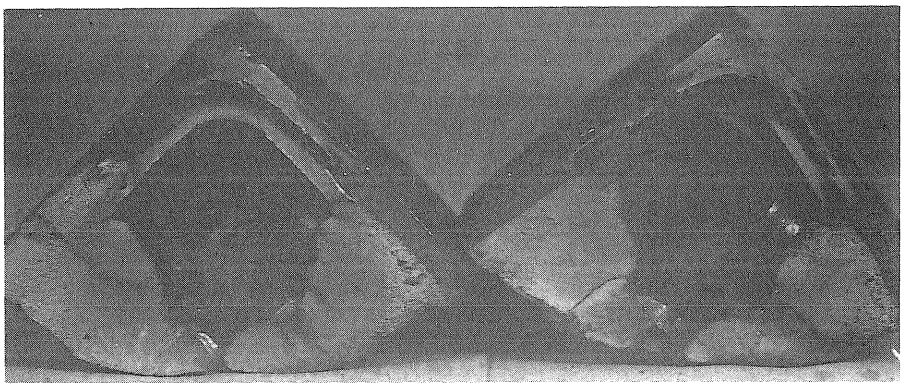

F. ANGLE SPLICE JOINT
(SPEC W28)

FIG. 8 TYPICAL FATIGUE FAILURES (CONTINUED)

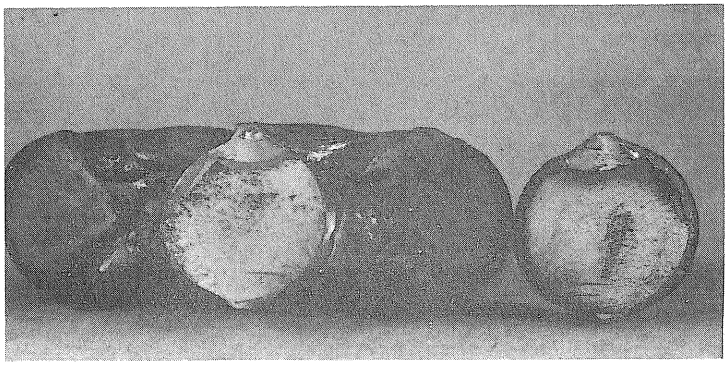

G. DOUBLE STRAP LAP JOINT
(SPEC WL1)

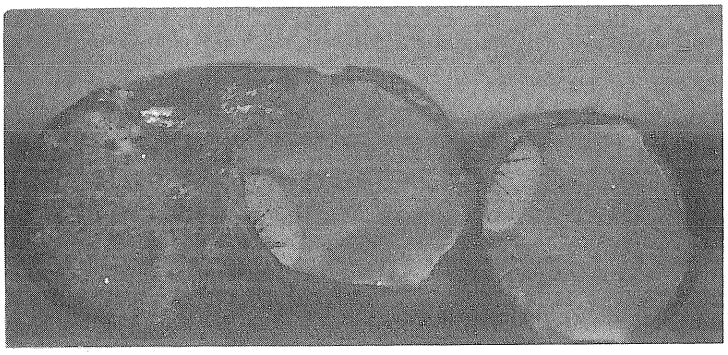

H. SINGLE STRAP LAP JOINT
(SPEC W33)

FIG. 8 TYPICAL FATIGUE FAILURES (CONTINUED)

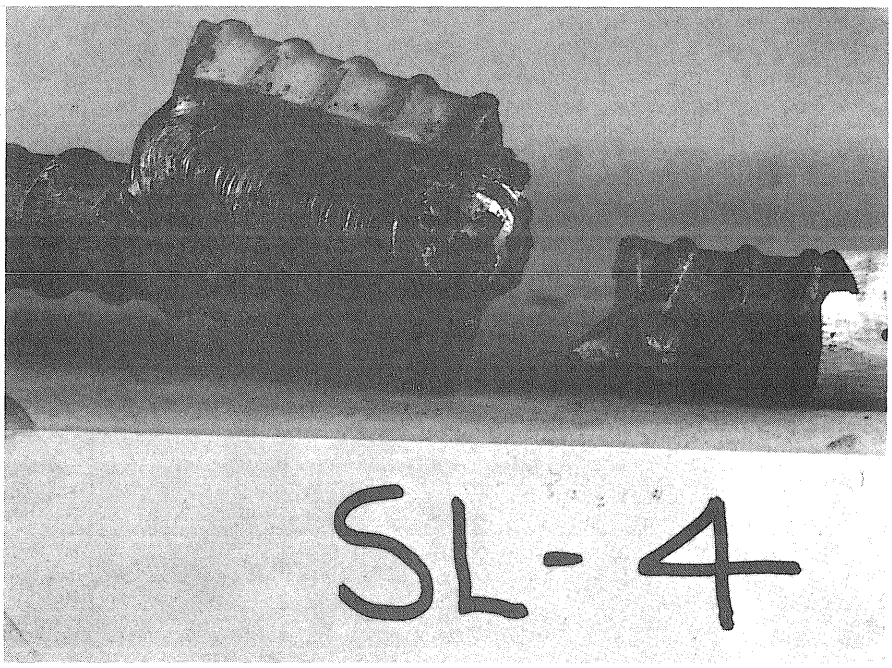

FIG. 9 EXAMPLE OF FAILURE AND SEVERE BENDING AT ENDS OF SINGLE LAP-WELDED JOINTS

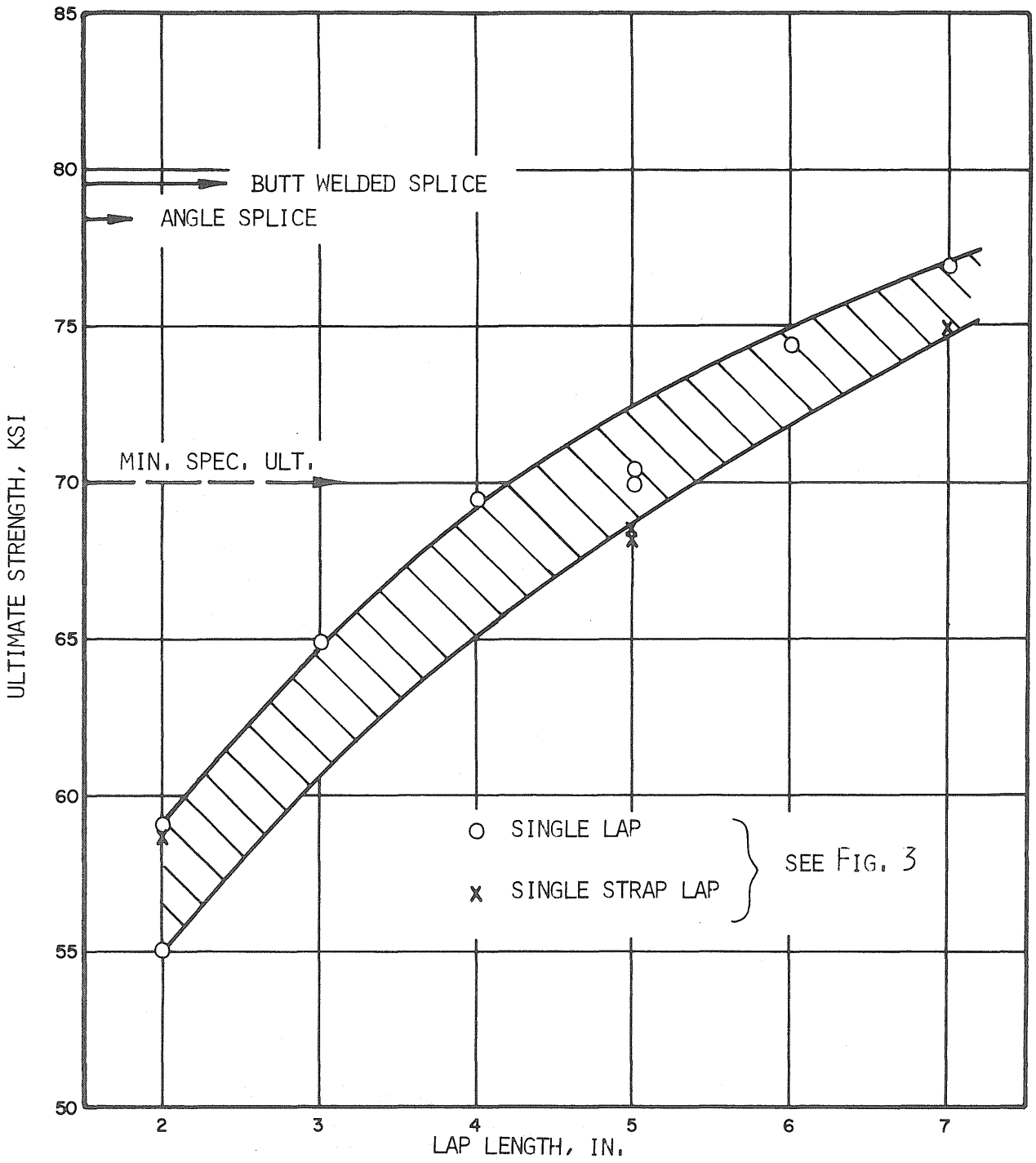

FIG. 10 EFFECT OF LAP LENGTH ON JOINT STRENGTH

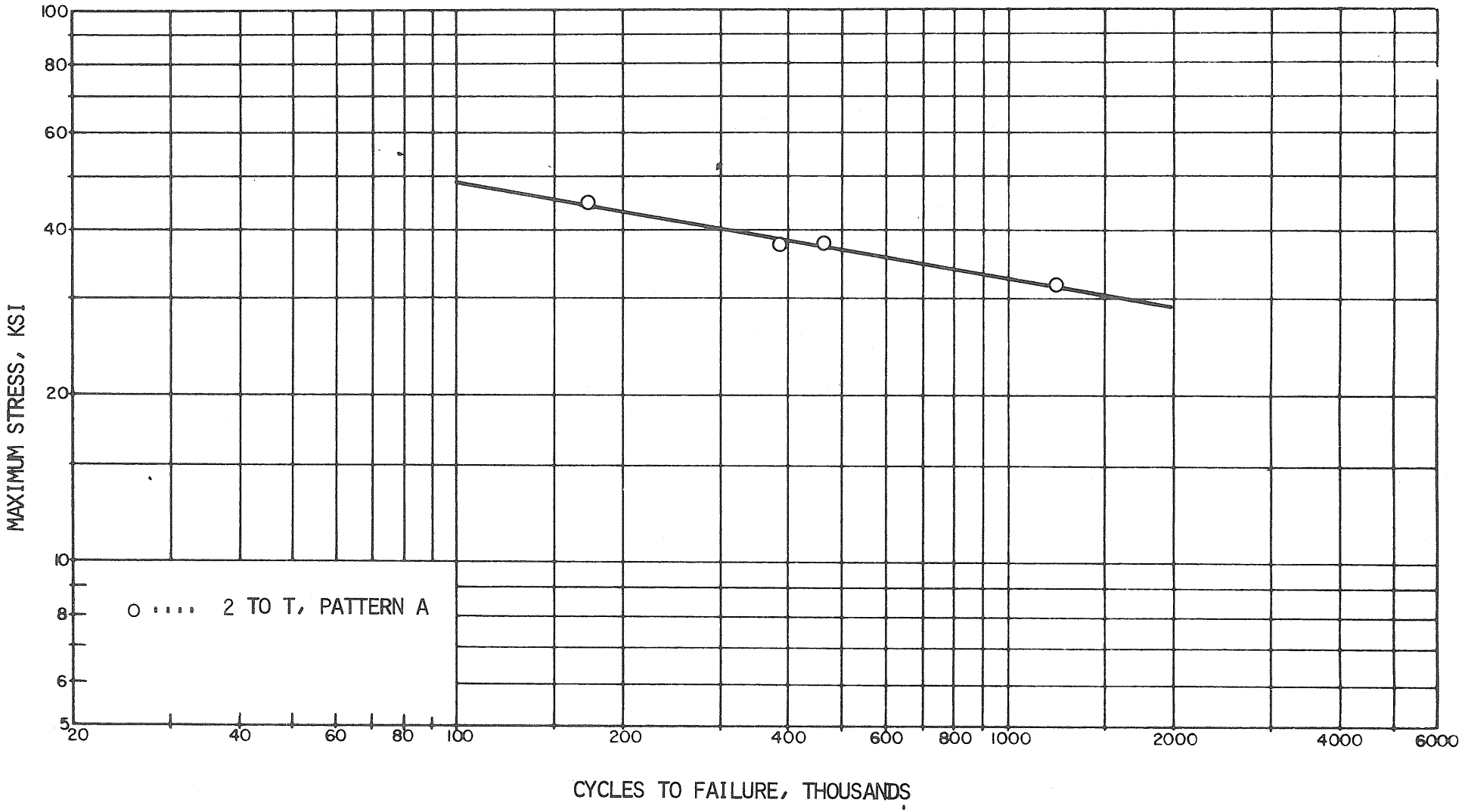

FIG. 11 S-N CURVE, AXIALLY LOADED INTERMEDIATE GRADE UNWELDED REINFORCING BARS, PATTERN A

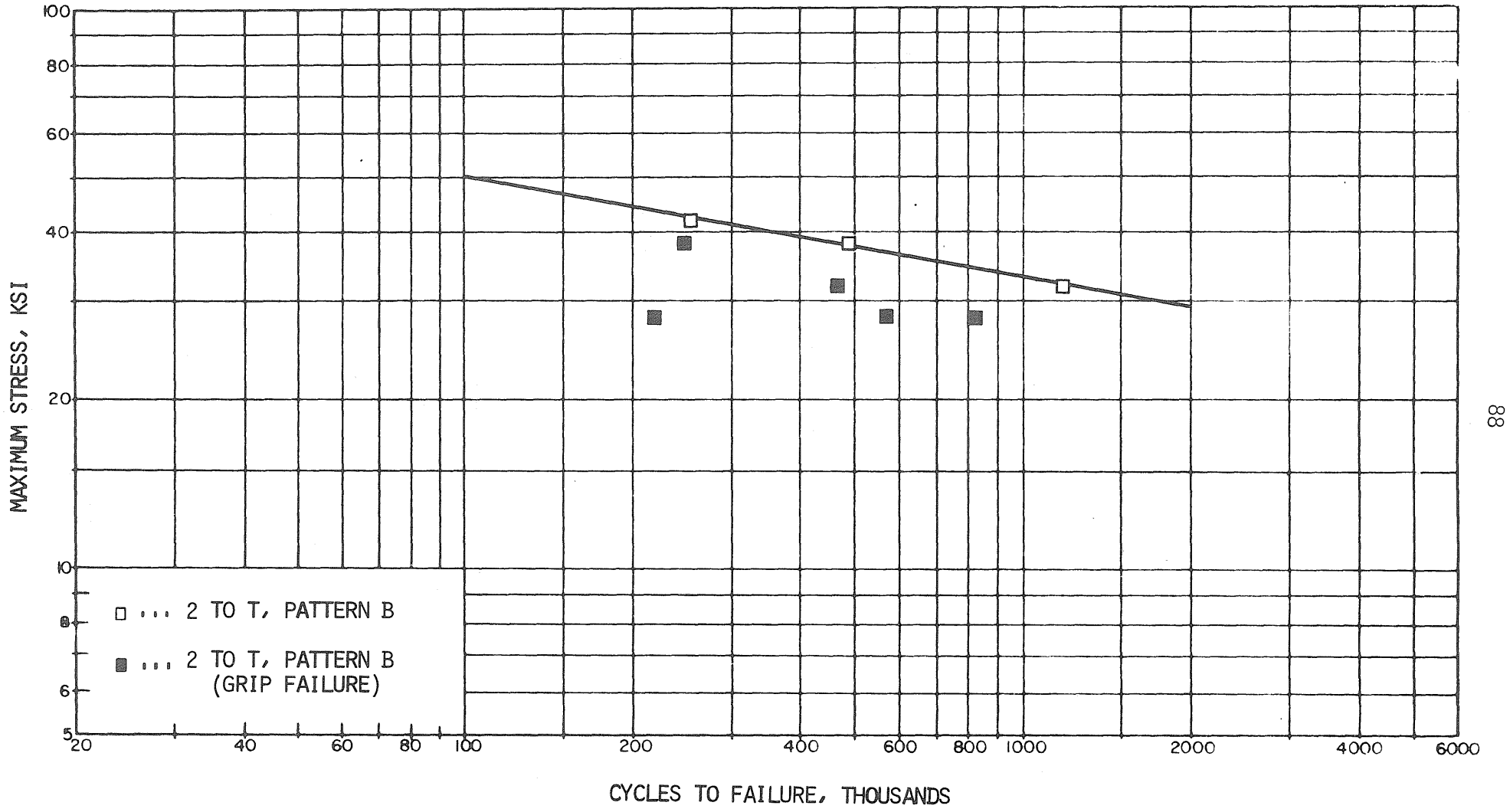

FIG. 12 S-N CURVE, AXIALLY LOADED INTERMEDIATE GRADE UNWELDED REINFORCING BARS, PATTERN B

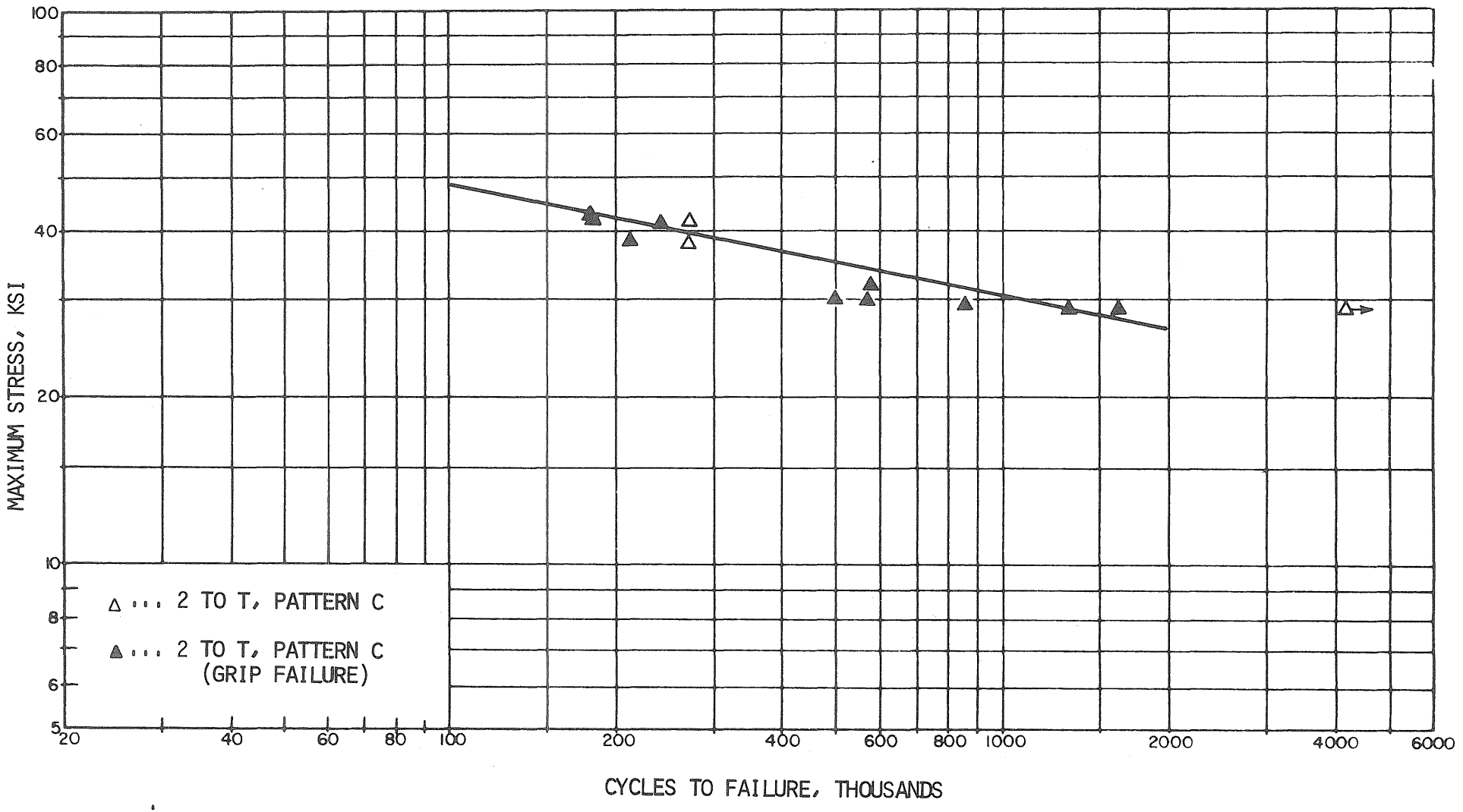

FIG. 13 S-N CURVE, AXIALLY LOADED INTERMEDIATE GRADE UNWELDED REINFORCING BARS, PATTERN C

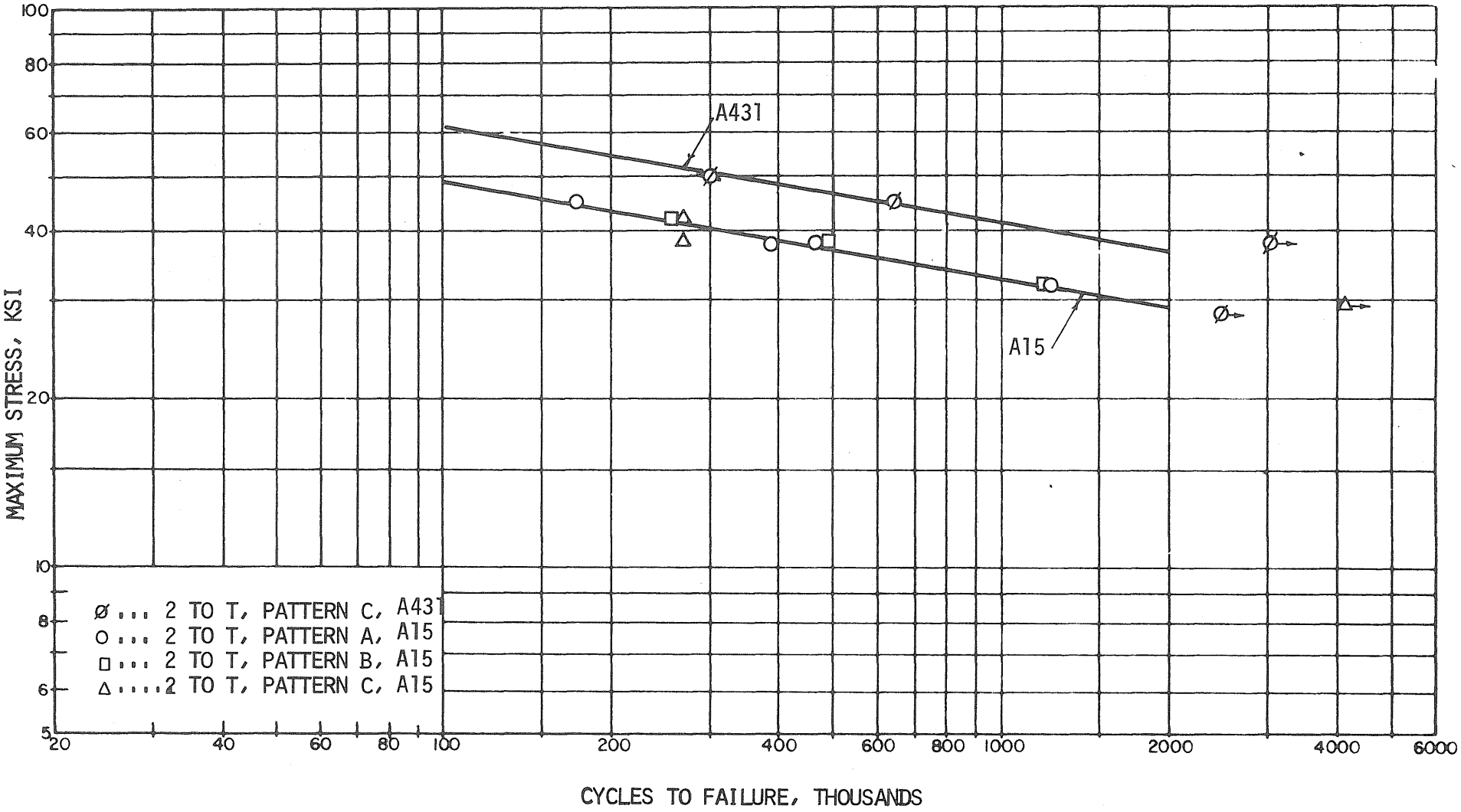

FIG. 14 S-N CURVES, AXIALLY LOADED INTERMEDIATE GRADE AND HIGH STRENGTH UNWELDED REINFORCING BARS

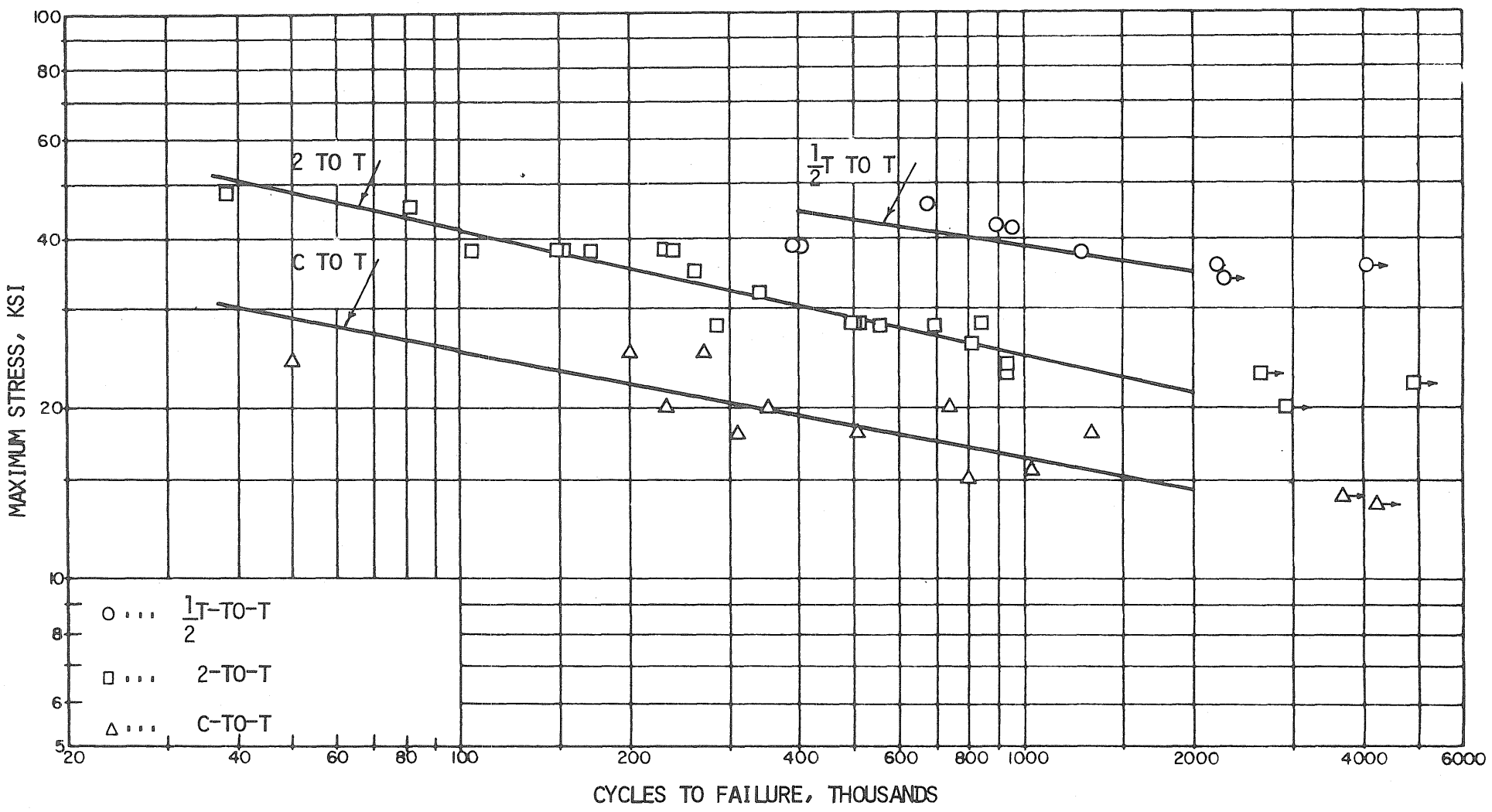

FIG. 15 S-N CURVES, AXIALLY LOADED INTERMEDIATE GRADE 60-DEGREE SINGLE-V BUTT-WELDED REINFORCING BARS

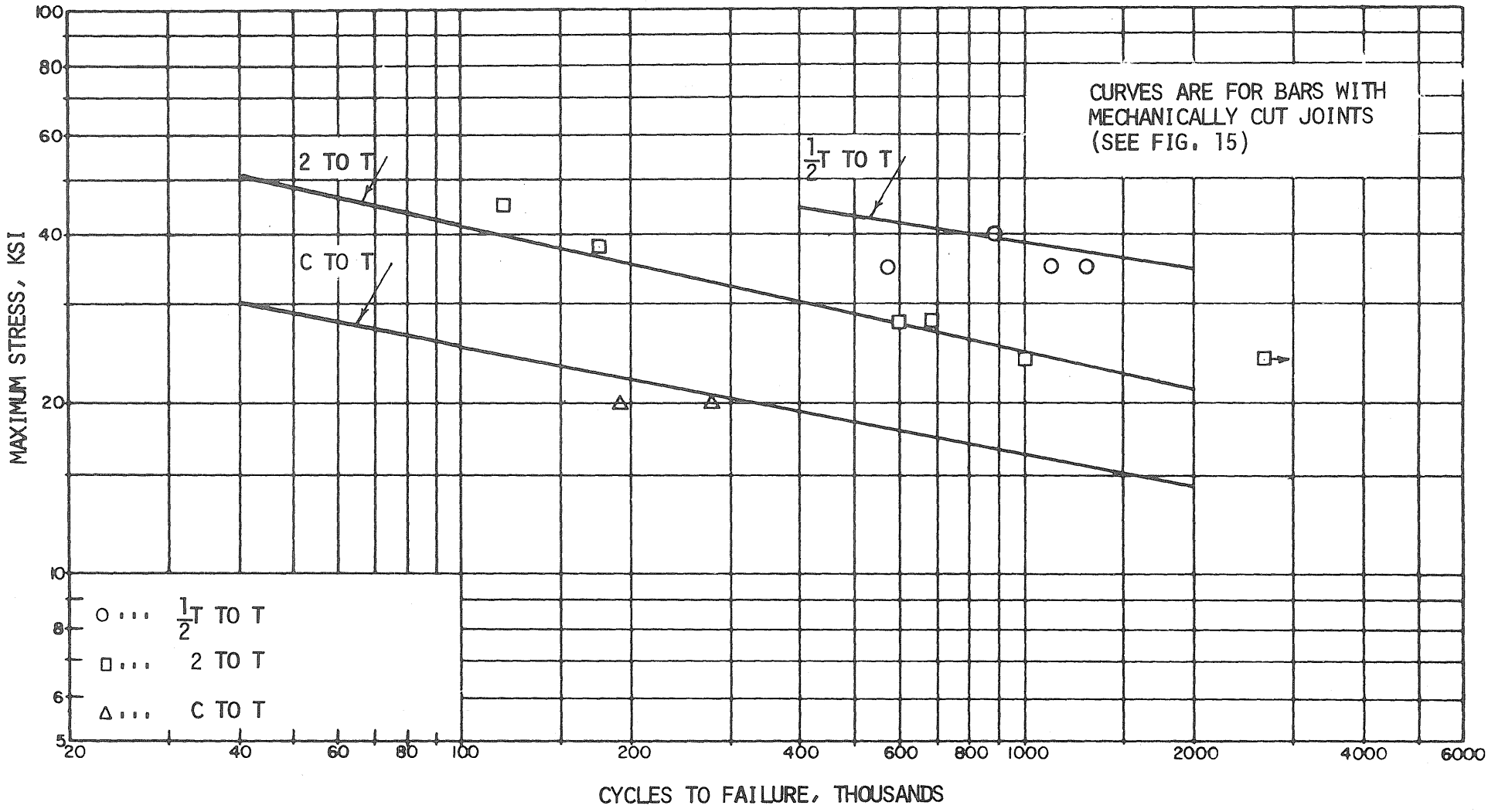

FIG. 16 FATIGUE TEST RESULTS FOR AXIALLY LOADED INTERMEDIATE GRADE 60-DEGREE SINGLE-V BUTT-WELDED REINFORCING BARS WITH FLAME CUT JOINT PREPARATION

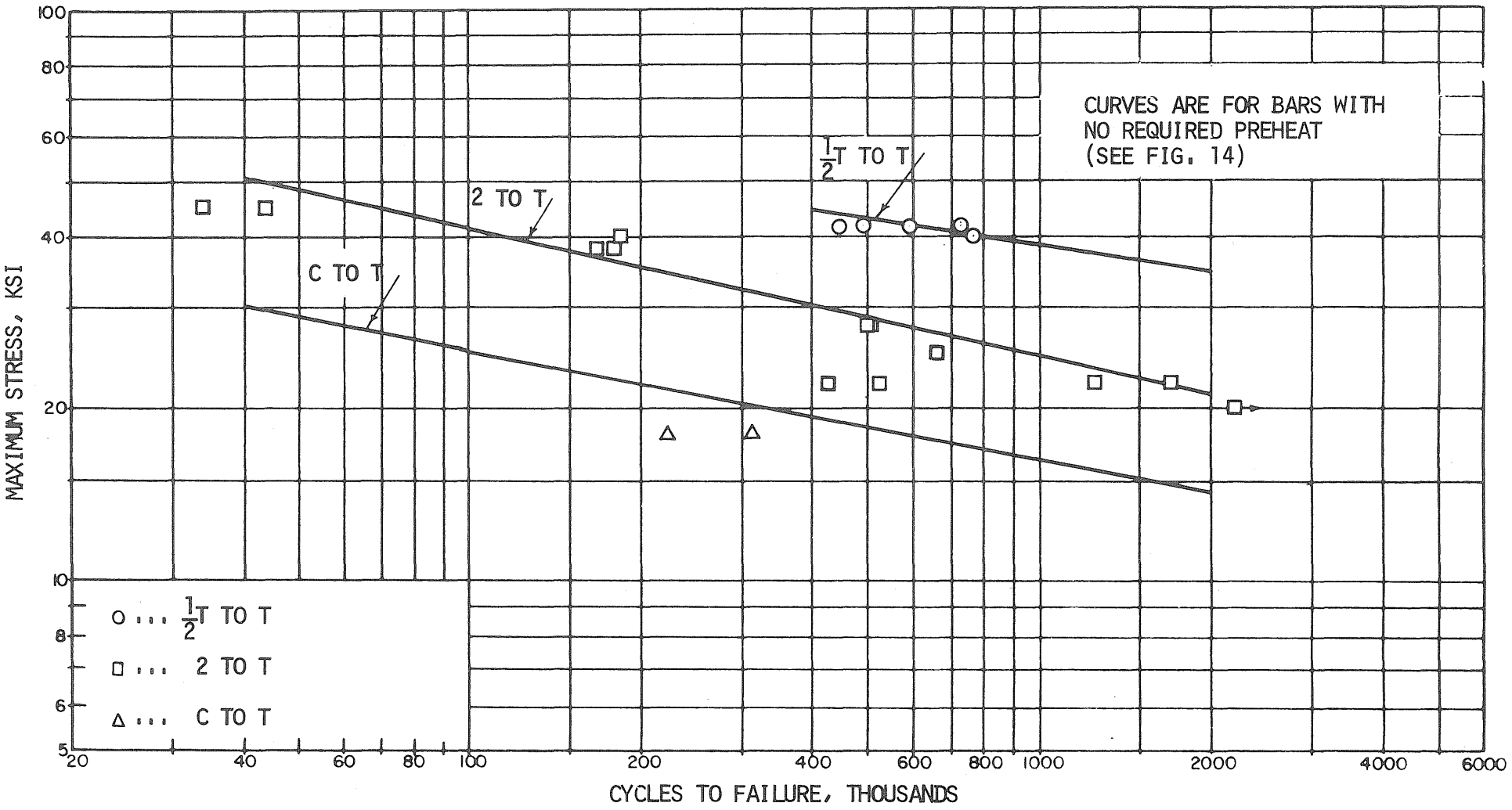

FIG. 17 FATIGUE TEST RESULTS FOR AXIALLY LOADED INTERMEDIATE GRADE 60-DEGREE SINGLE-V BUTT-WELDED REINFORCING BARS WITH 400°F PREHEAT

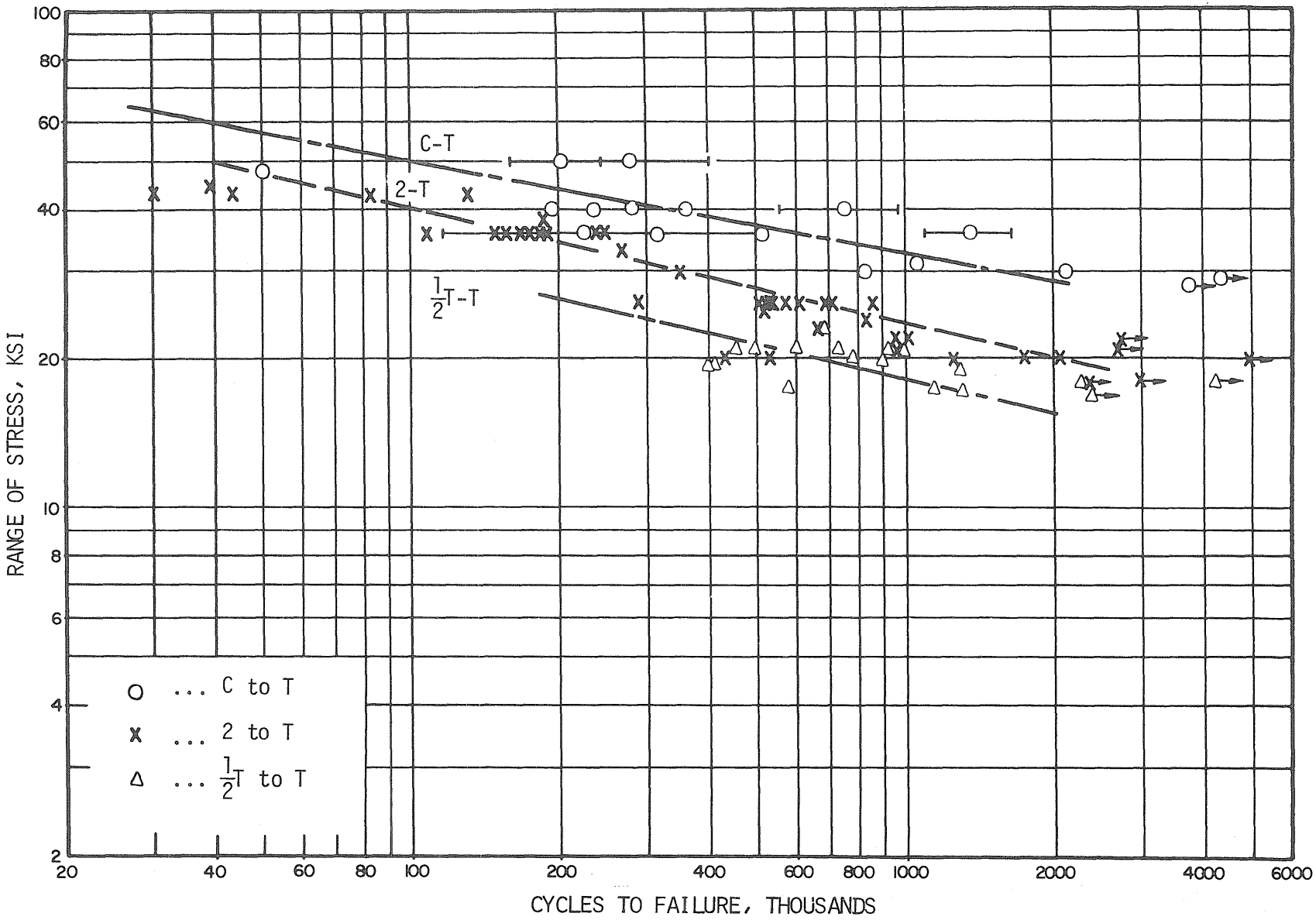

FIG. 18 S-N CURVES FOR AXIALLY LOADED INTERMEDIATE GRADE 60-DEGREE SINGLE-V BUTT WELDED REINFORCING BARS (RANGE OF STRESS)

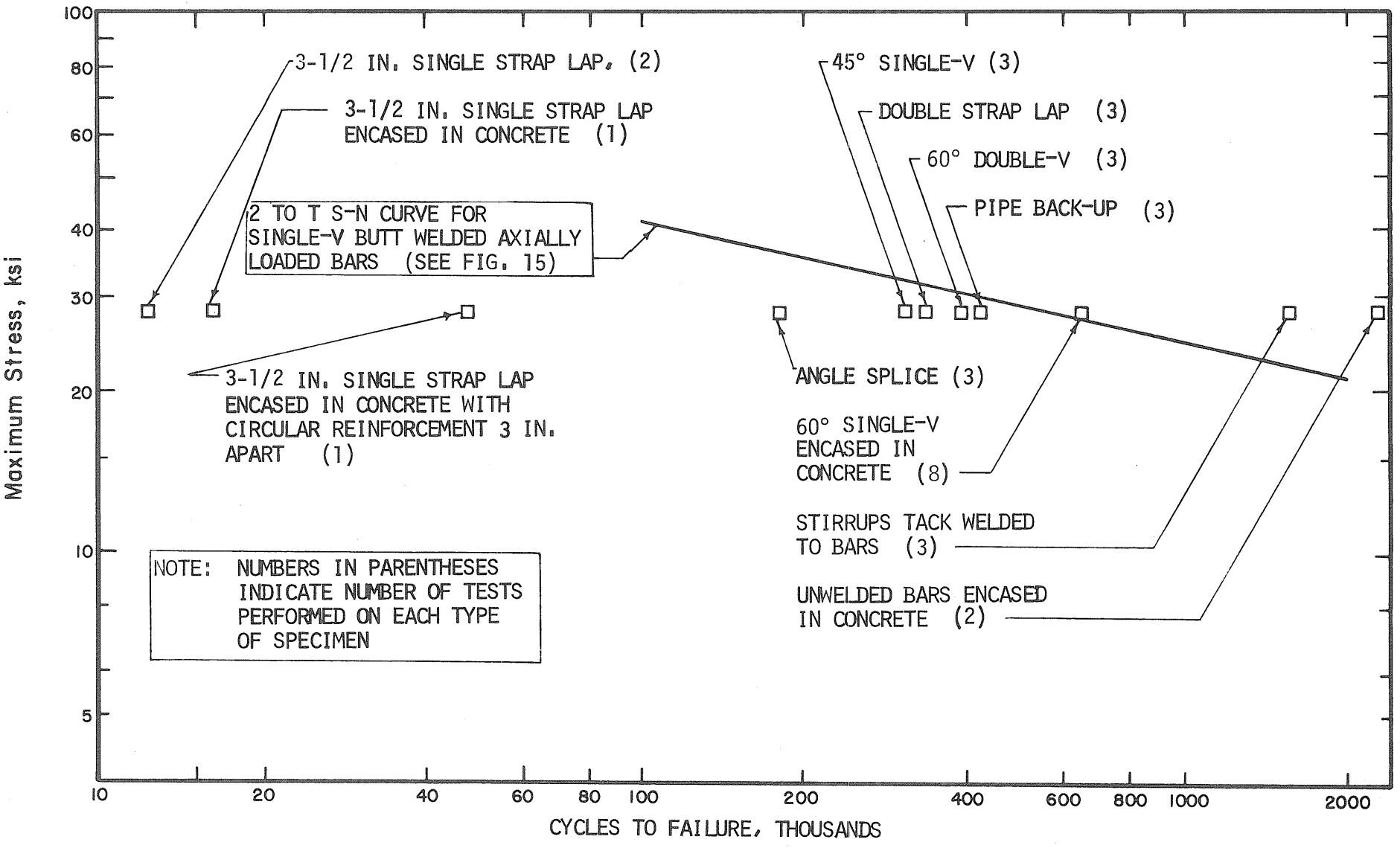

FIG. 19 RESULTS OF 2-28 KSI FATIGUE TESTS CONDUCTED ON AXIALLY LOADED WELDED REINFORCING BARS

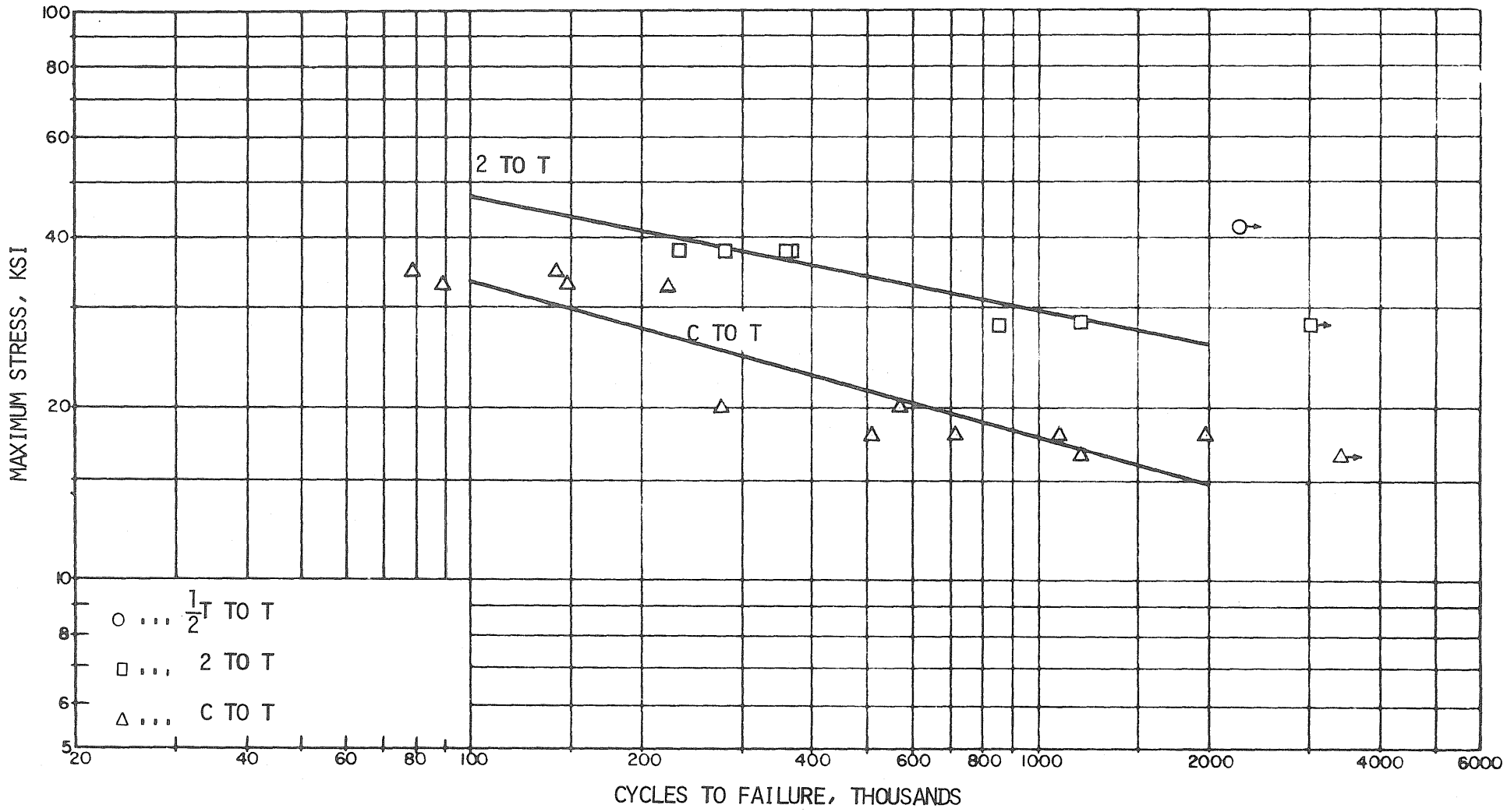

FIG. 20 S-N CURVES, AXIALLY LOADED HIGH STRENGTH 60-DEGREE SINGLE-V BUTT-WELDED REINFORCING BARS (ASTM-A431)

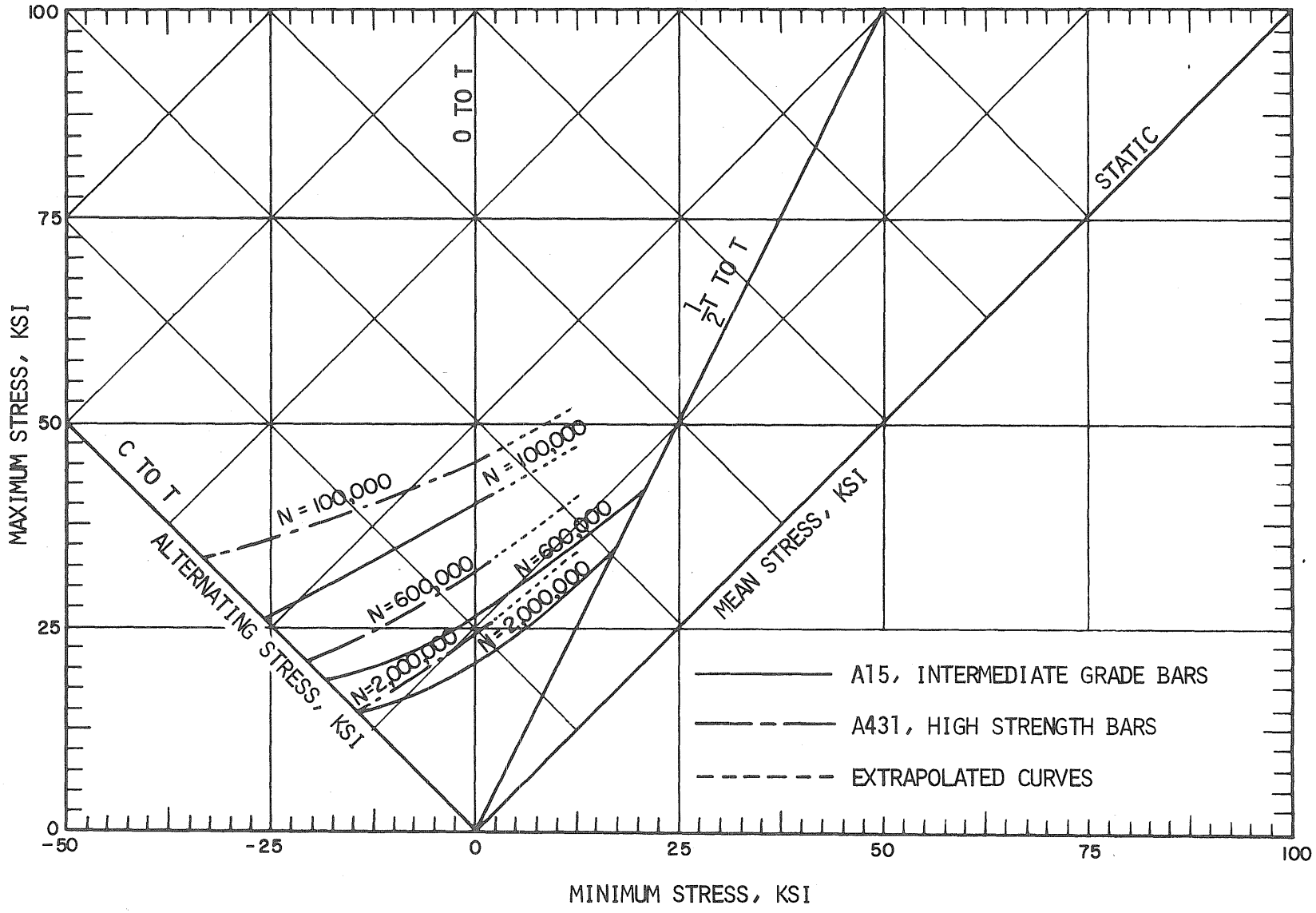

FIG. 21 MODIFIED GOODMAN DIAGRAM, AXIALLY LOADED 60-DEGREE SINGLE-V BUTT-WELDED REINFORCING BARS

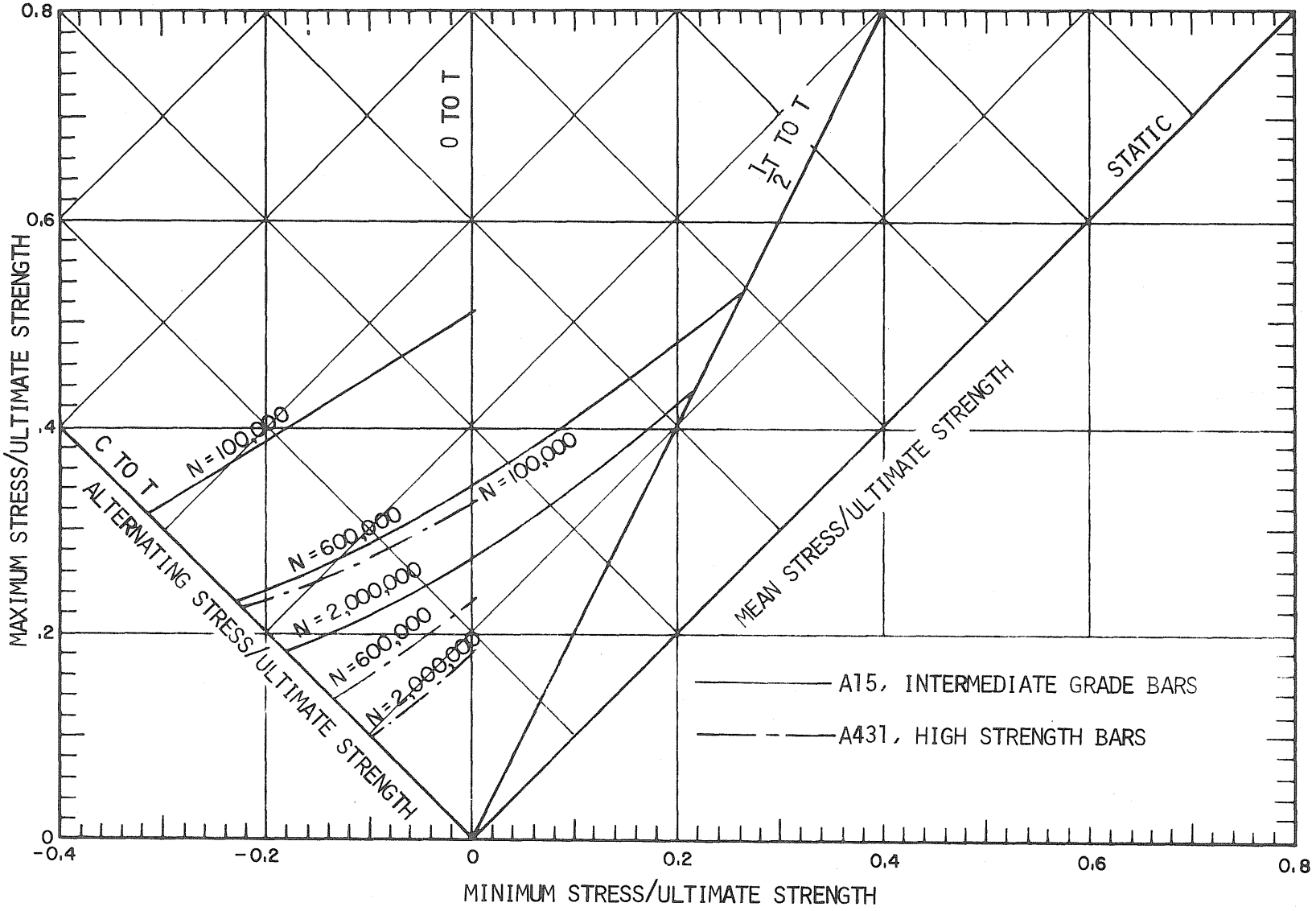

FIG. 22 NON-DIMENSIONALIZED MODIFIED GOODMAN DIAGRAM, 60-DEGREE SINGLE-V BUTT-WELDED REINFORCING BARS

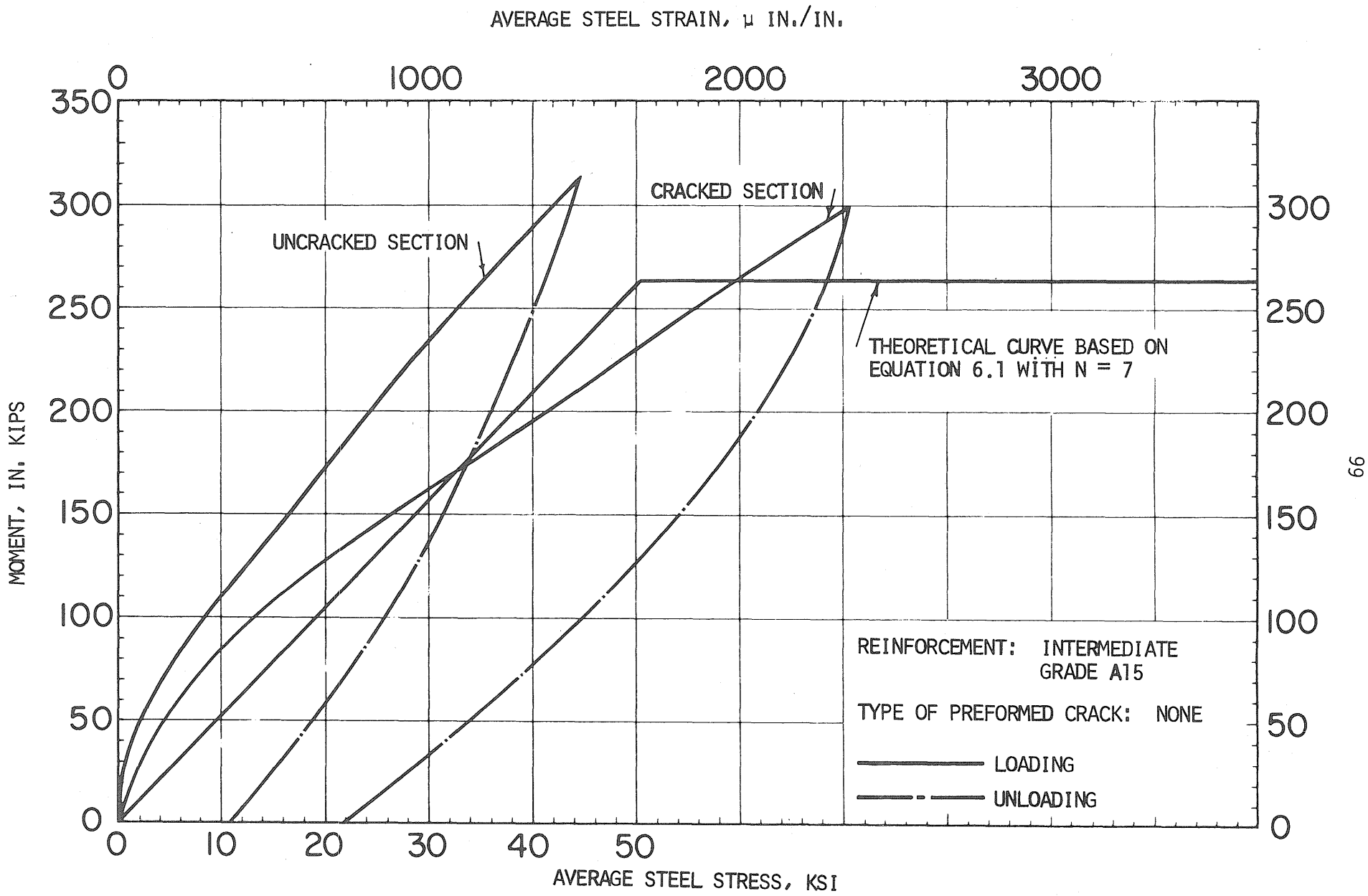

FIG. 23 MOMENT VS. AVERAGE MEASURED STEEL STRESS OR STRAIN

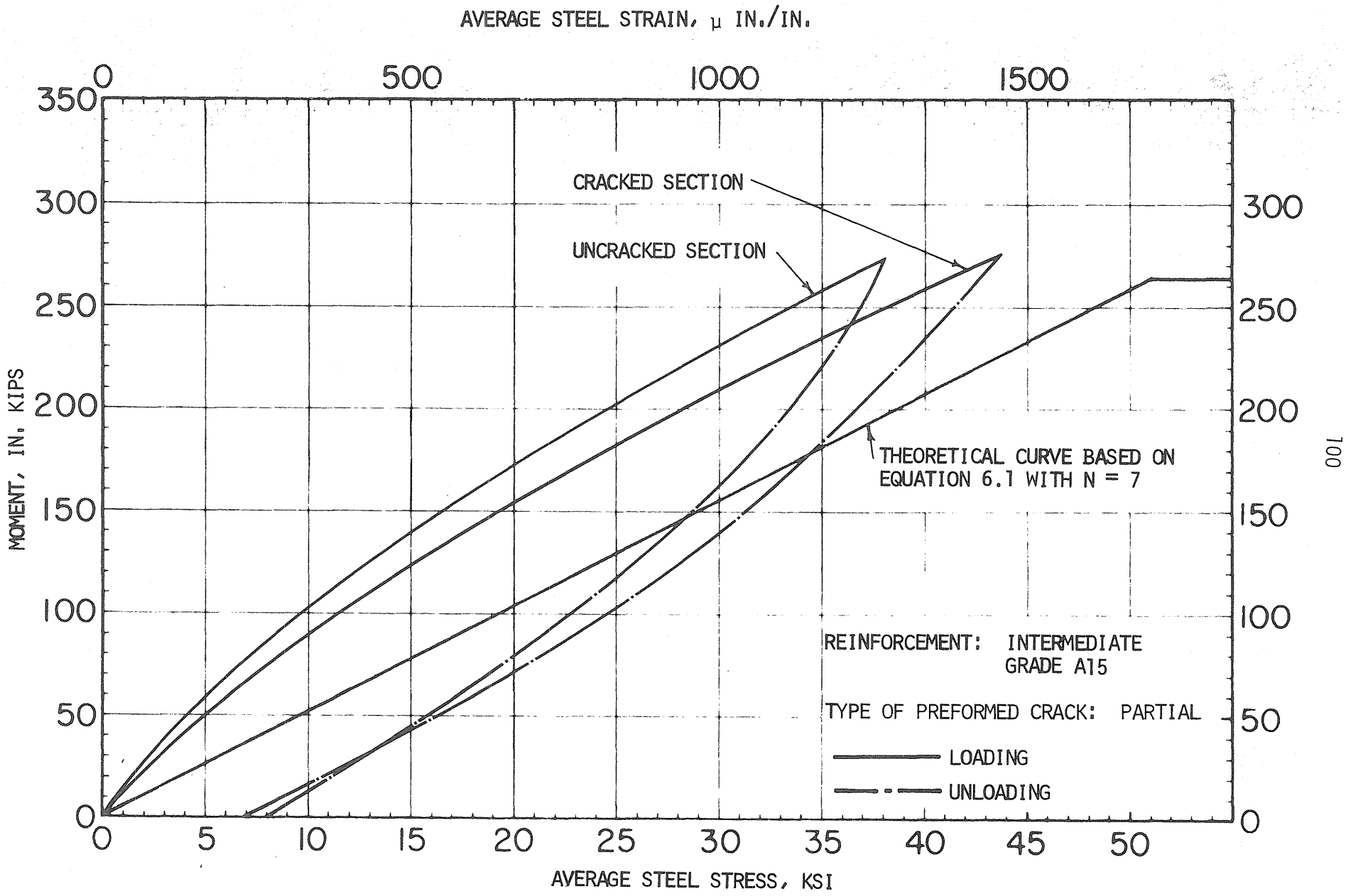

FIG. 24 MOMENT VS. AVERAGE MEASURED STEEL STRESS OR STRAIN

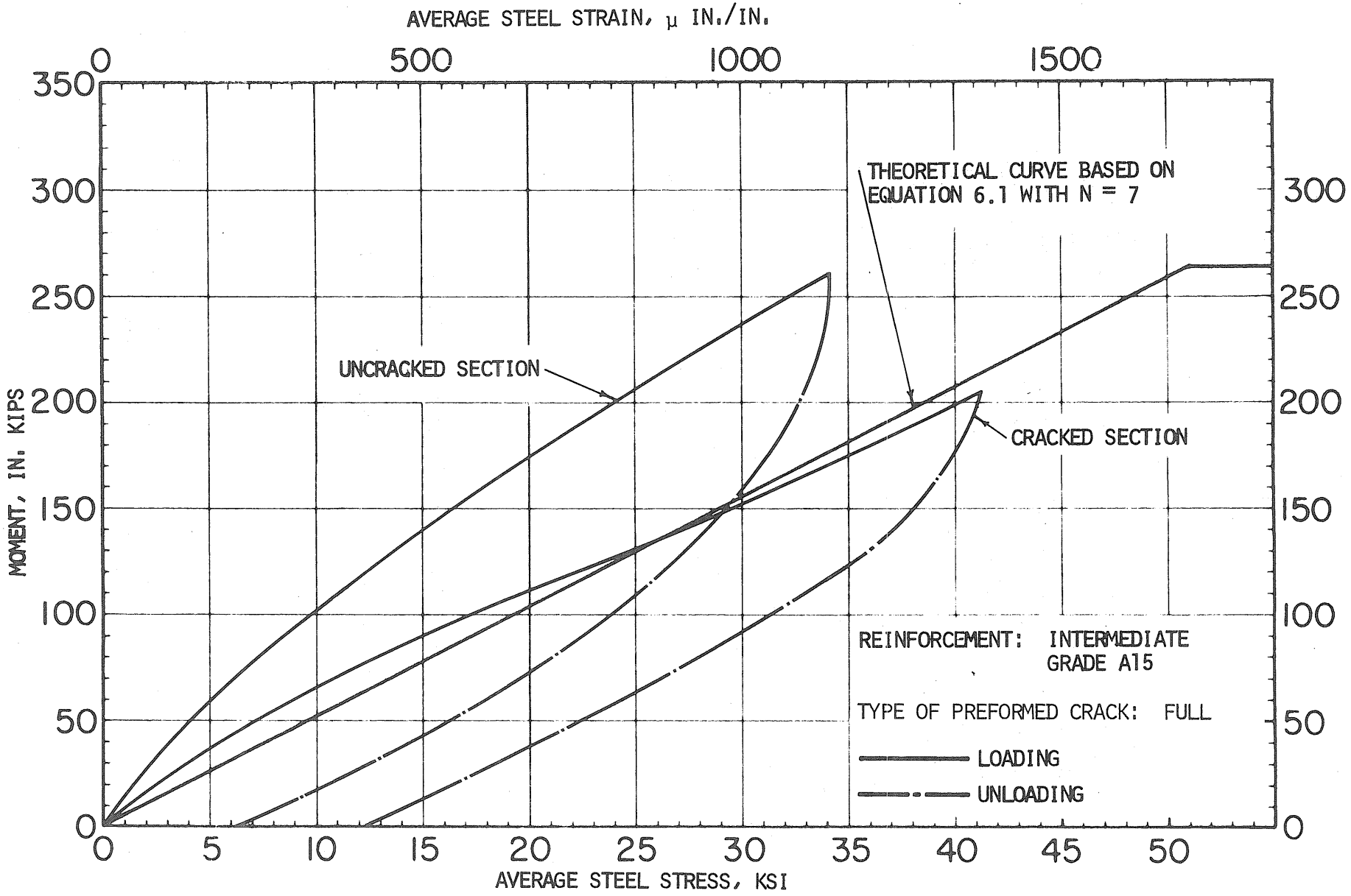

FIG. 25 MOMENT VS. AVERAGE MEASURED STEEL STRESS OR STRAIN

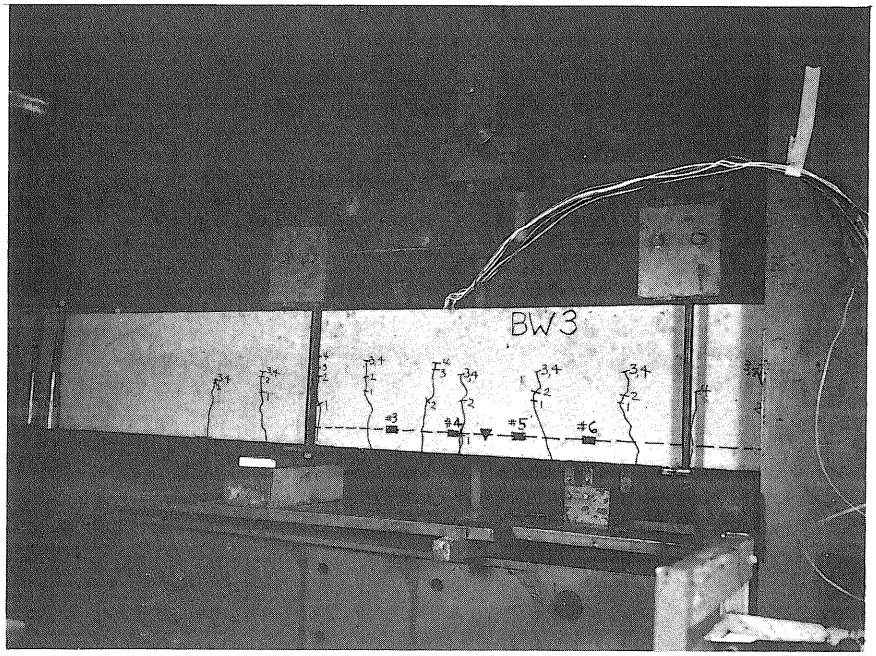

GAGES CONSIDERED TO BE AT CRACKED SECTIONS: #4

GAGES CONSIDERED TO BE AT UNCRACKED SECTIONS:
#3, #5, AND #6

FIG. 26 LOCATION OF STRAIN GAGES WITH RESPECT TO SURFACE CRACKS

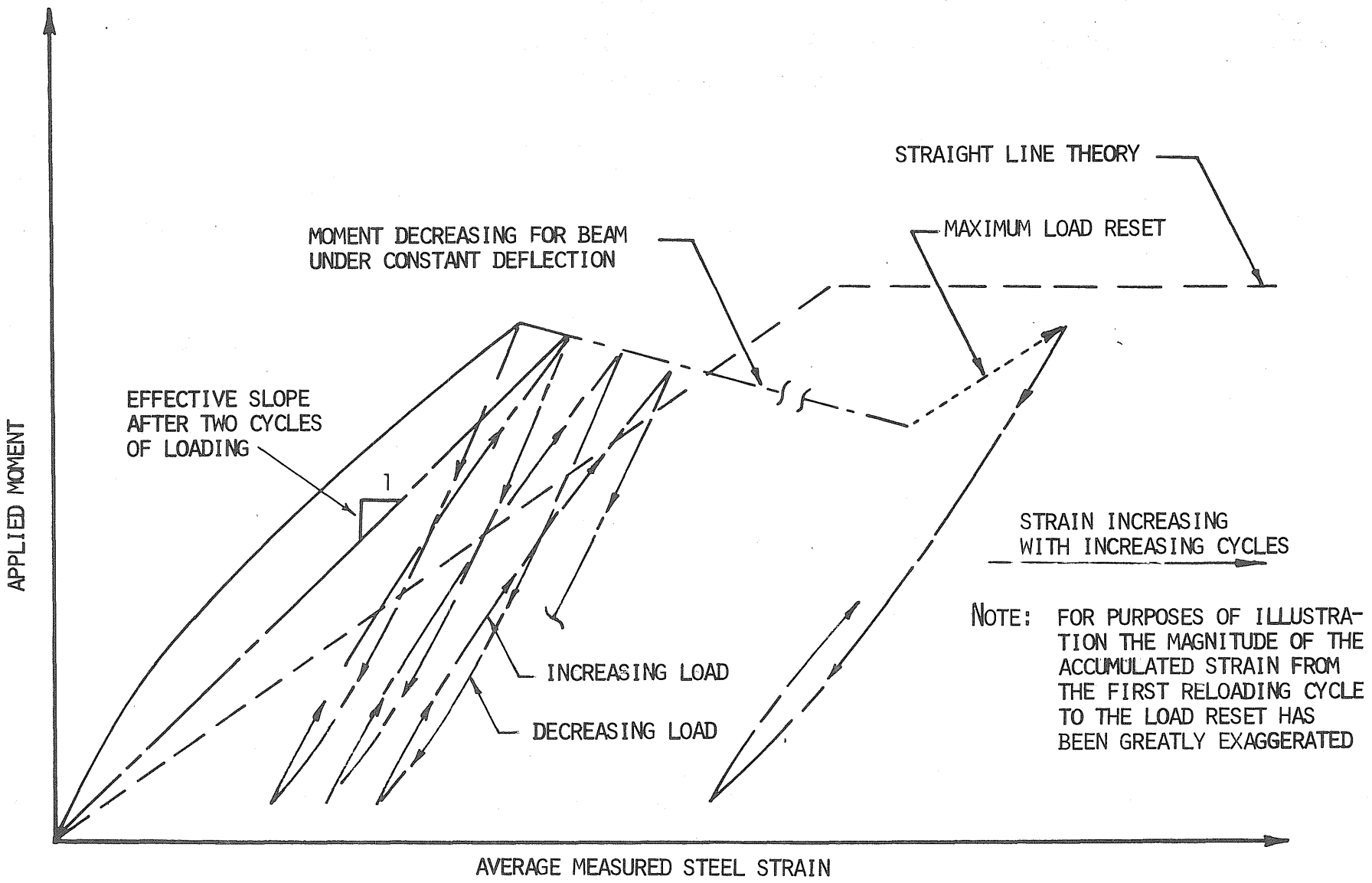

FIG. 27 SCHEMATIC REPRESENTATION OF THE AVERAGE STRAIN IN THE BEAM REINFORCEMENT AS AFFECTED BY REPEATED LOADING

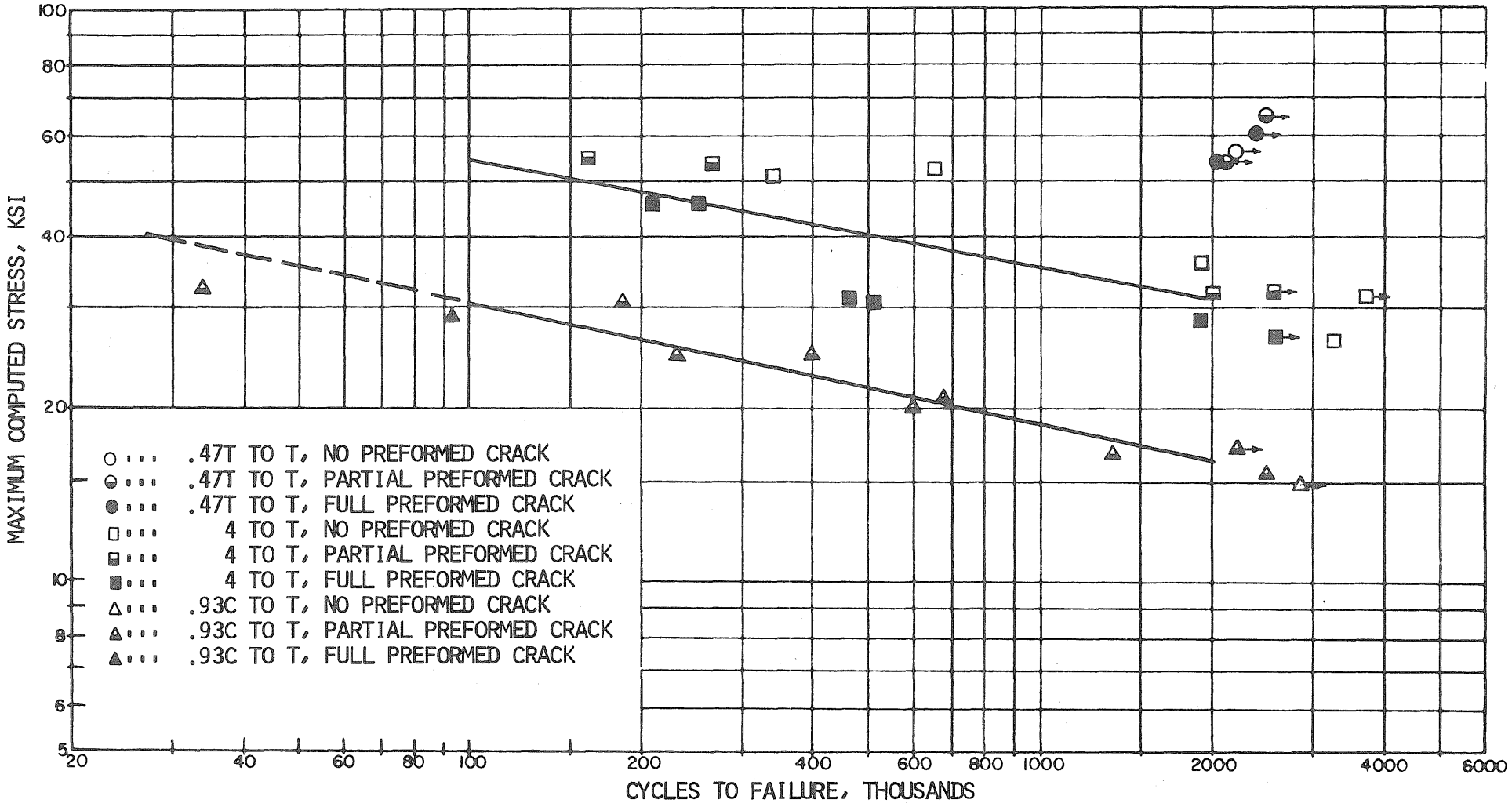

FIG. 28 S-N CURVES, CONCRETE BEAMS WITH INTERMEDIATE GRADE 60-DEGREE SINGLE-V BUTT-WELDED REINFORCEMENT

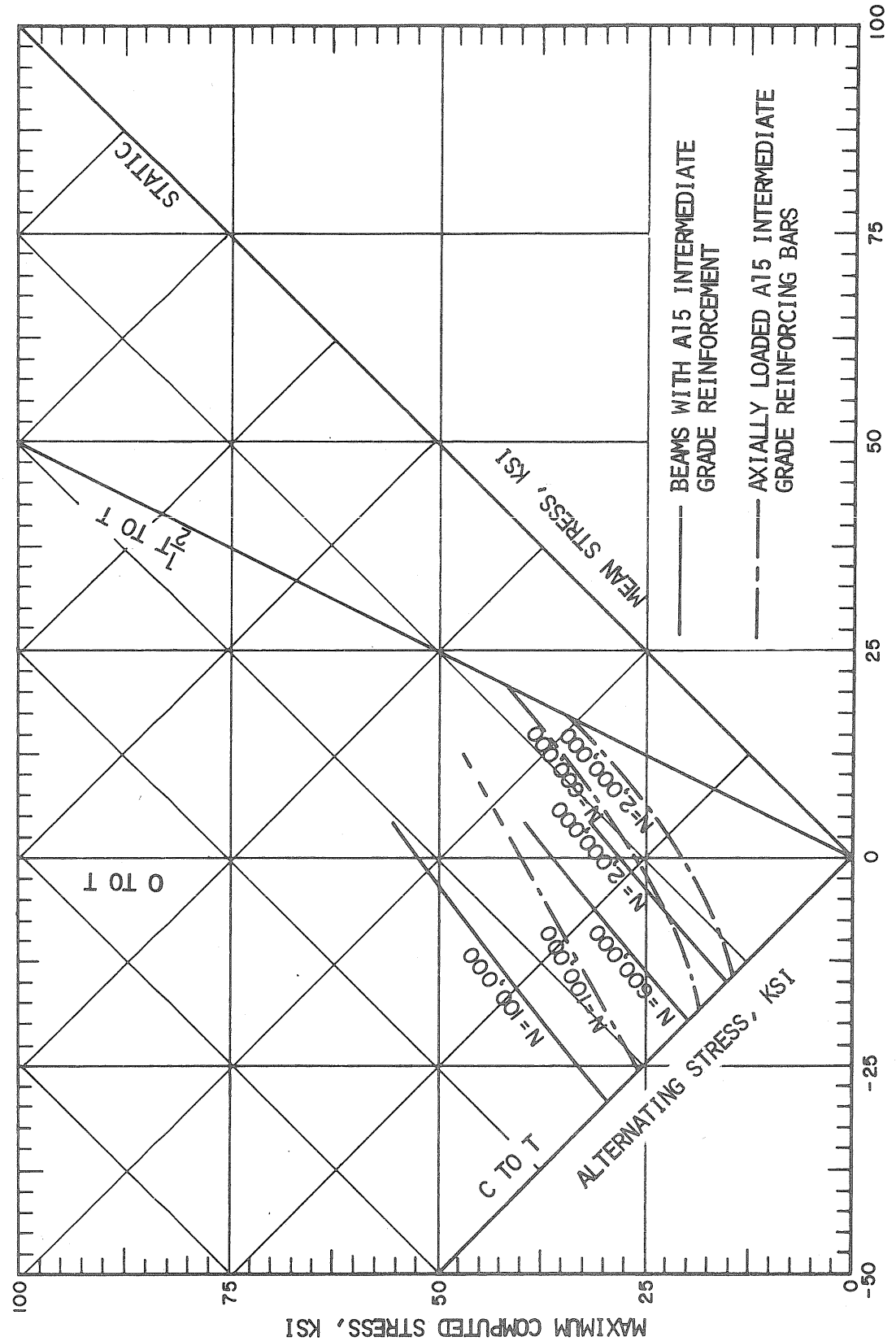

FIG. 29 MODIFIED GOODMAN DIAGRAM, BEAMS WITH 60-DEGREE SINGLE-V BUTT-WELDED REINFORCEMENT

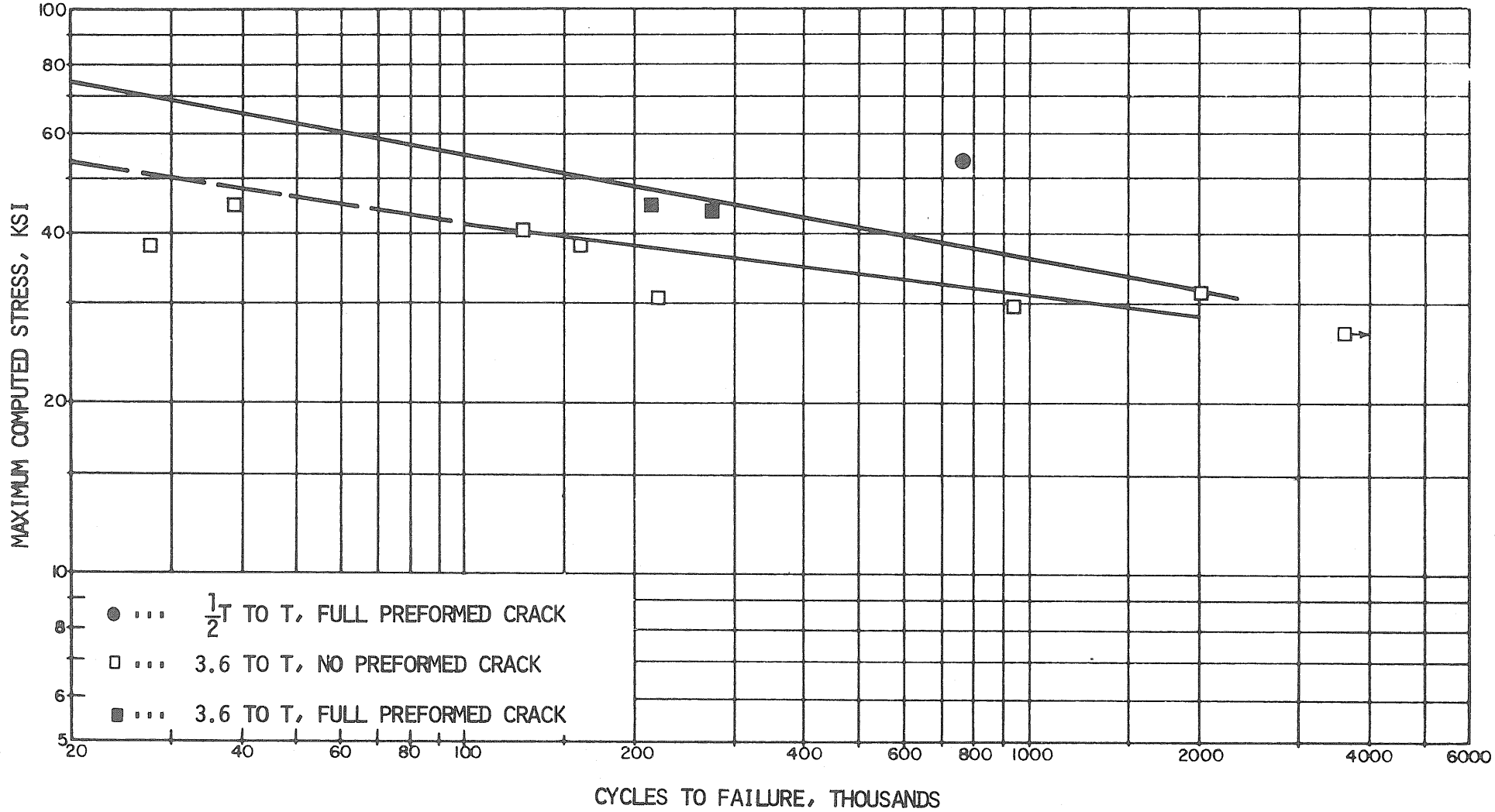

FIG. 30 S-N CURVES, CONCRETE BEAMS WITH INTERMEDIATE GRADE 3-1/2 IN. LAP WELDED REINFORCEMENT

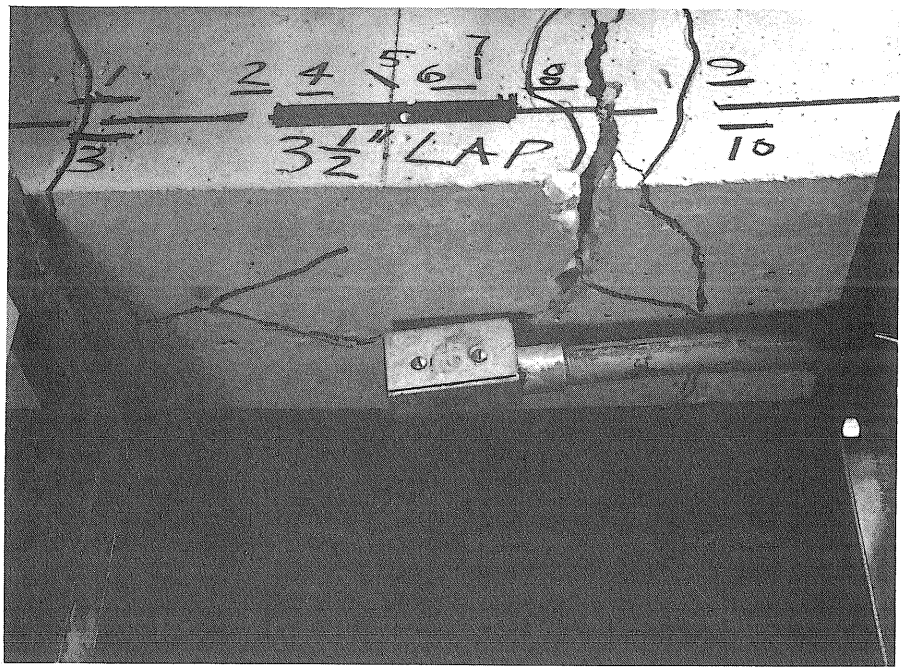

FIG. 31 AN EXAMPLE OF LONGITUDINAL CRACKING IN BEAMS WITH LAP-WELDED REINFORCEMENT

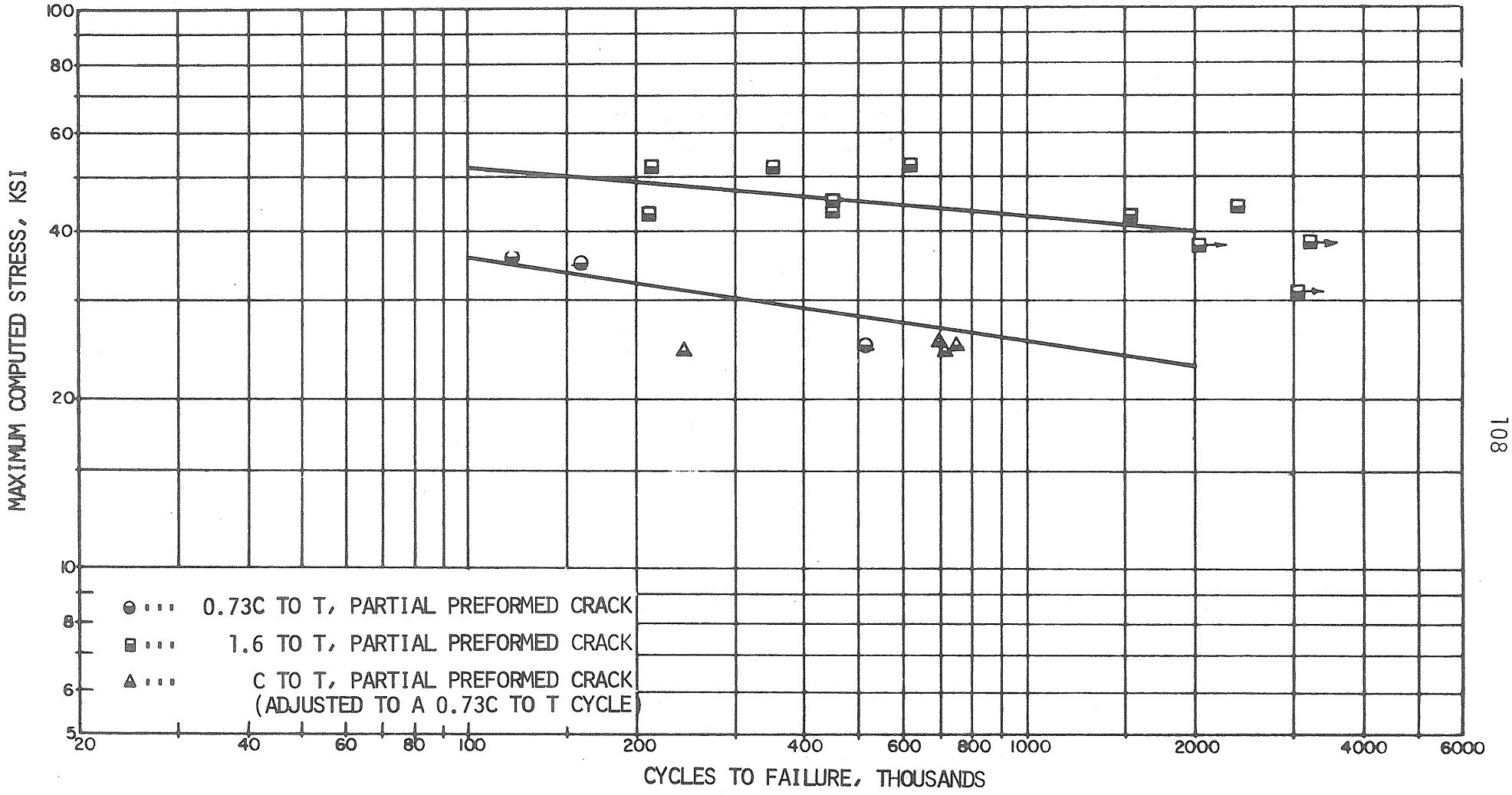

FIG. 32 S-N CURVES, CONCRETE BEAMS WITH HIGH STRENGTH 60-DEGREE SINGLE-V BUTT WELDED REINFORCEMENT

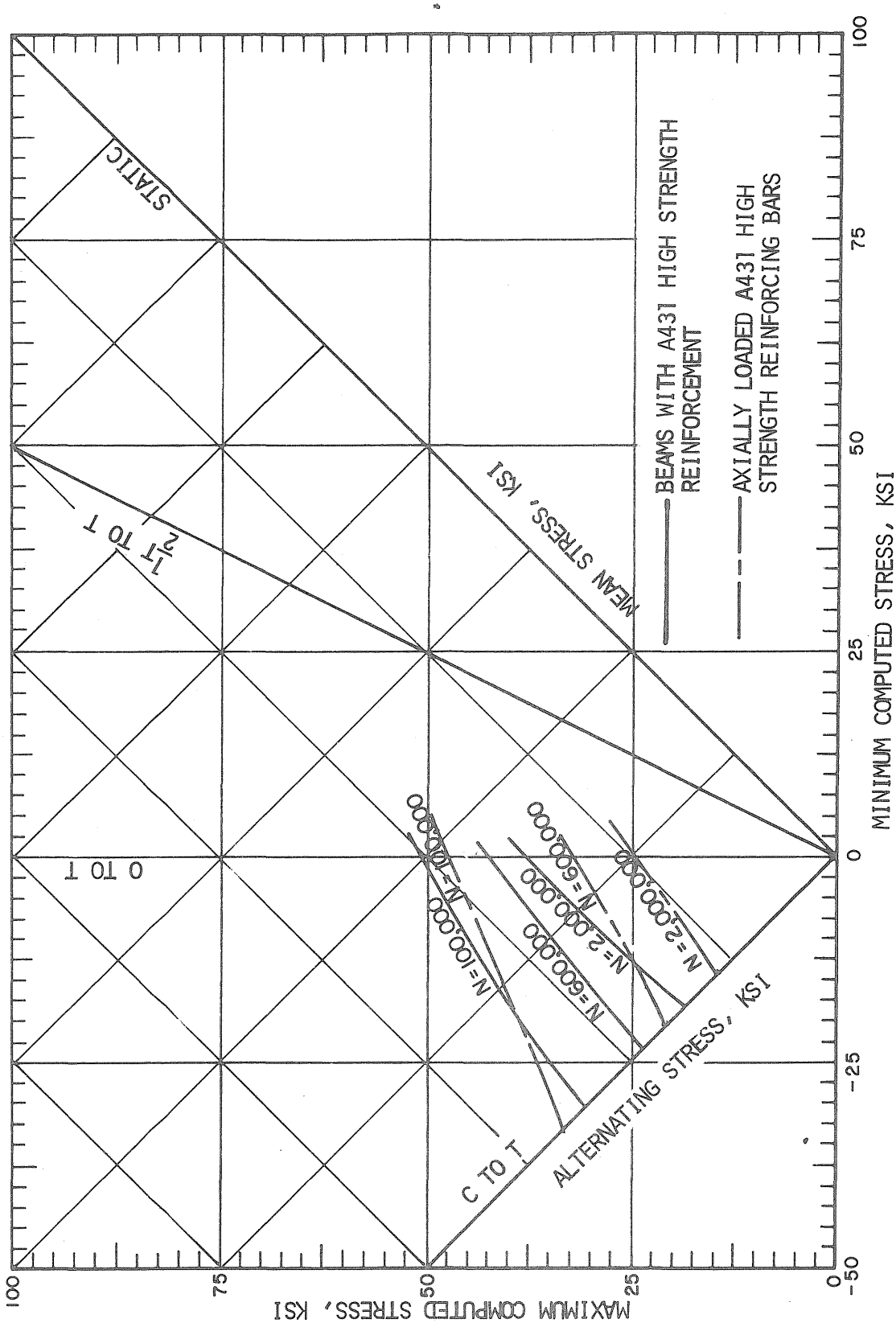

FIG. 33 MODIFIED GOODMAN DIAGRAM, BEAMS WITH 60-DEGREE SINGLE-V BUTT WELDED HIGH STRENGTH REINFORCEMENT

APPENDIX A

BEAM SIMULATION TESTS

A.1 General Description of Specimens and Tests

The simulated beam specimens shown in Fig. A1 consisted of a block of concrete that contained an intermediate grade reinforcing bar.* A steel collar was fastened to one side of the concrete block in an attempt to simulate flexural behavior. The collar tended to restrain a portion of the concrete block while the reinforcement was subjected to an axial load, thereby inducing compressive stresses in the restrained area of the concrete. Four of the six specimens tested contained 60-degree single-v butt-welded reinforcing bars and the remaining two specimens contained 3-1/2 in. single strap lap-welded reinforcement.

Prior to fatigue testing, surface strains in the reinforcement, concrete, and 3/4 in. round collar rods were measured at various levels of static loading. Following the initial static loading the specimens were subjected to a 2 to T computed fatigue stress cycle. The computed stresses were obtained by dividing the load applied to the grips by the nominal area of the reinforcement.

A.2 Test Results**

The measured reinforcing bar strains were close to the computed values near the ends of the concrete block and were generally lower than

---

* See Table 1.

** See Table A1 for fatigue test results.

the computed value at the mid-length of the reinforcing bar. This suggests that the concrete participated in carrying tensile load in the mid-length region of the specimen.

Simulated beams containing both lap and butt-welded reinforcement were tested. However, fatigue test results were obtained only for those specimens which contained 60-degree single-v butt-welded reinforcement. The fatigue tests on the specimens that contained the lap-welded reinforcement were not completed because of excessive cracking and spalling of the concrete.

If the simulated beam specimens--none of which contained preformed cracks at the welds--had fulfilled their intended function, they should have behaved like the reinforced concrete beams without preformed cracks.* The fatigue strength of the reinforcement contained in the simulated beams was found to be considerably lower than the fatigue strength of the reinforcement contained in the concrete beams without preformed cracks. This can be more clearly seen in the data shown in Fig. A2.

---

* The types of preformed cracks used in the reinforced concrete beams are shown in Fig. 4.

TABLE A1[1]

RESULTS OF FATIGUE TESTS ON BEAM SIMULATION SPECIMENS

Specimen Number	Joint Type	Bar Pattern	Stress Cycle,[2] ksi	Cycles to Failure	Remarks
WX-2	60-degree single-v	C	+3 to +31	124,000	
WX-3	60-degree single-v	C	+2 to +31	906,800	Failed about 2 in. from weld
WX-4	60-degree single-v	C	+2 to +31	832,500	Failed about 2-1/2 in. from weld
WX-5	60-degree single-v	C	+2 to +28	<505,800[3]	Failed about 2 in. from weld (machine did not shut off)
LX-1	3-1/2 in. single strap lap	C	---	---	Concrete cracked severely before maximum load was reached
LX-1	3-1/2 in. single strap lap	C	---	---	Concrete cracked severely before maximum load was reached

[1] None of the simulated beam specimens contained preformed cracks.

[2] The stress in the reinforcement was computed by dividing the load which was applied directly to the reinforcement by the nominal area of the reinforcement.

[3] The inequality symbol indicates that the specimen had failed sometime before 505,800 cycles.

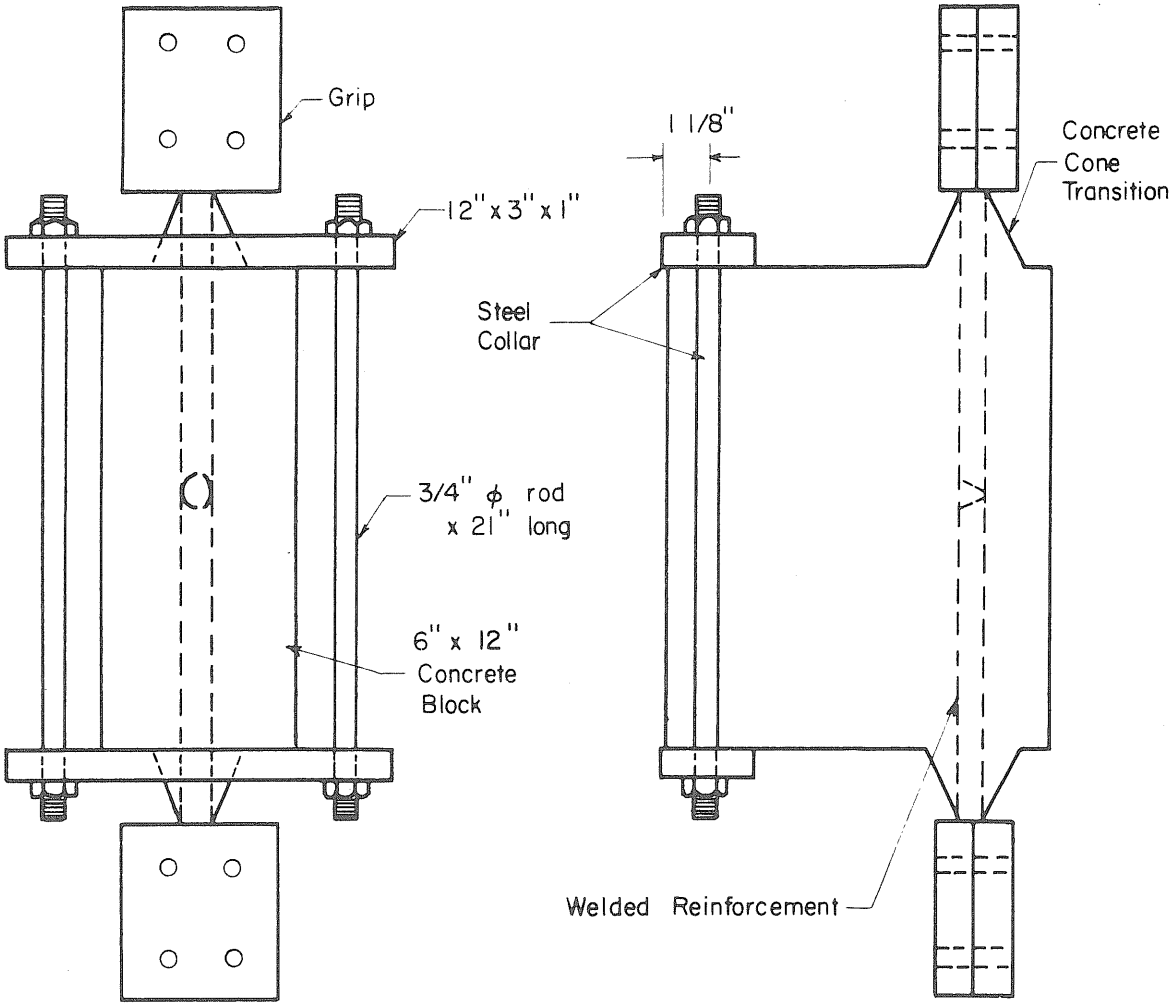

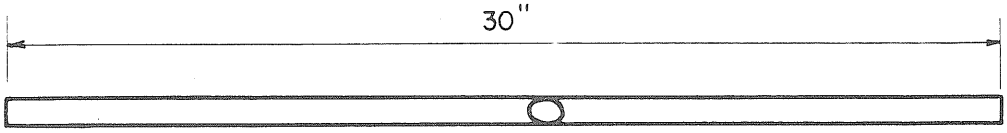

60° Single-V Butt-Welded Reinforcing Bar

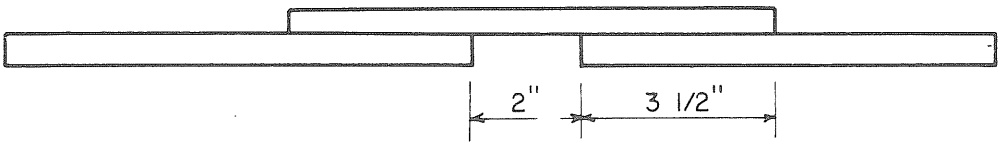

3 1/2 in. Single Strap Lap-Welded Reinforcing Bar

FIG. A1 DETAILS OF BEAM SIMULATION TEST SPECIMENS

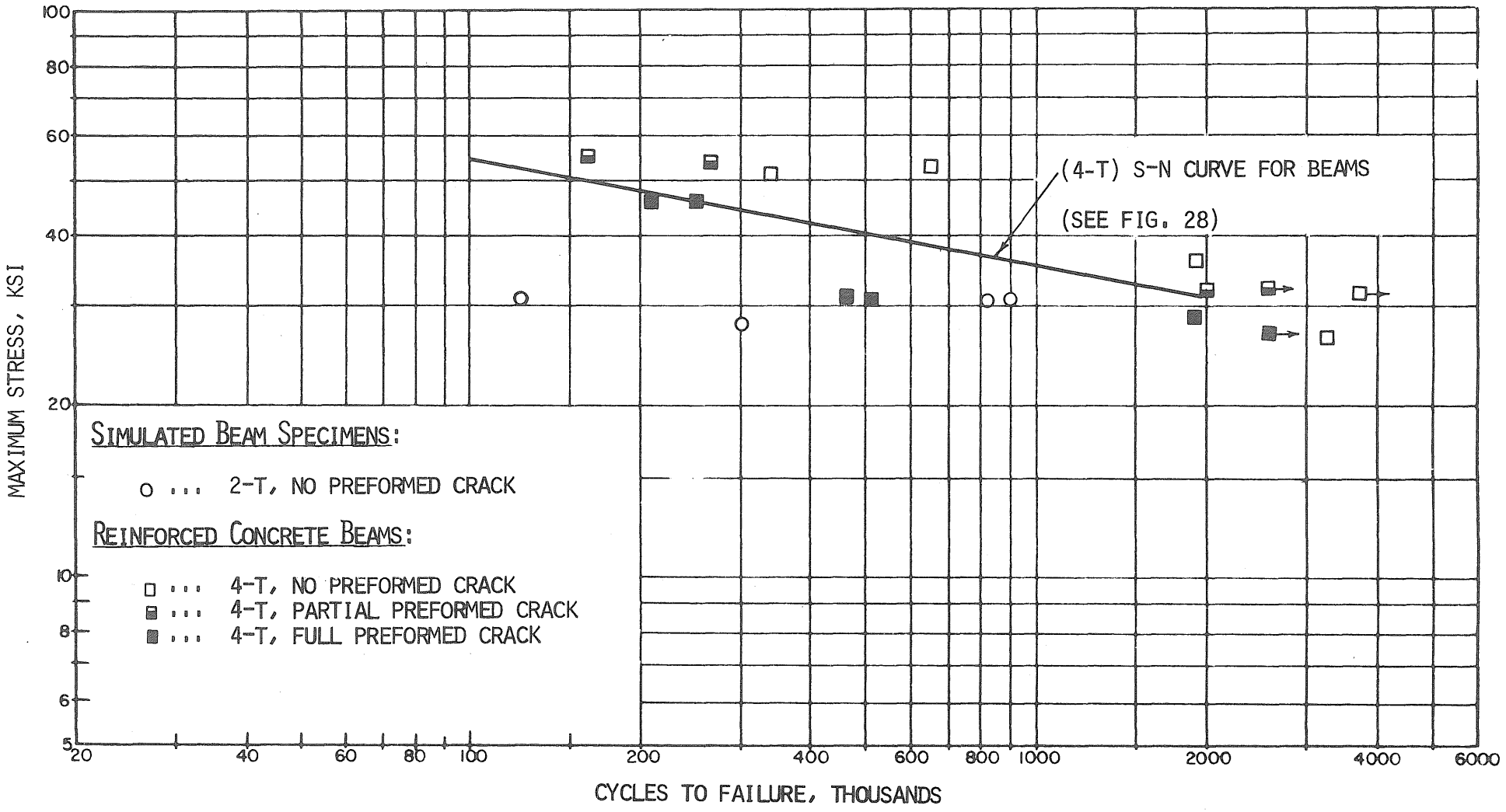

FIG. A2 RESULTS OF FATIGUE TESTS CONDUCTED ON SIMULATED BEAM SPECIMENS WITH 60-DEGREE SINGLE-V BUTT-WELDED REINFORCEMENT

APPENDIX B

MATERIALS AND WELDING PROCEDURES

Information concerning the physical properties of the various reinforcing bars were obtained in laboratory tests as well as from mill reports. The results of these tests are summarized in Table B1. It can be seen that all of the bars met the requirements of the appropriate ASTM Specification.[1]

The chemical composition of the reinforcing bars, as reported by the mill have been tabulated also. These are summarized in Table B2.

The properties of the concrete were also determined during the investigation. A summary of the compression strength and of the modulus of rupture is given in Table B3 for each of the test beams for the beginning of the test and the compressive strength at the end of the fatigue test. The age of the concrete at the time of testing is also noted.

Finally, data are presented in Table B4 concerning the welding procedures used for each of the welded joints. Data are included both for the butt-welded joints and also for the fillet welded joints.

The butt welds were all specified to be full-penetration multiple pass groove welds prepared with electrodes approximately matching the tensile strength of the reinforcing bars being welded. Such welds can generally be expected to develop the full strength of the bars. In the case of the angle splices and the double and single lap joints also matching electrodes were used to deposit the multiple pass welds. As shown in Table 2, the fillet welds detailed in the procedures of Table B4 were all adequate to develop the full strength of the lap and angle splice joints; the failures all occurred at the ends or outside of the joints.

TABLE B1

PHYSICAL PROPERTIES OF REINFORCING BARS USED FOR STATIC AND FATIGUE TESTS

Static and Fatigue Test Specimens				Yield Strength (ksi)		Ultimate Strength (ksi)		Elongation in 8 in. (percent)		Reduction in Area (percent)	
Specimen Designation	Specimen Type*	Test Type	Bar Pattern	Lab.	Mill	Lab.	Mill	Lab.	Mill	Lab.	Mill
SO-1	A(U)	Static	C	52.5	51.0	79.8	77.3	21.5	20.0	44.8	--
SO-2	A(U)	Static	C	51.2	51.0	80.0	77.3	21.0	20.0	49.8	--
			C	51.0	51.0	80.2	77.3	18.8	20.0	37.7	--
SW-1; SW-2; SW-3	A(W)	Static	C	51.0	51.0	80.1	77.3	23.0	20.0	43.1	--
SW41	A(W)	Static	C	51.8	51.0	80.0	77.3	21.2	20.0	37.7	--
SL-1	A(W)	Static	C	51.1	51.0	80.0	77.3	23.0	20.0	43.1	
SL-2	A(W)	Static	C	50.0	51.0	78.8	77.3	18.5	20.0	43.1	--
SL-3 to SL-8	A(W)	Static	C	--	51.0	--	77.3	--	30.0	--	--
SLL-1 to SLL-4	A(W)	Static	C	--	51.0	--	77.3	--	20.0	--	--
10 to 16	A(U)	Fatigue	C	--	51.0	--	77.3	--	20.0	--	--
A-9 to A-12	A(U)	Fatigue	A	50.8	49.8	85.3	84.6	18.8	18.75	--	--
B1-9 to B1-12	A(U)	Fatigue	B	49.3	50.0	78.1	79.3	22.0	18.0	48.1	--
WDO-1 to WDO-4	A(U)	Fatigue	B	51.8	51.0	80.0	77.3	21.2	20.0	--	--

*The symbols used in this column are defined as follows:
A(U) - Unwelded axial bar; B(U) - Beam with unwelded reinforcement
A(W) - Welded axial bar; B(W) - Beam with welded reinforcement

TABLE B1 (Continued)

Static and Fatigue Test Specimens				Yield Strength (ksi)		Ultimate Strength (ksi)		Elongation in 8 in. (percent)		Reduction in Area (percent)	
Specimen Designation	Specimen Type*	Test Type	Bar Pattern	Lab.	Mill	Lab.	Mill	Lab.	Mill	Lab.	Mill
01 to 04	A(U)	Fatigue	C	52.5	51.0	79.8	77.3	21.5	20.0	44.8	--
1 to 9; 18; 19	A(U)	Fatigue	C	--	51.0	--	77.3	--	20.0	--	--
C-1 to C-5	A(U)	Fatigue	C	51.8	51.0	80.0	77.3	21.2	20.0	--	--
WHO-1; WHO-2	A(U)	Fatigue	B	--	89.7	--	123.7	--	7.7	--	--
HB9 to HB12	A(U)	Fatigue	C	124.9	93.3	149.8	149.2	9.4	10.0	35.8	--
A-5 to A-8	A(W)	Fatigue	B	49.3	50.0	78.1	79.3	22.0	18.0	48.1	--
B1-5; B1-6	A(W)	Fatigue	B	49.3	50.0	78.1	79.3	22.0	18.0	48.1	--
W-12; W-14 W-15	A(W)	Fatigue	C	50.2	51.0	78.0	77.3	23.1	20.0	43.1	--
W-13; W-18	A(W)	Fatigue	C	50.2	51.0	78.1	77.3	22.7	20.0	37.7	--
W-19; W-20	A(W)	Fatigue	C	51.1	51.0	80.1	77.3	23.0	20.0	43.1	--
W-21	A(W)	Fatigue	C	50.0	51.0	78.8	77.3	18.5	20.0	43.1	--
A-1 to A-4	A(W)	Fatigue	A	50.8	49.8	85.3	84.6	18.8	18.75	--	--
B1-1 to B1-4	A(W)	Fatigue	B	49.3	50.0	78.1	79.3	22.0	18.0	48.1	--
B1-7; B1-8	A(W)	Fatigue	B	49.3	50.0	78.1	79.3	22.0	18.0	48.1	--

TABLE B1 (Continued)

Static and Fatigue Test Specimens				Yield Strength (ksi)		Ultimate Strength (ksi)		Elongation in 8 in. (percent)		Reduction in Area (percent)	
Specimen Designation	Specimen Type*	Test Type	Bar Pattern	Lab.	Mill	Lab.	Mill	Lab.	Mill	Lab.	Mill
W-1; W-2	A(W)	Fatigue	C	52.5	51.0	79.8	77.3	21.5	20.0	44.8	--
W-3	A(W)	Fatigue	C	51.1	51.0	80.1	77.3	23.0	20.0	43.1	--
W-4; W-7	A(W)	Fatigue	C	50.0	51.0	78.8	77.3	18.5	20.0	43.1	--
W-8 to W-11	A(W)	Fatigue	C	50.2	51.0	78.0	77.3	23.1	20.0	43.1	--
W-16; W-17	A(W)	Fatigue	C	50.2	51.0	78.1	77.3	22.7	20.0	37.7	--
FC1 to FC21	A(W)	Fatigue	C	53.3	53.0	83.3	80.0	21.9	22.0	48.1	--
W58; W59; W68; W69	A(W)	Fatigue		53.3	53.0	83.3	80.0	21.9	22.0	48.1	--
W-60 to W-67	A(W)	Fatigue		53.3	53.0	83.3	80.0	21.9	22.0	48.1	--
W-31; W-32	A(W)	Fatigue	C	51.7	51.0	81.1	77.3	23.4	20.0	48.8	--
W-33	A(W)	Fatigue	C	51.7	51.0	81.1	77.3	23.4	20.0	48.8	--
W-35; W-36	A(W)	Fatigue	C	51.6	51.0	79.2	77.3	--	20.0	37.7	--
W-28 to W-30	A(W)	Fatigue	C	51.4	51.0	81.0	77.3	22.7	20.0	48.8	--

TABLE B1 (Continued)

Static and Fatigue Test Specimens				Yield Strength (ksi)		Ultimate Strength (ksi)		Elongation in 8 in. (percent)		Reduction in Area (percent)	
Specimen Designation	Specimen Type*	Test Type	Bar Pattern	Lab.	Mill	Lab.	Mill	Lab.	Mill	Lab.	Mill
W22 to W24	A(W)	Fatigue	C	51.9	51.0	80.5	77.3	24.2	20.0	37.7	--
WL-1	A(W)	Fatigue	C	51.8	51.0	80.0	77.3	21.2	20.0	--	--
WL-2; WL-3	A(W)	Fatigue	C	52.0	51.0	79.2	77.3	--	20.0	--	--
W25; W26	A(W)	Fatigue	C	51.9	51.0	80.5	77.3	24.2	20.0	37.7	--
W-27	A(W)	Fatigue	C	51.4	51.0	81.0	77.3	22.7	20.0	48.8	--
WP-1 to WP-3	A(W)	Fatigue	C	51.0	51.0	79.7	77.3	--	20.0	--	--
W-37; W-39	A(W)	Fatigue	C	51.6	51.0	79.2	77.3	--	20.0	37.7	--
W-40	A(W)	Fatigue	C	51.6	51.0	79.2	77.3	--	20.0	37.7	--
W-48 to W-51 W-55 to W-57	A(W)	Fatigue	C	51.8	51.0	80.0	77.3	21.2	20.0	--	--
WT-1 to WT-3	A(W)	Fatigue	C	51.8	51.0	80.0	77.3	21.2	20.0	--	--
HB-1 to HB-8 HB-13 to HB-18	A(W)	Fatigue	C	124.3	93.3**	149.8	149.2	9.4	10	35.8	--
H-20 to H-24	A(W)	Fatigue	X	--	89.6	--	124.0	--	11.0	--	--
WH-1 to WH-3	A(W)	Fatigue	B	90.0	89.7	123.7	123.7	7.7	7.7	--	--

** The yield strength given by the mill report is believed to be in error.

TABLE B1 (Continued)

Static and Fatigue Test Specimens				Yield Strength (ksi)		Ultimate Strength (ksi)		Elongation in 8 in. (percent)		Reduction in Area (percent)	
Specimen Designation	Specimen Type*	Test Type	Bar Pattern	Lab.	Mill	Lab.	Mill	Lab.	Mill	Lab.	Mill
SBC1	B(U)	Fatigue	C	51.8	51.0	80.0	77.3	21.2	20.0	--	--
$\overline{BT1}$; $\overline{BT2}$	B(U)	Fatigue	C	124.3	93.3**	149.8	149.2	9.4	10.0	35.8	--
BR1 to BR12	B(W)	Fatigue	C	53.3	53.0	83.3	80.0	21.9	22.0	48.1	--
BW1; BW4; BW6 BW7A; BW8A; BW9; BW10A; BW11A; BW12; BW13A; BW14; BW15; BW17	B(W)	Fatigue	C	51.8	51.0	80.0	77.3	21.2	20.0	--	--
BW2; BW3	B(W)	Fatigue	C	52.1	51.0	80.0	77.3	--	20.0	--	--
BW18; to BW20 BW22; BW23	B(W)	Fatigue	C	51.8	51.0	80.0	77.3	21.2	20.0	--	--
$\overline{BT1}$; $\overline{BT2}$	B(W)	Fatigue	A	69.0	--	82.0	--	21.0	--	61.0	--
BF1; BF2	B(W)	Fatigue	A	51.8	51.0	80.0	77.3	21.2	20.0	--	--
BL1;to BL11	B(W)	Fatigue	C	51.8	51.0	80.0	77.3	21.2	20.0	--	--

** The yield point given by mill reports is believed to be in error

TABLE B1 (Continued)

Static and Fatigue Test Specimens				Yield Strength (ksi)		Ultimate Strength (ksi)		Elongation in 8 in. (percent)		Reduction in Area (percent)	
Specimen Designation	Specimen Type*	Test Type	Bar Pattern	Lab.	Mill	Lab.	Mill	Lab.	Mill	Lab.	Mill
BR13 to BR17	B(W)	Fatigue	C	124.3	93.3	149.8	149.2	9.4	10.0	35.8	--
BR18; BR20; BR21	B(W)	Fatigue	X	--	89.6	--	124.0	--	11.0	--	--
BT-3 to BT-13	B(W)	Fatigue	C	124.3	93.3	149.8	149.2	9.4	10.0	35.8	--
WX-2 to WX-5 LX-1; LX-2	--**	Fatigue	C	51.8	51.0	80.0	77.3	21.2	20	--	--

**Beam simulation specimens with welded reinforcement.

TABLE B2

CHEMICAL COMPOSITIONS OF REINFORCING BARS
USED IN STATIC AND FATIGUE TESTS

Static and Fatigue Test Specimen Designations	Chemical Compositions from Mill Reports, %						
	C	Mn	P	S	Si	Cr	Mo
(A) Axially Loaded Bar Specimens							
SO-1 to SO-3; SW-1 to SW-3 SW-41; SL-1 to SL-8; SLL-1 to SLL-4; O1 to O4; 1 to 19; WDO-1 to WDO-4	0.43	0.39	0.19	0.035	0.15	--	--
A-1 to A-12	0.45	0.46	0.014	0.045	--	--	--
B1-1 to B1-12	0.35	0.64	0.019	0.04	--	--	--
W-1 to W-40; W-48 to W-51; W-55 to W-57; WL-1 to WL-3; WT-1 to WT-3; WP-1 to WP-3; C-1 to C-5	0.43	0.39	0.019	0.035	--	--	--
FC-1 to FC-21; W-58 to W-69	0.43	0.40	0.013	0.030	0.14	--	--
WHO-1 to WHO-2; WH-1 to WH-3	0.4	0.81	0.010	0.03	0.25	0.87	0.17
HB-1 to HB-18	0.45	0.89	0.022	0.016	0.35	0.97	0.22
H-20 to H-24	0.4	--	0.016	0.020	--	--	--
(B) Beam Specimens							
BR1 to BR12	0.43	0.40	0.013	0.030	0.14	--	--
BW1 to BW4, BW6, BW7A; BW8A; BW9, BW10A, BW11A; BW12; BW13A; BW15 to BW25; BF1, BF2; BL1 to BL11	0.43	0.39	0.019	0.035	0.15	--	--
BR13 to BR17	0.45	0.89	0.022	0.016	0.35	0.91	0.22
BR18; BR20; BR21	0.4	--	0.016	0.02	--	--	--
BT1 to BT13	0.45	0.89	0.022	0.016	0.35	0.91	0.22
(C) Beam Simulation Specimens							
WX-2 to WX-5 LX-1; LX-2	0.43	0.39	0.019	0.035	0.15	--	--

TABLE B3

PROPERTIES OF THE CONCRETE USED IN THE BEAMS

Beam Number	Ave. Compressive Strength fc' and Modulus of Rupture fr at Beginning of Test			Ave. Compressive Strength fc' at End of Test	
	fc' (psi)	fr (psi)	Age (days)	fc' (psi)	Age (days)
SBC1	4860	417	7	5720	27
BT1	4510	500	15	4910	55
BT2	5330	550	13	6150	33
BR1	4825	504	25	5190	28
BR2	4670	546	9	4960	12
BR3	5640	558	14	5660	16
BR4	4560	538	--	5160	--
BR5	4740	516	--	4980	--
BR6	4630	496	8	5250	25
BR7	4050	429	7	4315	8
BR8	5340	467	27	5350	30
BR9	5170	471	12	5400	14
BR10	5010	479	9	5610	21
BR11	5415	621	17	--	--
BR12	5645	550	15	--	--
BW1	6055	--	10	6440	37
BW2	6620	490	27	6730	43
BW3	6340	520	27	6380	34
BW4	5140	410	26	5400	29

TABLE B3 (Continued)

Beam Number	Ave. Compressive Strength f'_c and Modulus of Rupture f_r at Beginning of Test			Ave. Compressive Strength f'_c at End of Test	
	f'_c (psi)	f_r (psi)	Age (days)	f'_c (psi)	Age (days)
BW6	4230	450	7	5090	21
BW7A	5720	--	16	6420	28
BW8A	4930	527	10	4980	12
BW9	5220	--	41	5480	45
BW10A	5030	412	19	--	--
BW11A	3940	474	8	4860	19
BW12	4610	--	9	5220	13
BW13A	4000	396	16	4090	17
BW14	4500	454	16	4980	26
BW15	--	381	--	4795	21
BW17	--	446	--	4980	20
BW18	4830	600	15	5405	33
BW19	5375	608	13	5460	27
BW20	5505	670	21	5495	31
BW22	5890	533	34	5990	49
$\overline{BT1}$	4230	442	7	4560	11
$\overline{BT2}$	--	--	--	5370	15
BF1	4540	417	12	--	--
BF2	4740	458	12	4950	19

TABLE B3 (Continued)

Beam Number	Ave. Compressive Strength fc and Modulus of Rupture fr at Beginning of Test			Ave. Compressive Strength fc at End of Test	
	fc (psi)	fr (psi)	Age (days)	fc (psi)	Age (days)
BL1					
BL2	3750	420	12	4043	17
BL3	3660	366	15	3920	24
BL4	5160	528	11	5585	36
BL5	5230	520	13	--	--
BL6	4720	421	15	4785	17
BL7	3430	450	6	3800	8
BL8	4490	467	6	4715	8
BL9	5570	456	--	5800	--
BL10	5540	522	--	5250	--
BL11	5480	604	--	5450	--
BR13	--	500	--	5680	26
BR14	5330	590	--	--	--
BR15	5845	521	18	5860	25
BR16	5840	479	10	5980	14
BR17	5280	500	15	--	--
BR18	4180	458	7	4910	16
BR20	4030	500	2	5370	10
BR21	5380	583	7	5562	15

TABLE B3 (Continued)

Beam Number	Ave. Compressive Strength fc' and Modulus of Rupture fr at Beginning of Test			Ave. Compressive Strength fc' at End of Test	
	fc' (psi)	fr (psi)	Age (days)	fc' (psi)	Age (days)
BT3	5305	490	14	5385	16
BT4	5740	540	18	5850	19
BT5	4700	512	8	5060	14
BT6	4700	520	16	4850	34
BT7	5820	570	31	5780	35
BT8	5615	535	8	5920	23
BT9	5410	660	18	6290	39
BT10	5510	625	26	5980	40
BT11	6030	548	12	6240	17
BT12	4980	550	8	5690	19
BT13	4700	521	4	4705	11
WX3[1]	--	815	--	6740	53
WX5[1]	--	635	--	6220	49

[1] Simulated Beam Specimens

TABLE B4

WELDING PROCEDURES

Joint Classification	Electrode	Current (Amp)	Pass Sequence
(a) V-Shaped Butt Welds			
(Intermediate Grade Reinforcing Bars)			±18 puddles
60-Degree Single-V	1/8" ϕ E7018	120	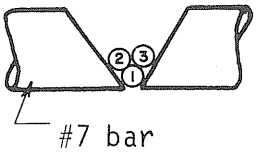
60-Degree Single-V with Flame Cut Joint Preparation	1/8" ϕ E7018	120	#7 bar
60-Degree Single-V with 400°F Preheating	1/8" ϕ E7018	120	
60-Degree Double-V	1/8" ϕ E7018	110	±16 puddles 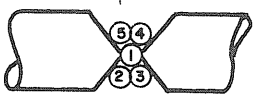 #7 bar
45-Degree Single-V	1/8" ϕ E7018	110	±16 puddles 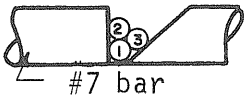 #7 bar
60-Degree Single-V Pipe Back Up	1/8" ϕ E7018	120	±18 puddles  #7 bar
(High Strength Reinforcing Bars)			±13 puddles
60-Degree Single-V	1/8" ϕ E12018	120	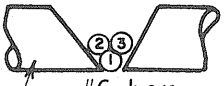 #6 bar
60-Degree Single-V	1/8" ϕ E12018	120	±18 puddles 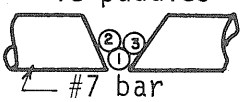 #7 bar

TABLE B4 (Continued)

Joint Classification	Electrode	Current (Amp)	Pass Sequence
(b) Fillet Welds			
(Intermediate Grade Reinforcing Bars)			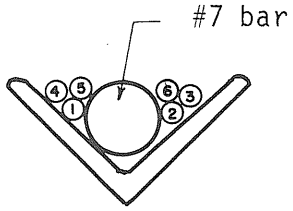
Angle Splice	5/32" ϕ E7018 First Two Passes 3/16" ϕ E7018 Remaining Passes	160 First Two Passes 210 Remaining Passes	
Double and Single Lap	5/32" ϕ E7018 First Two Passes 3/16" ϕ E7018 Remaining Passes	160 First Two Passes 210 Remaining Passes	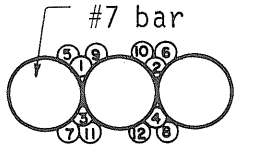 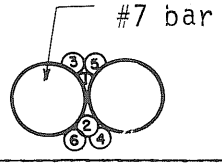

Note:

1. All intermediate grade bars were subjected to preheating temperatures which varied between room temperature and 150°F, and interpass temperatures not greater than 250°F unless stated otherwise above.

2. All high strength bars were subjected to a preheating temperature of 400°F and an interpass temperature not greater than 400°F or less than 350°F.

3. All joints were saw cut unless stated otherwise above.

APPENDIX C

FIRST CYCLE MOMENT VS. MEASURED STEEL STRAIN CURVES

The strain data from the individual beam tests used in constructing the first cycle, moment vs. average steel stress (or strain) curves shown in Figs. 23, 24 and 25 are plotted in Figs. C1 to C25. These data were obtained from strain gage readings taken at successive load increments and from gages located within the region of the beam subjected to a constant moment. The strain readings taken at the various load increments were then averaged for each beam in order to construct the moment vs. average stress (or strain) curves shown in Figs. C26 to C31. It can be seen from these curves that the gage readings at cracked and uncracked sections were averaged separately so that a moment vs. average stress curve for both cracked and uncracked concrete sections could be obtained for each beam. The average strains plotted on the curves shown in Figs. C26 to C31 were in turn averaged for various levels of applied moment to obtain the curves shown in Figs. 23, 24 and 25.

It should be noted that the character of the first cycle unloading curves was influenced by the magnitude of the maximum applied first cycle load. Therefore, it was necessary to use some discretion in obtaining the unloading curves shown in Figs. 23, 24 and 25. Only those unloading curves for beams subjected to relatively high maximum moments of nearly equal magnitudes were averaged for this purpose.

All the beam data available were used in constructing the first cycle loading curves since, ideally speaking, the character of the curve

for first cycle moment vs. stress should not be influenced by the magnitude of the maximum first cycle load. That is the character of the first cycle loading curves should depend only on whether the concrete section to which the curves pertain are cracked or uncracked.

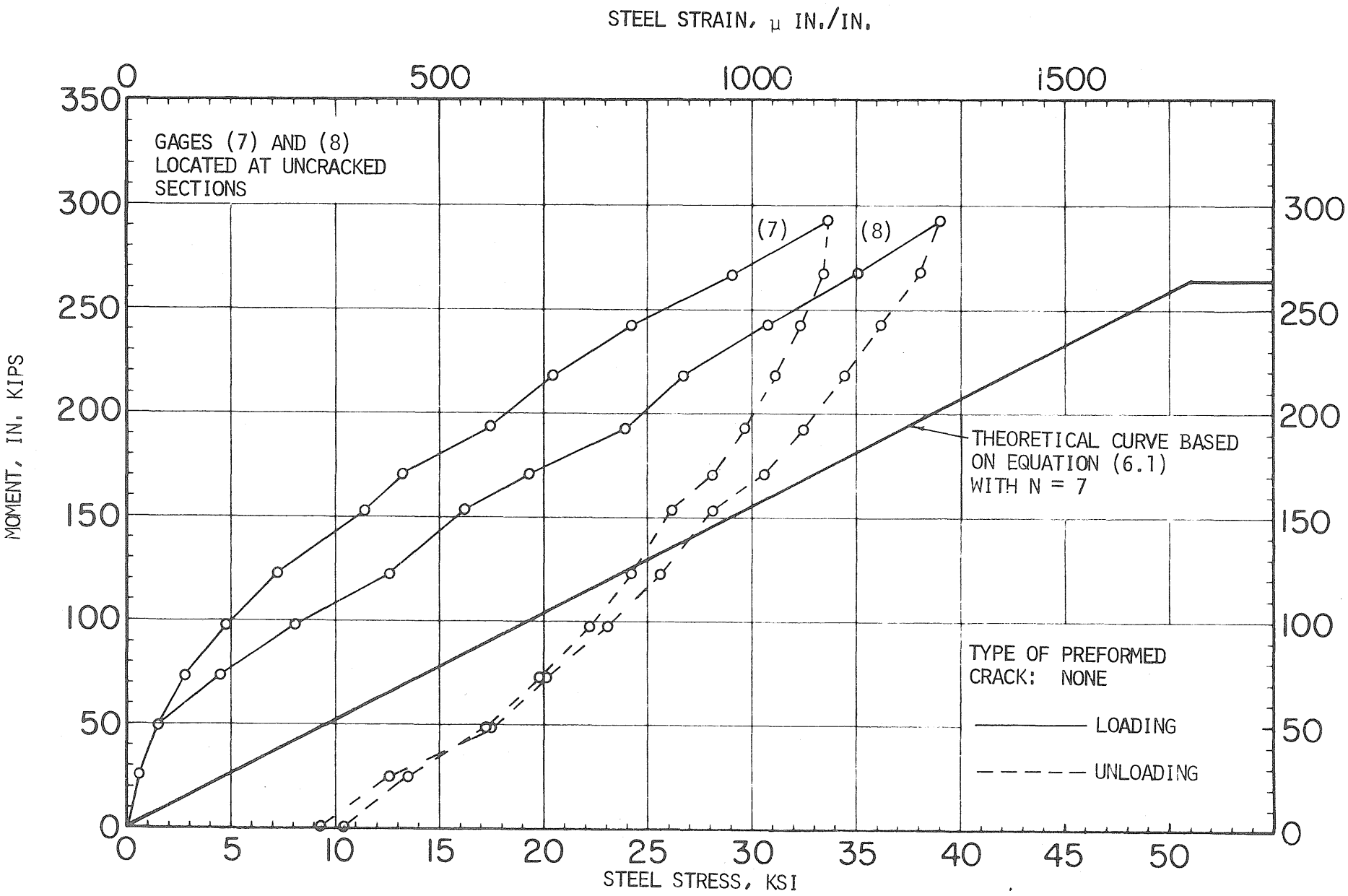

FIG. C1 MOMENT VS. STRESS OR STRAIN FOR BEAM SPECIMEN SBC1

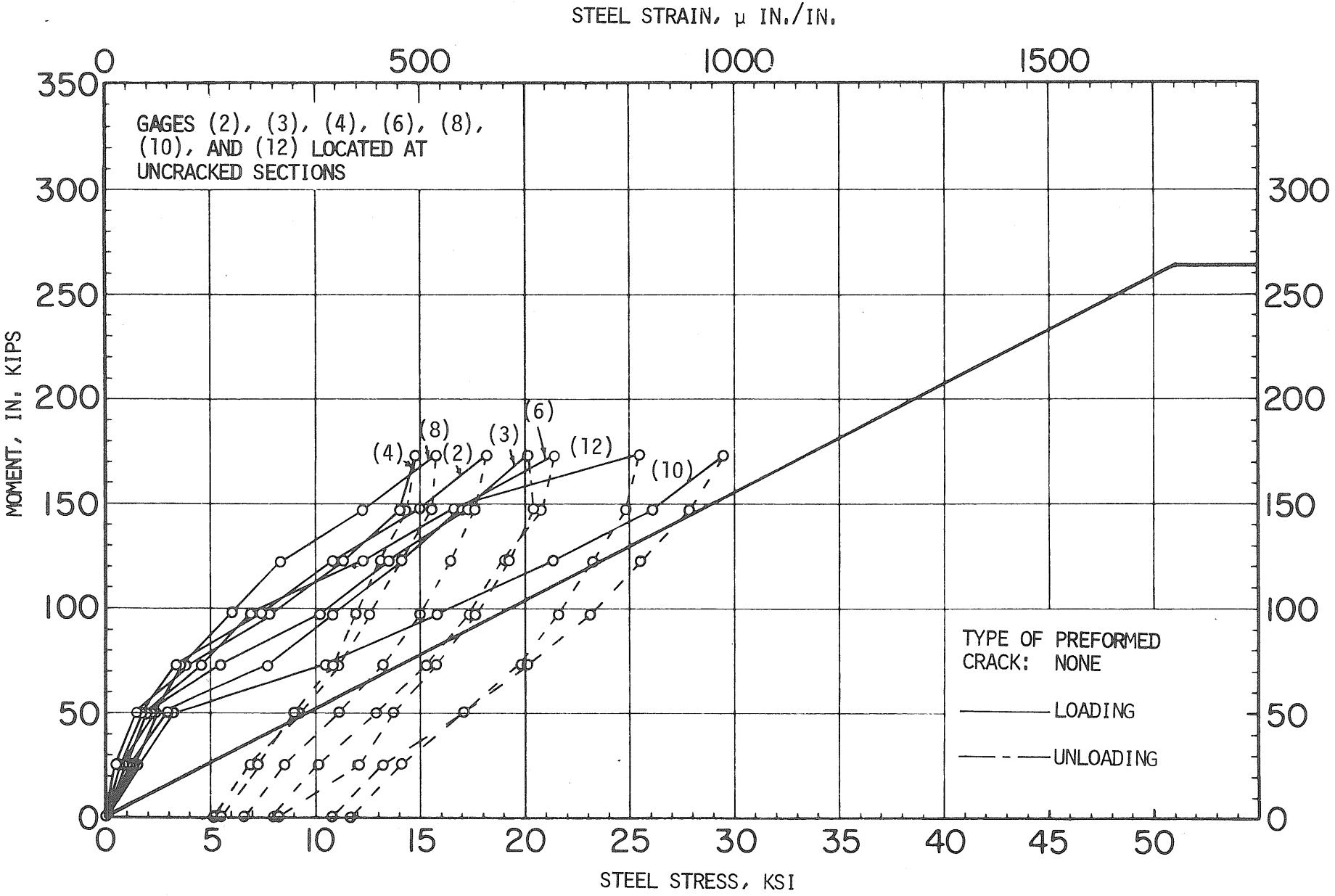

FIG. C2 MOMENT VS. STRESS OR STRAIN FOR BEAM SPECIMEN BW1

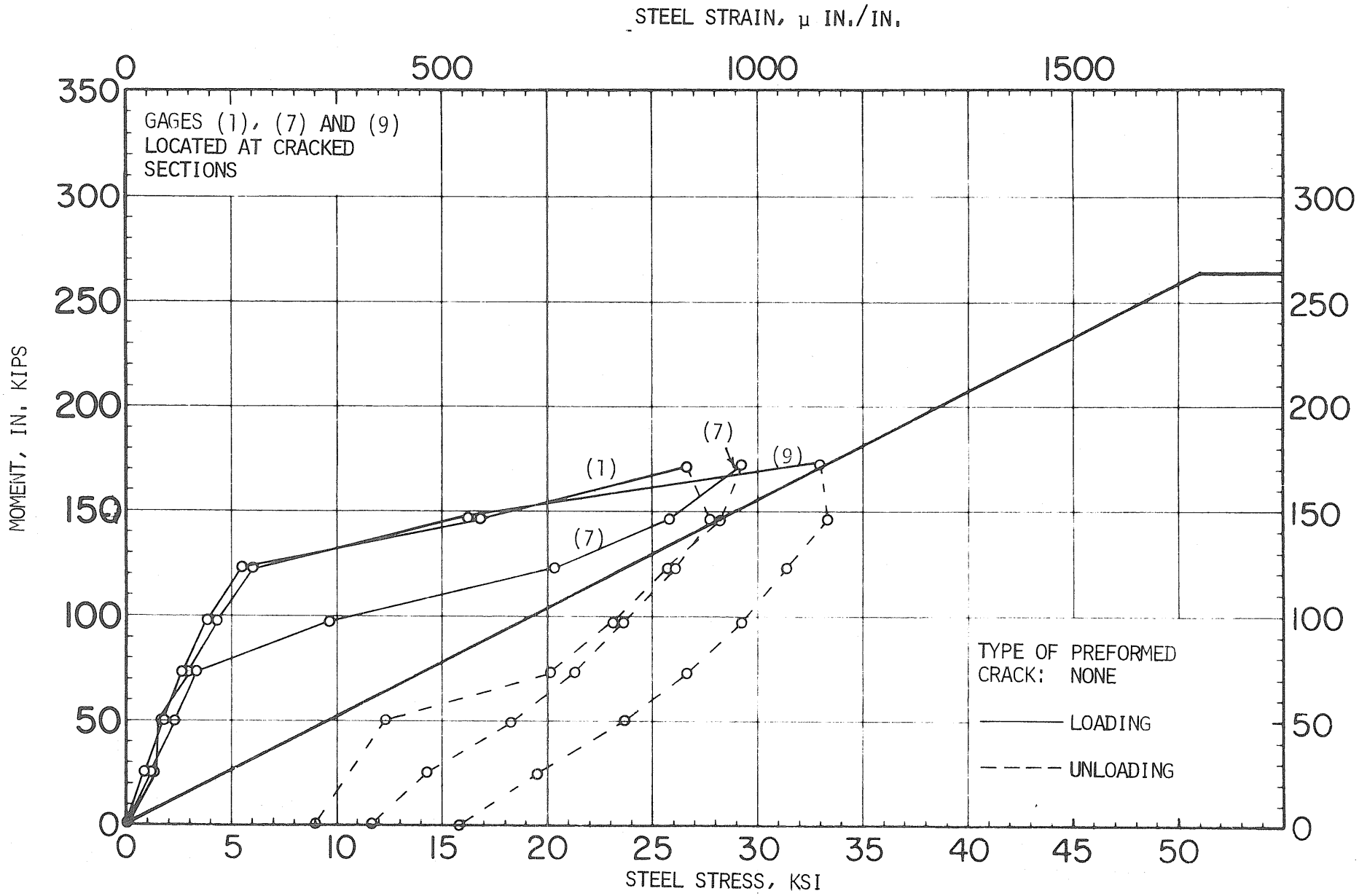

FIG. C3 MOMENT VS. STRESS OR STRAIN FOR BEAM SPECIMEN BW1

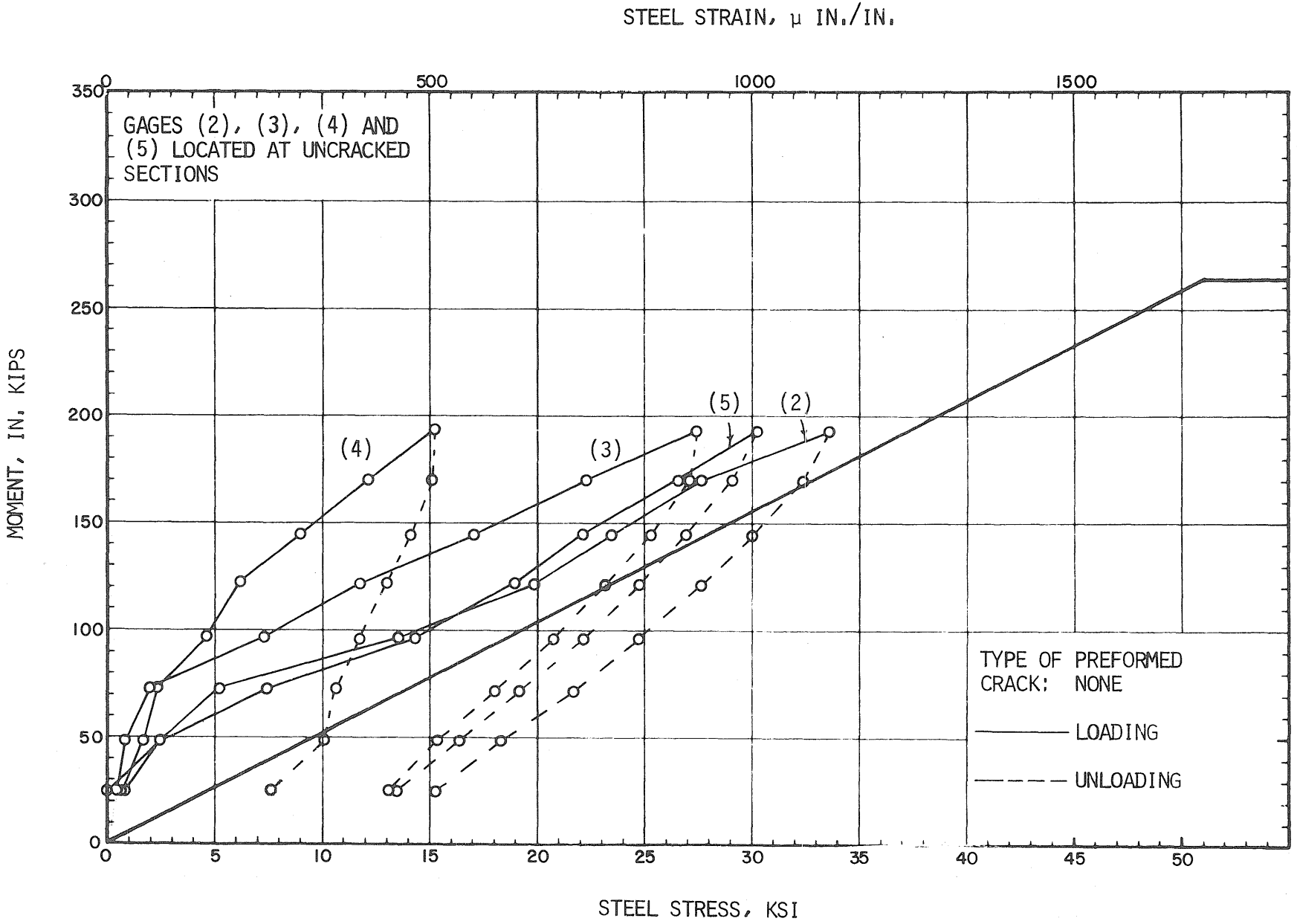

FIG. C4 MOMENT VS. STRESS OR STRAIN FOR BEAM SPECIMEN BW2

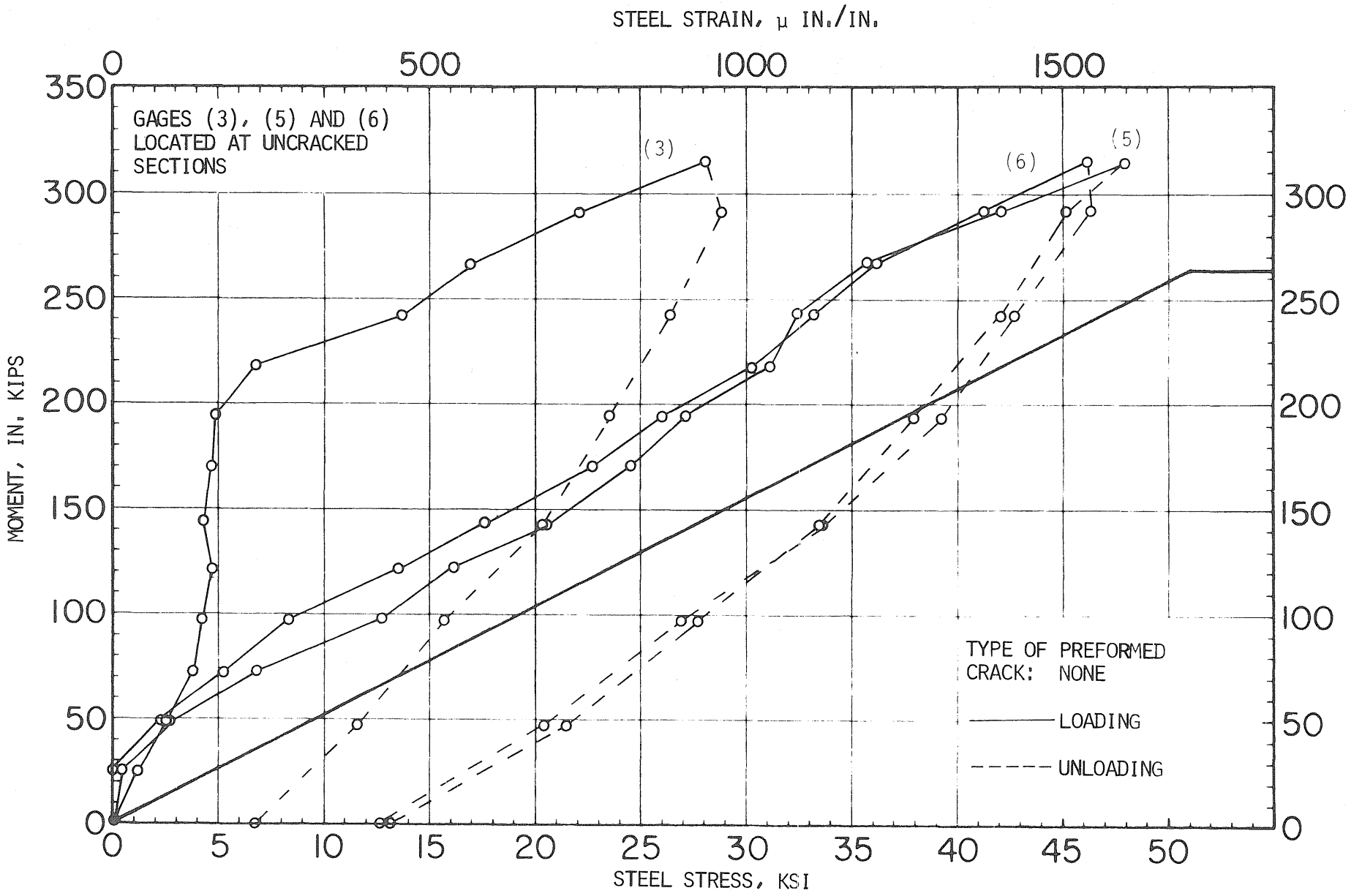

FIG. C5 MOMENT VS. STRESS OR STRAIN FOR BEAM SPECIMEN BW3

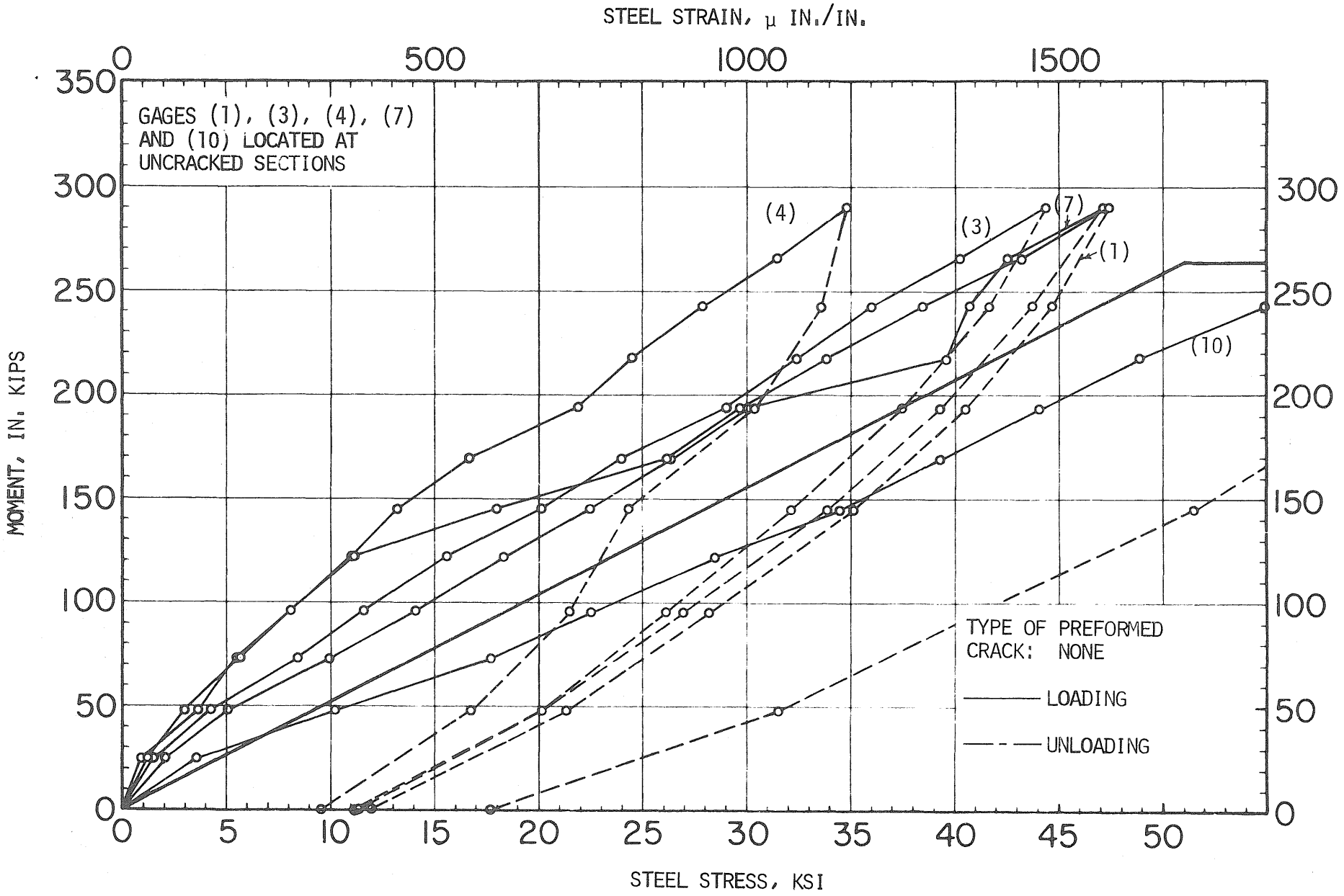

FIG. C6 MOMENT VS. STRESS OR STRAIN FOR BEAM SPECIMEN BW4

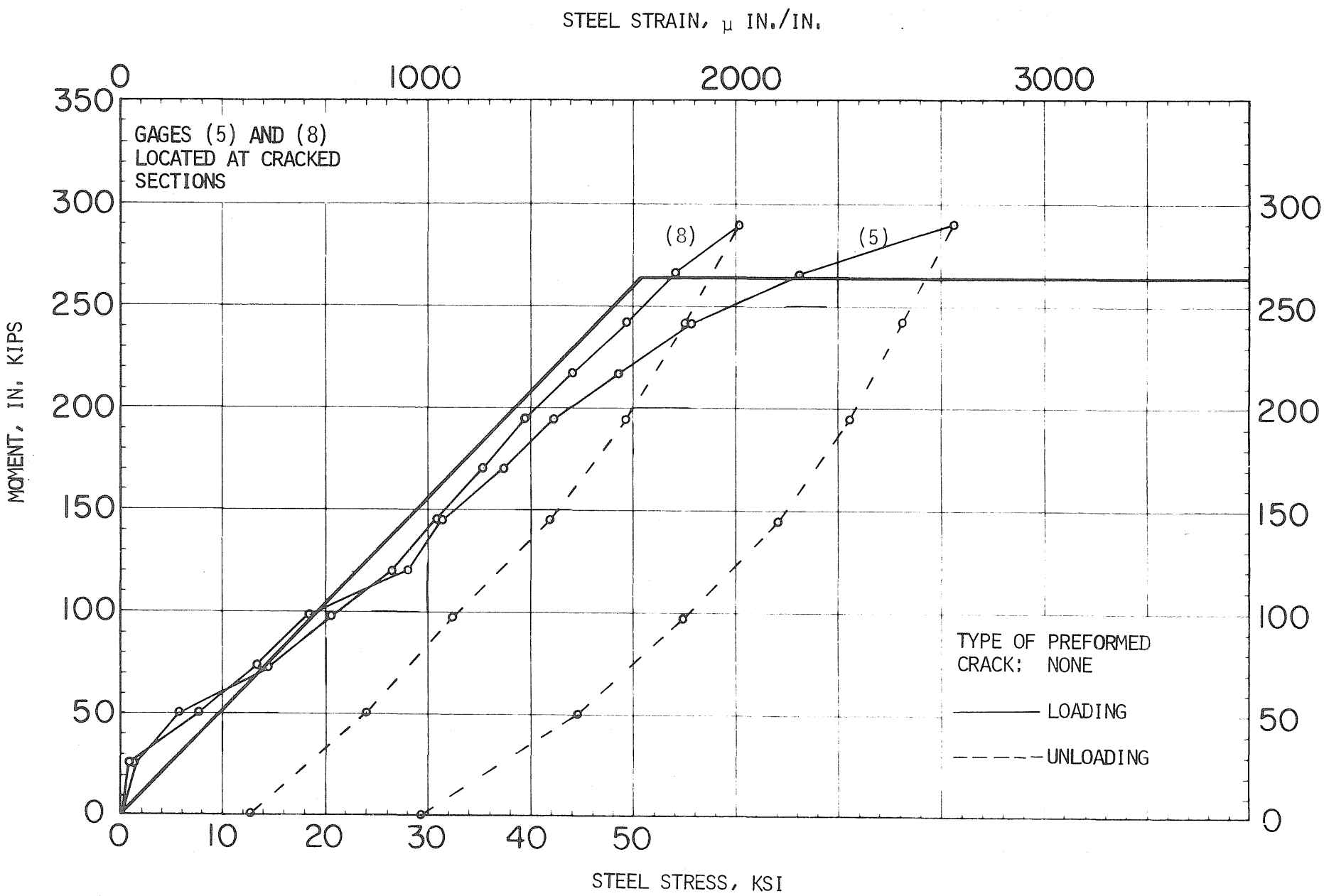

FIG. C7 MOMENT VS. STRESS OR STRAIN FOR BEAM SPECIMEN BW4

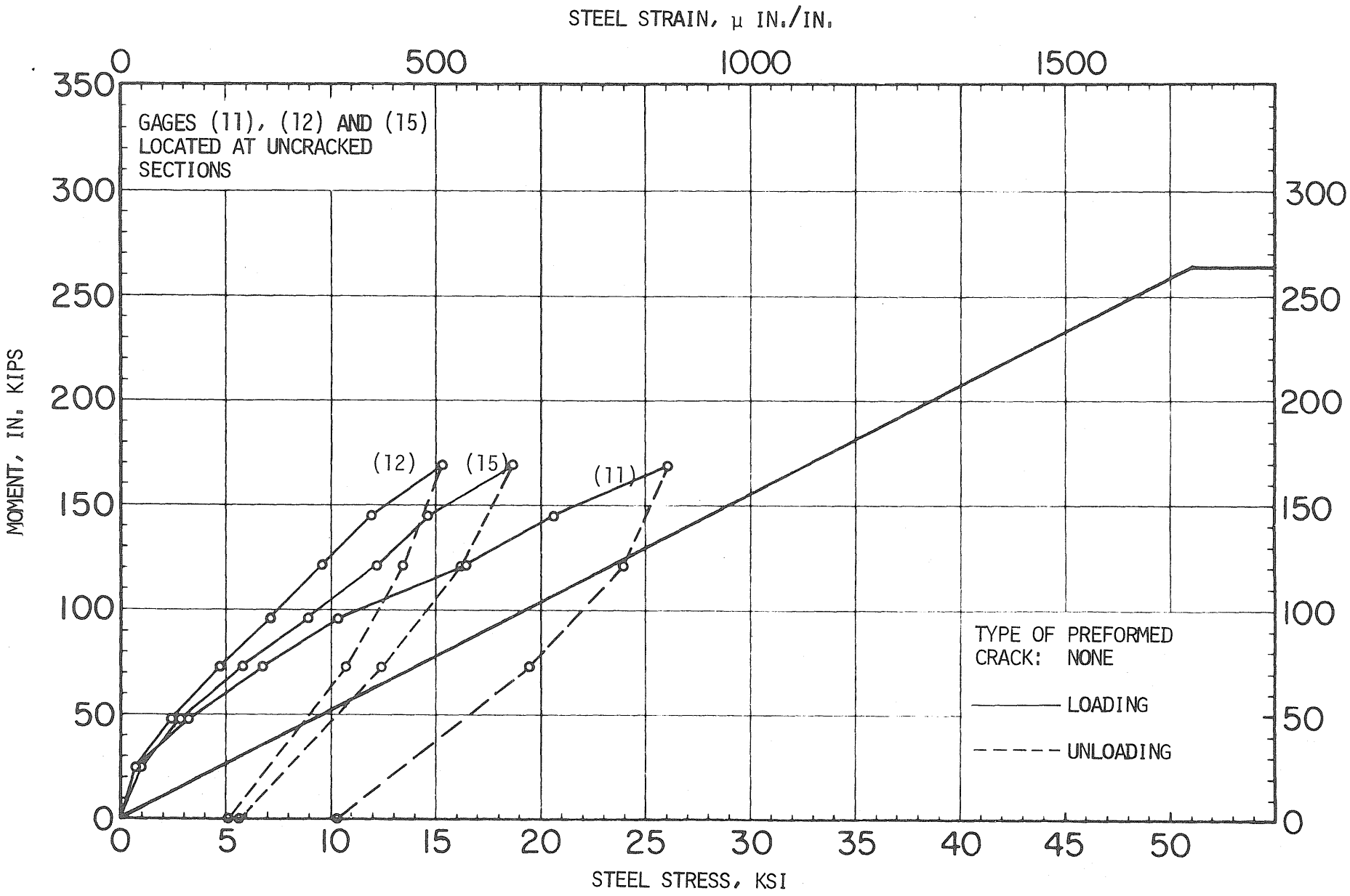

FIG. C8 MOMENT VS. STRESS OR STRAIN FOR BEAM SPECIMEN BW7A

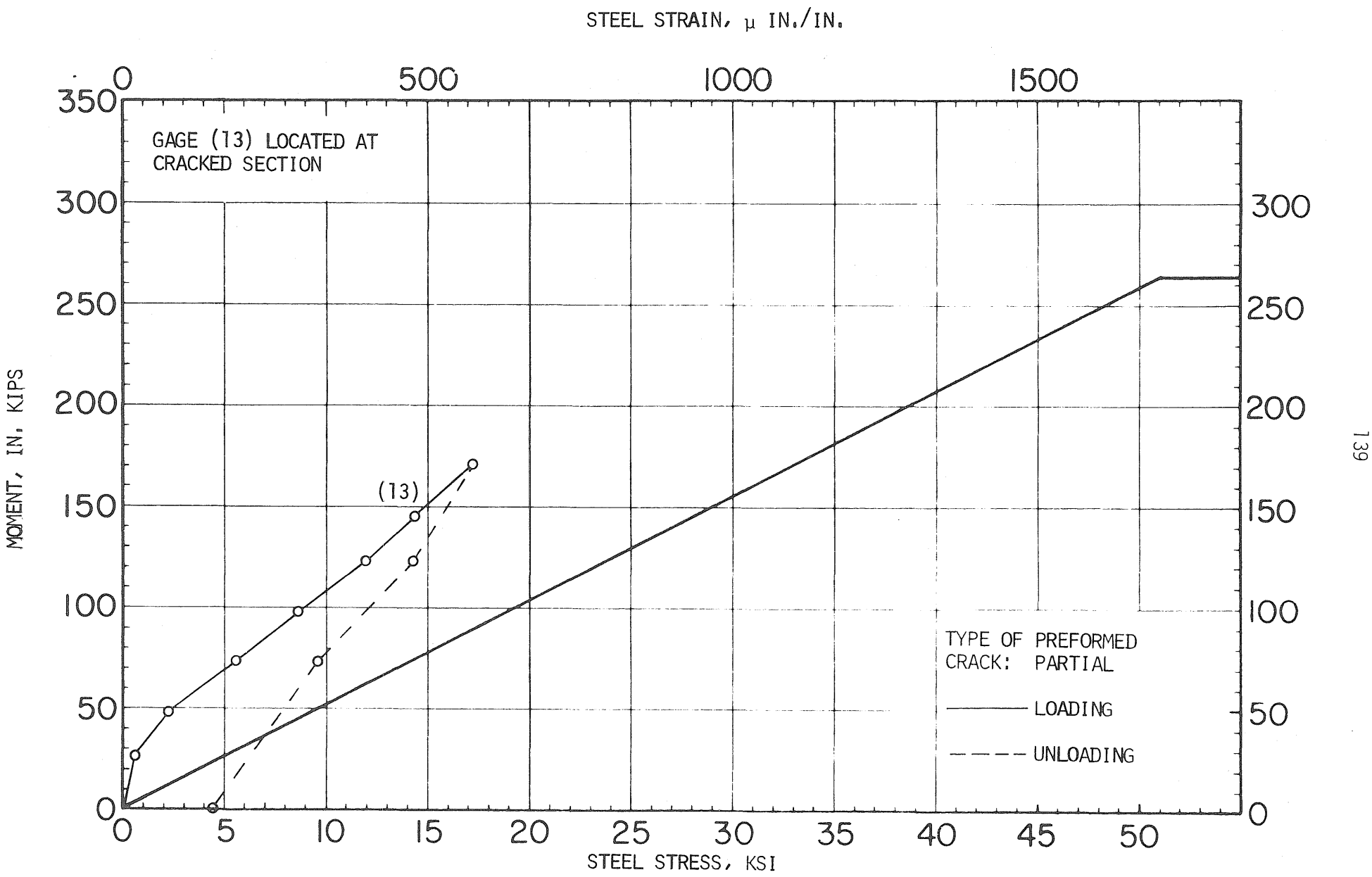

FIG. C9 MOMENT VS. STRESS OR STRAIN FOR BEAM SPECIMEN BW7A

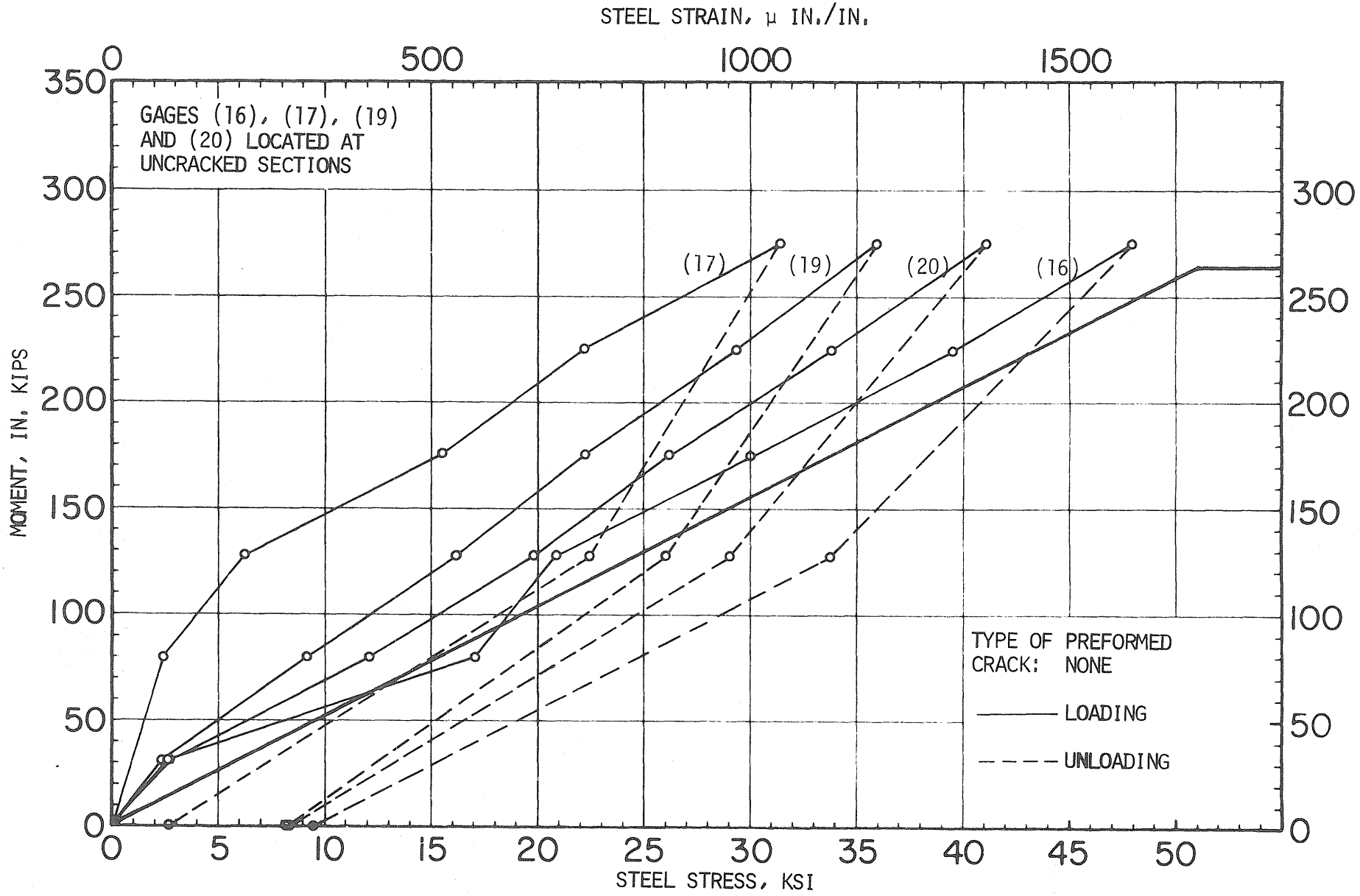

FIG. C10 MOMENT VS. STRESS OR STRAIN FOR BEAM SPECIMEN BW10A

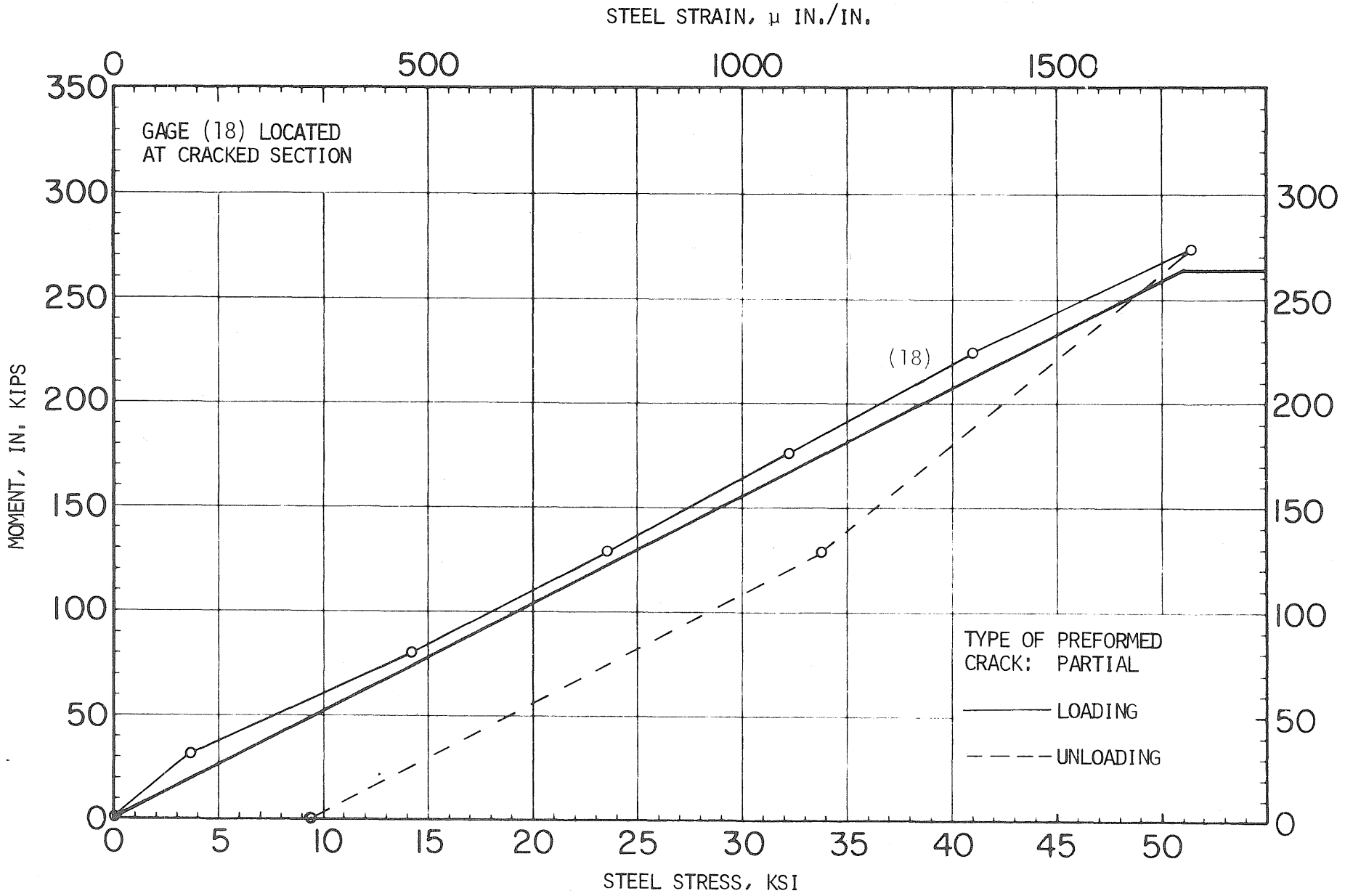

FIG. C11 MOMENT VS. STRESS OR STRAIN FOR BEAM SPECIMEN BW10A

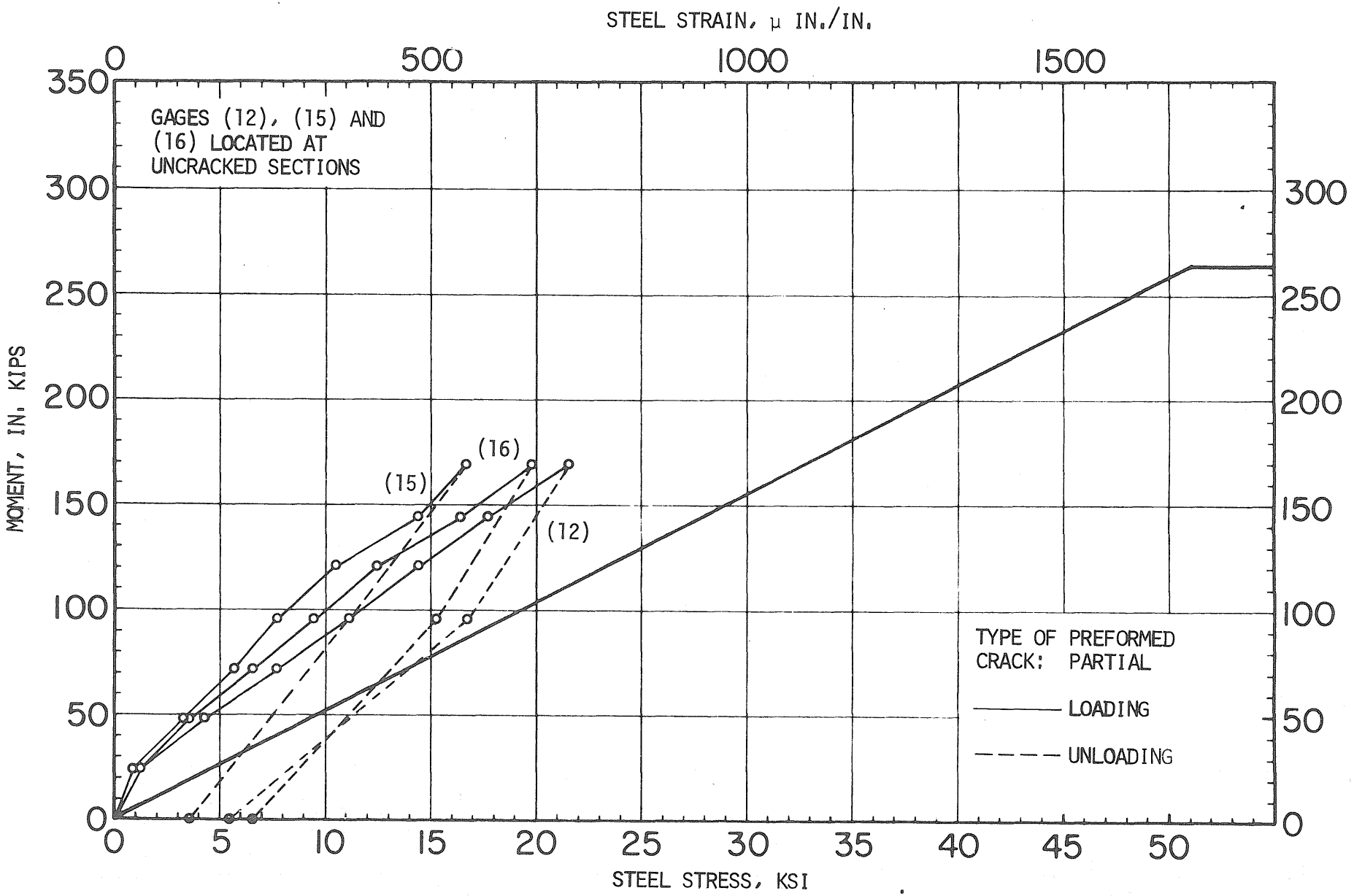

FIG. C12 MOMENT VS. STRESS OR STRAIN FOR BEAM SPECIMEN BW15

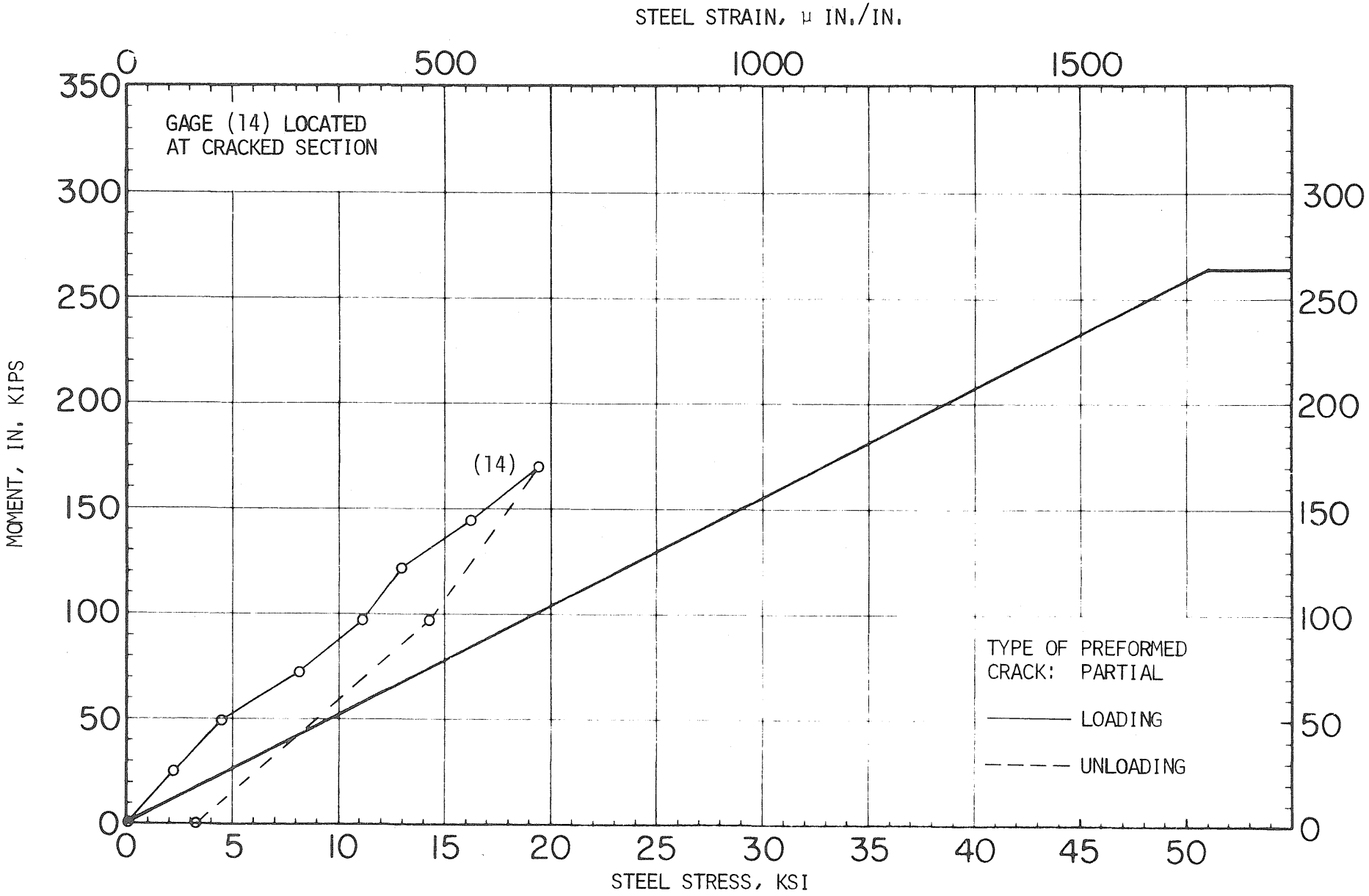

FIG. C13 MOMENT VS. STRESS OR STRAIN FOR BEAM SPECIMEN BW15

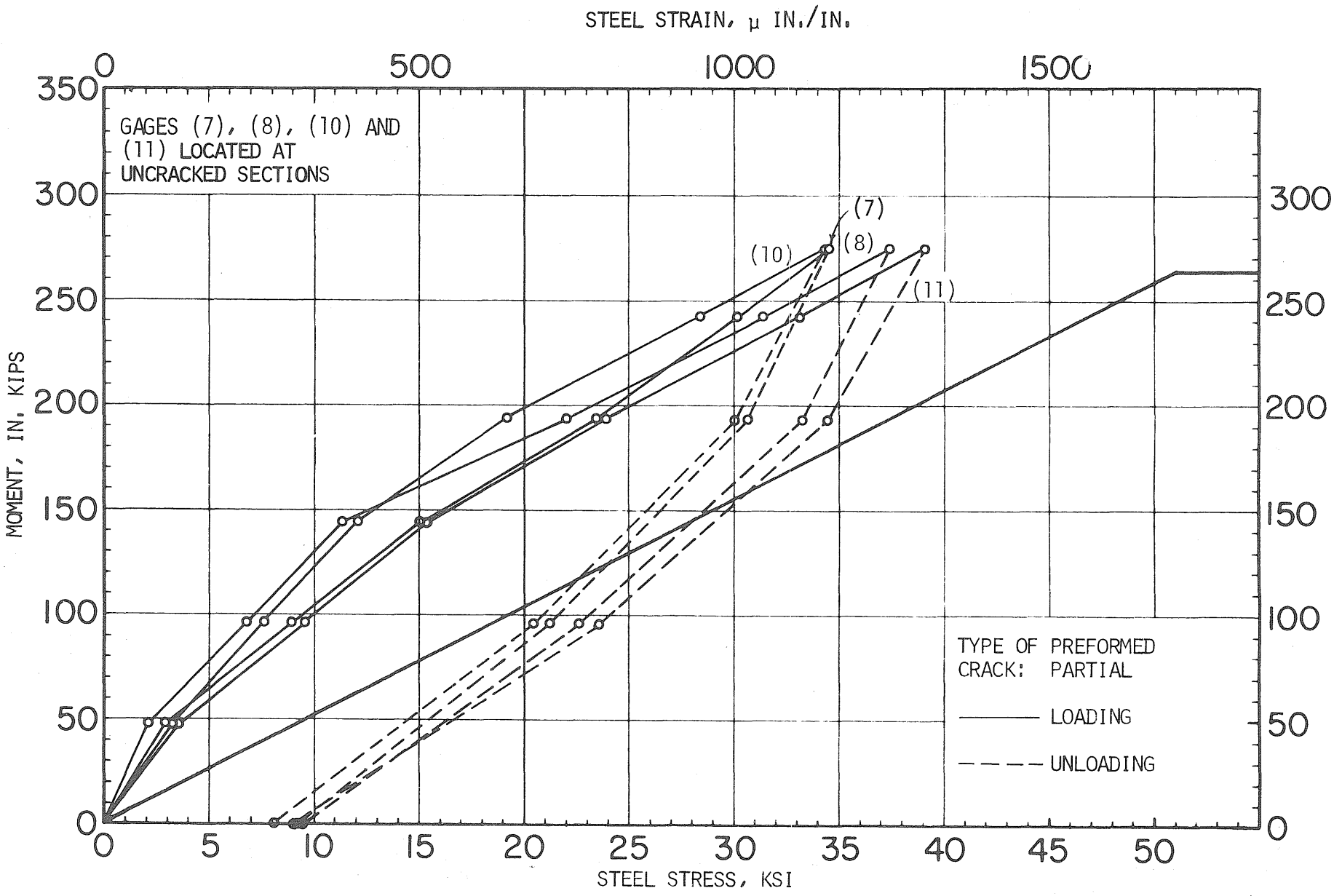

FIG. C14 MOMENT VS. STRESS OR STRAIN FOR BEAM SPECIMEN BW17

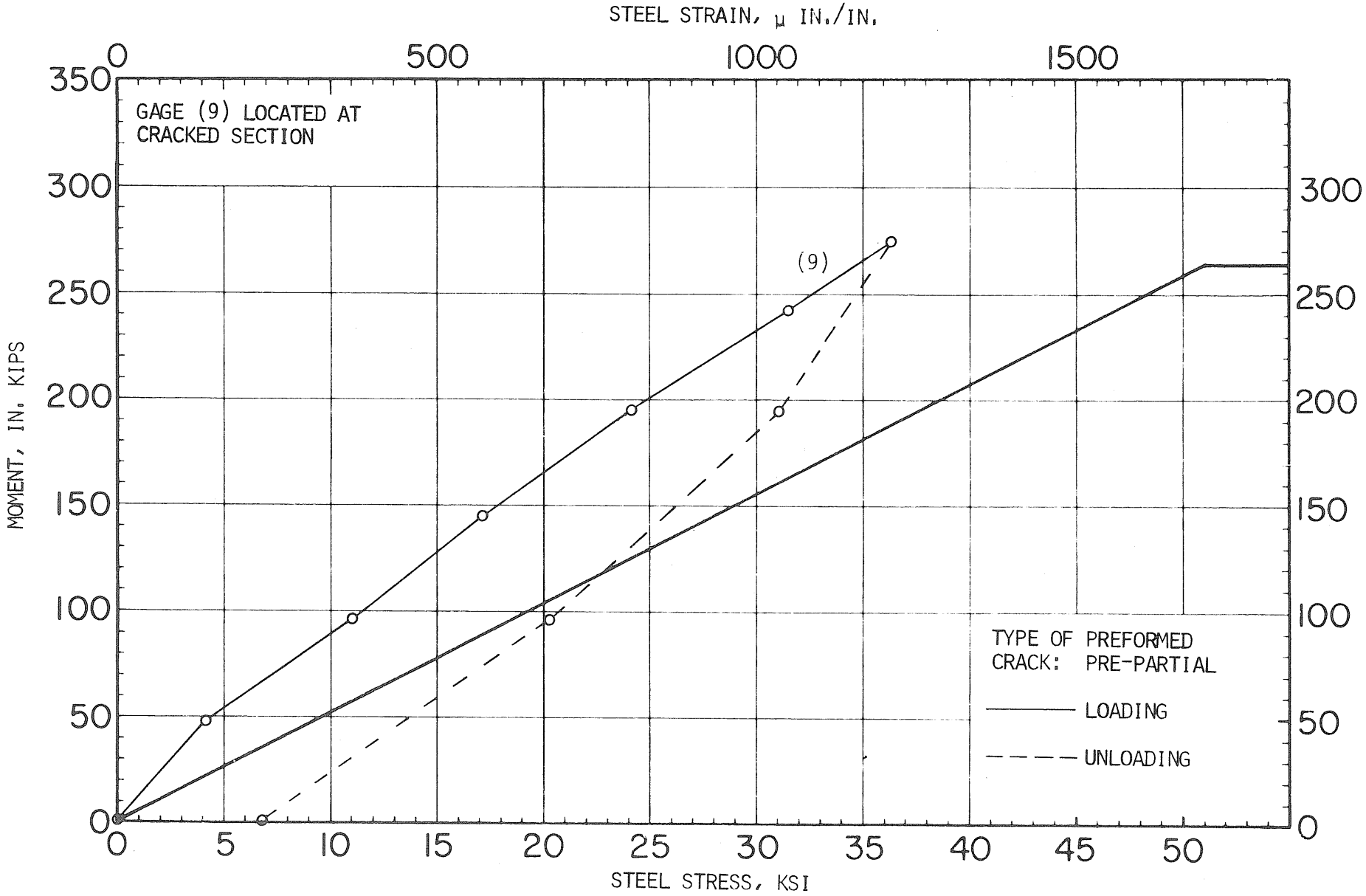

FIG. C15 MOMENT VS. STRESS OR STRAIN FOR BEAM SPECIMEN BW17

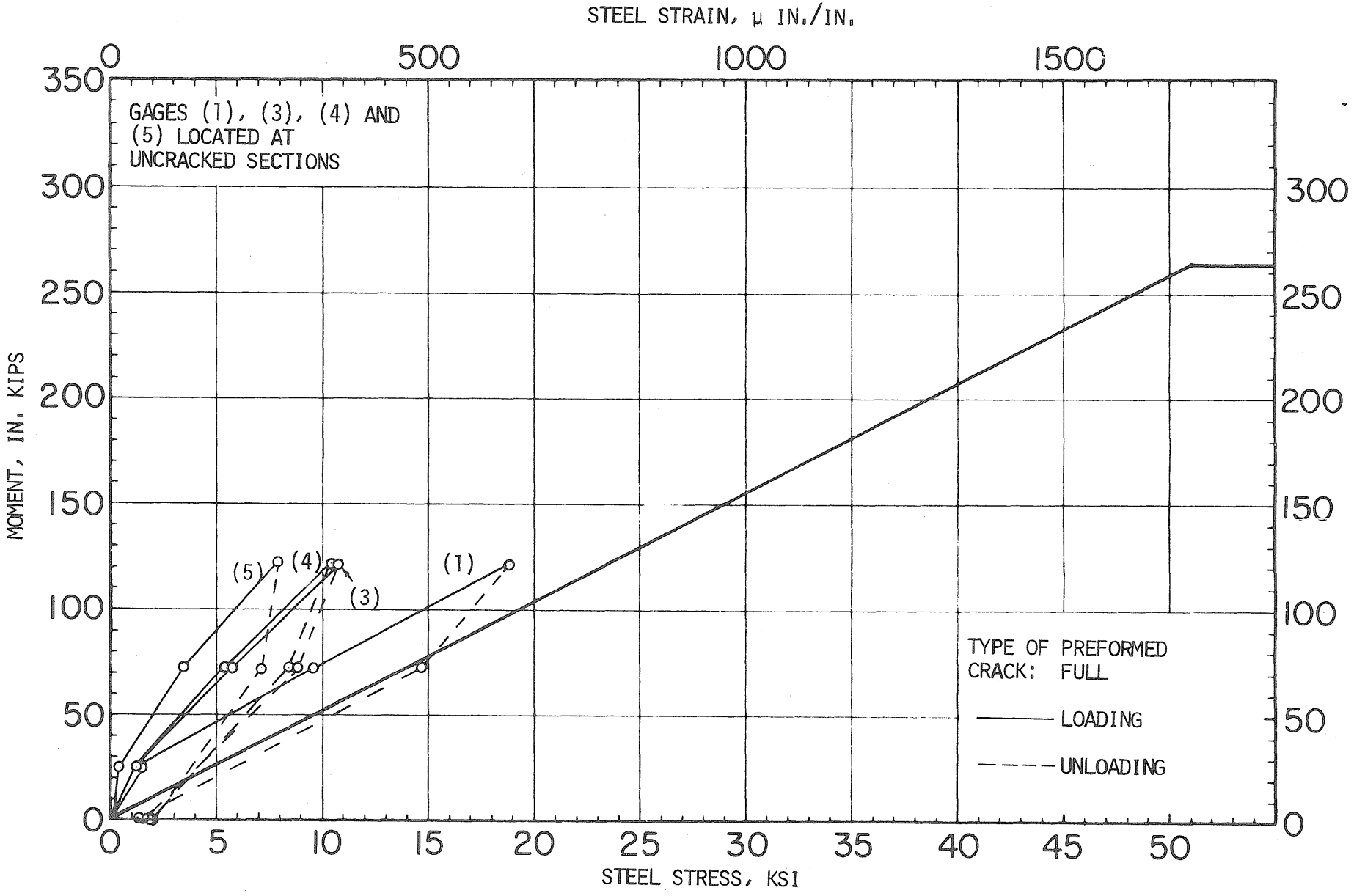

FIG. C16 MOMENT VS. STRESS OR STRAIN FOR BEAM SPECIMEN BW6

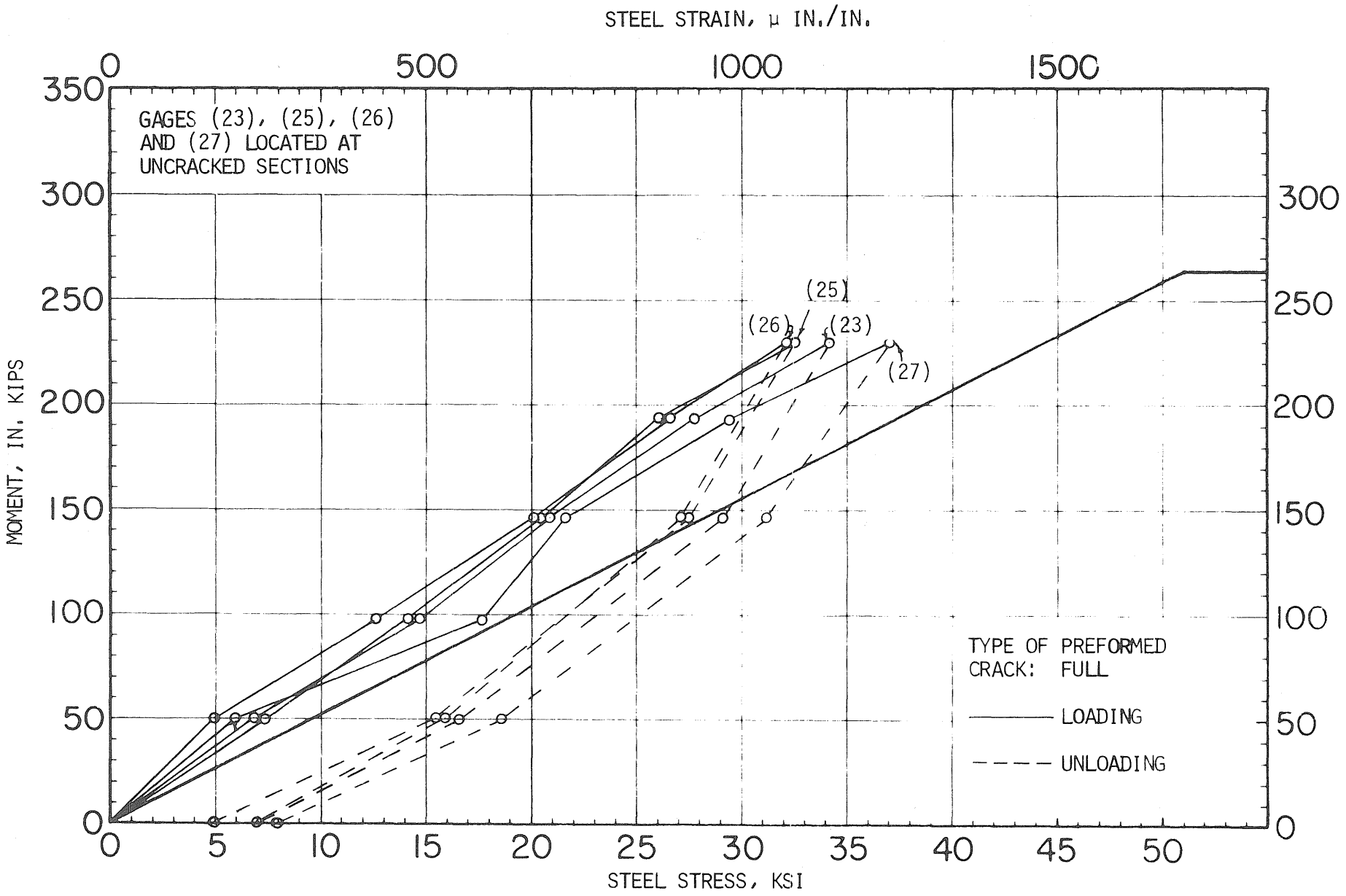

FIG. C17 MOMENT VS. STRESS OR STRAIN FOR BEAM SPECIMEN BW8A

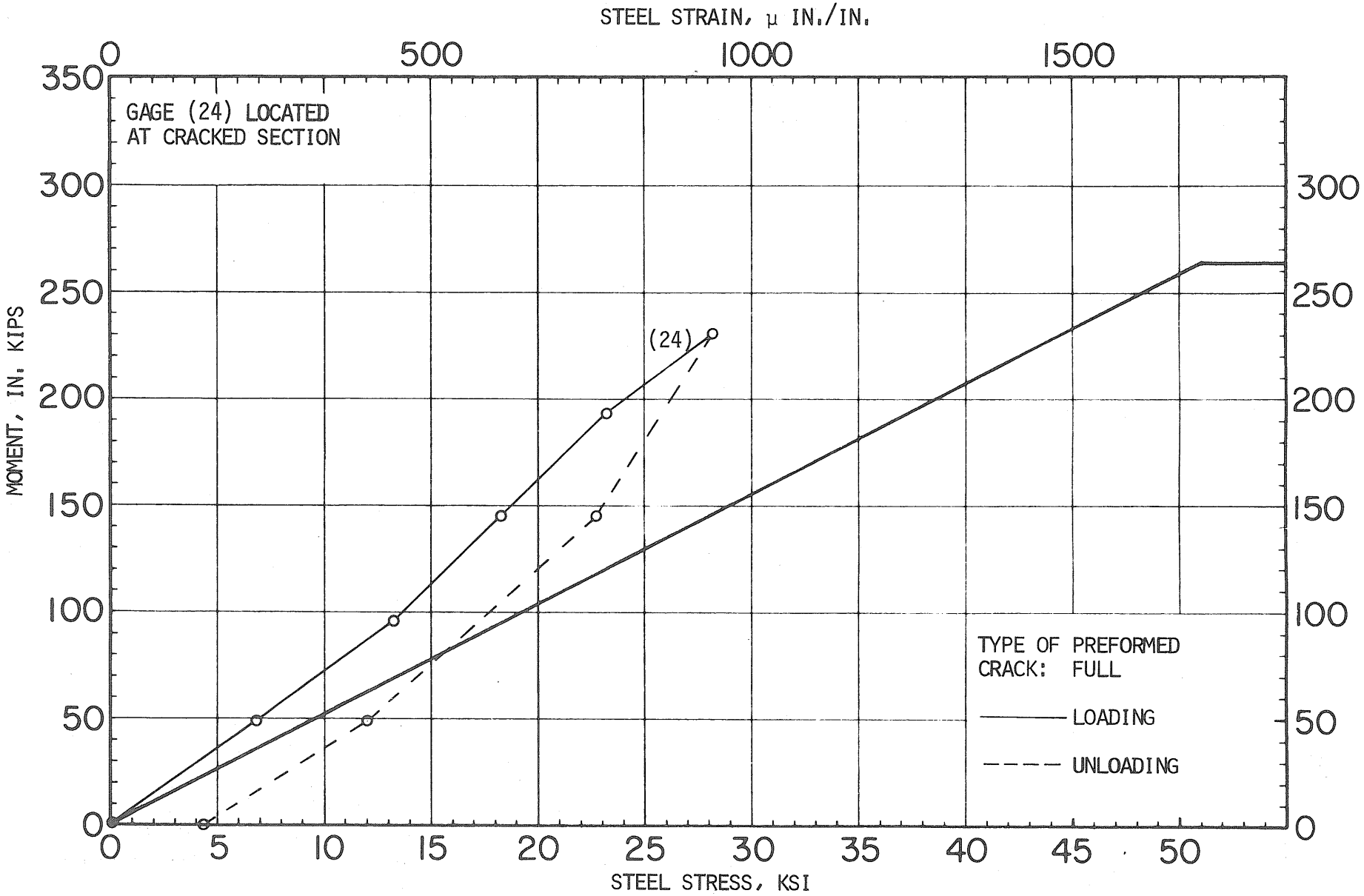

FIG. C18 MOMENT VS. STRESS OR STRAIN FOR BEAM SPECIMEN BW8A

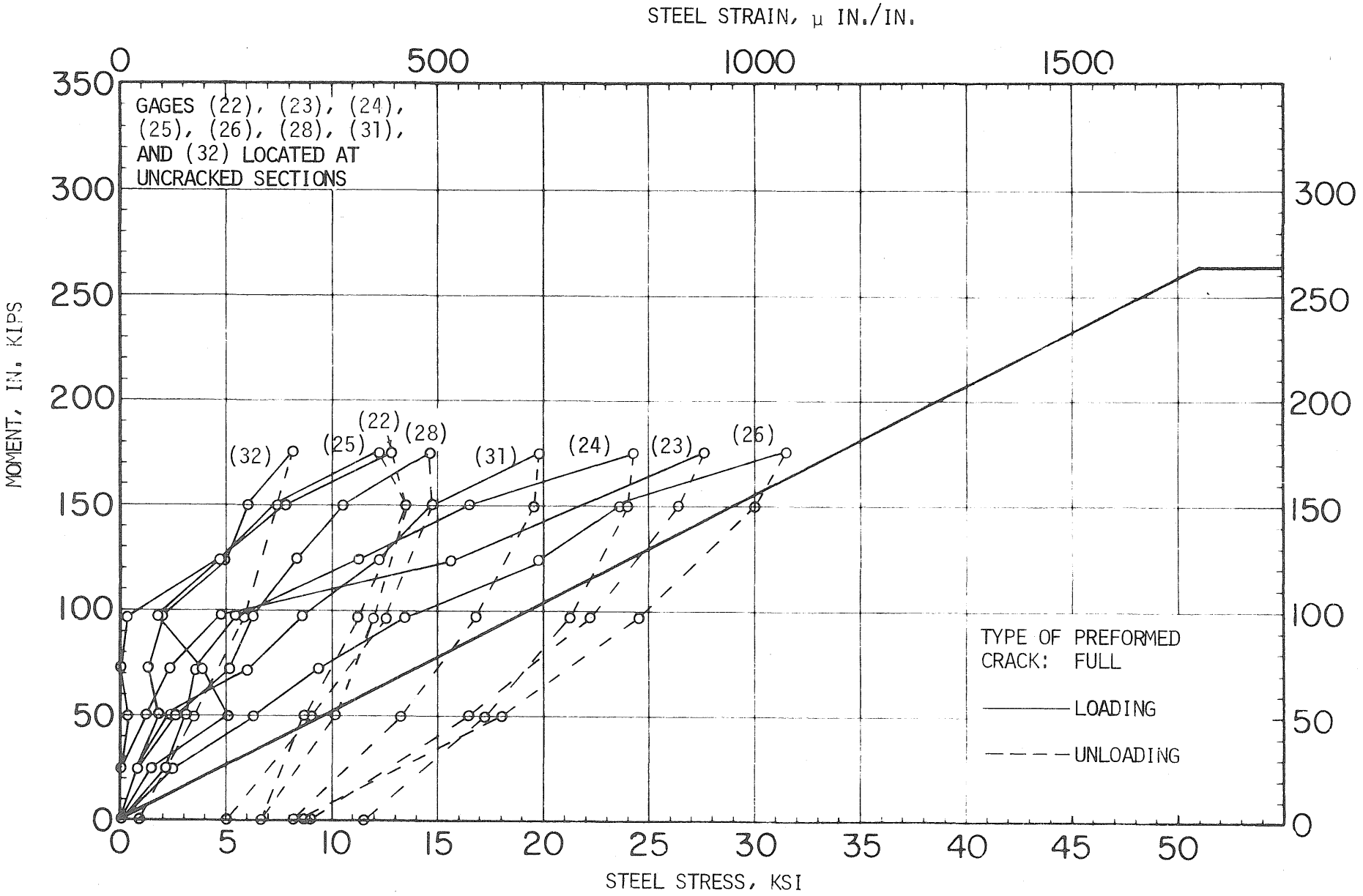

FIG. C19 MOMENT VS. STRESS OR STRAIN FOR BEAM SPECIMEN BW9

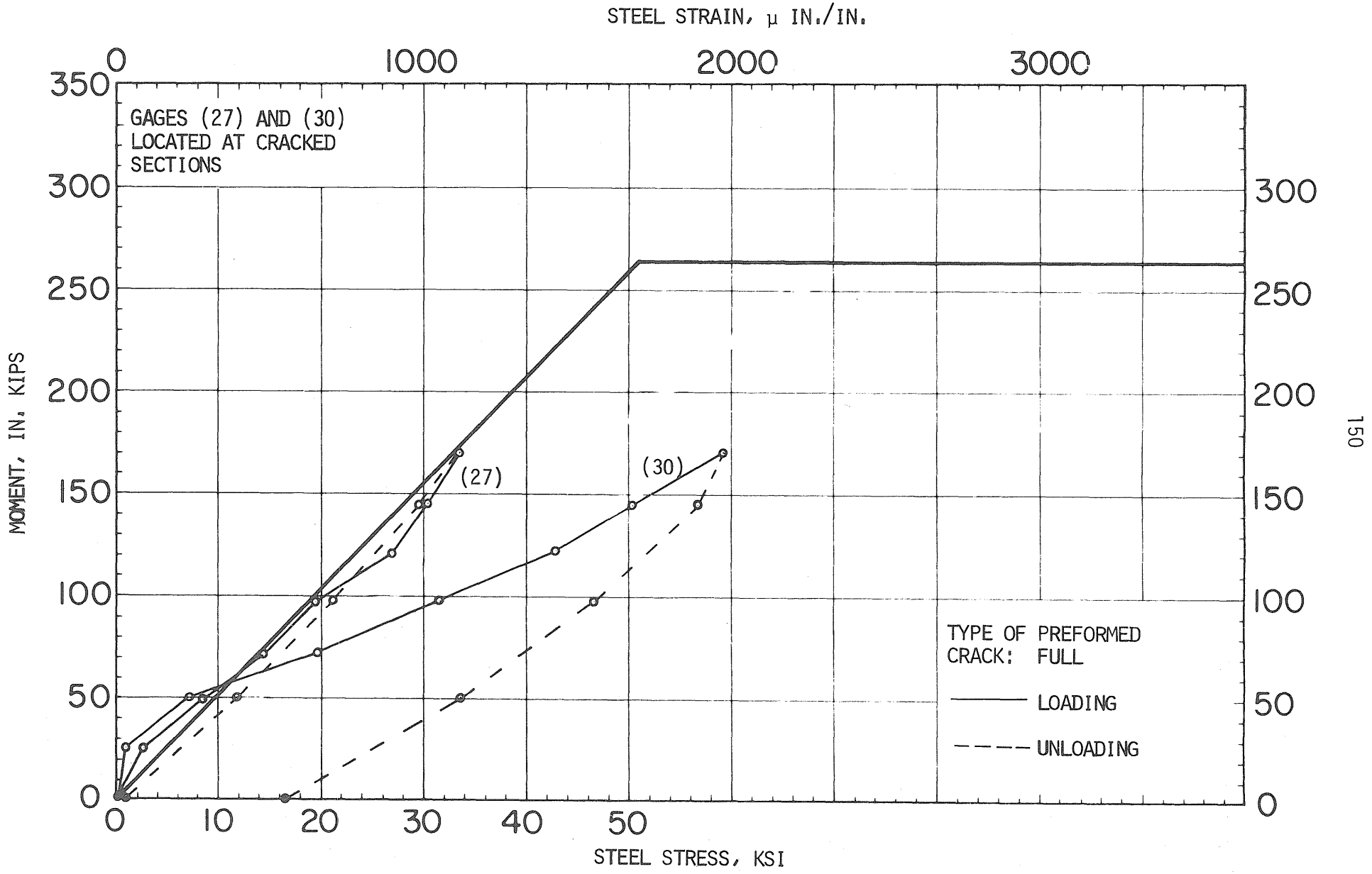

FIG. C20 MOMENT VS. STRESS OR STRAIN FOR BEAM SPECIMEN BW9

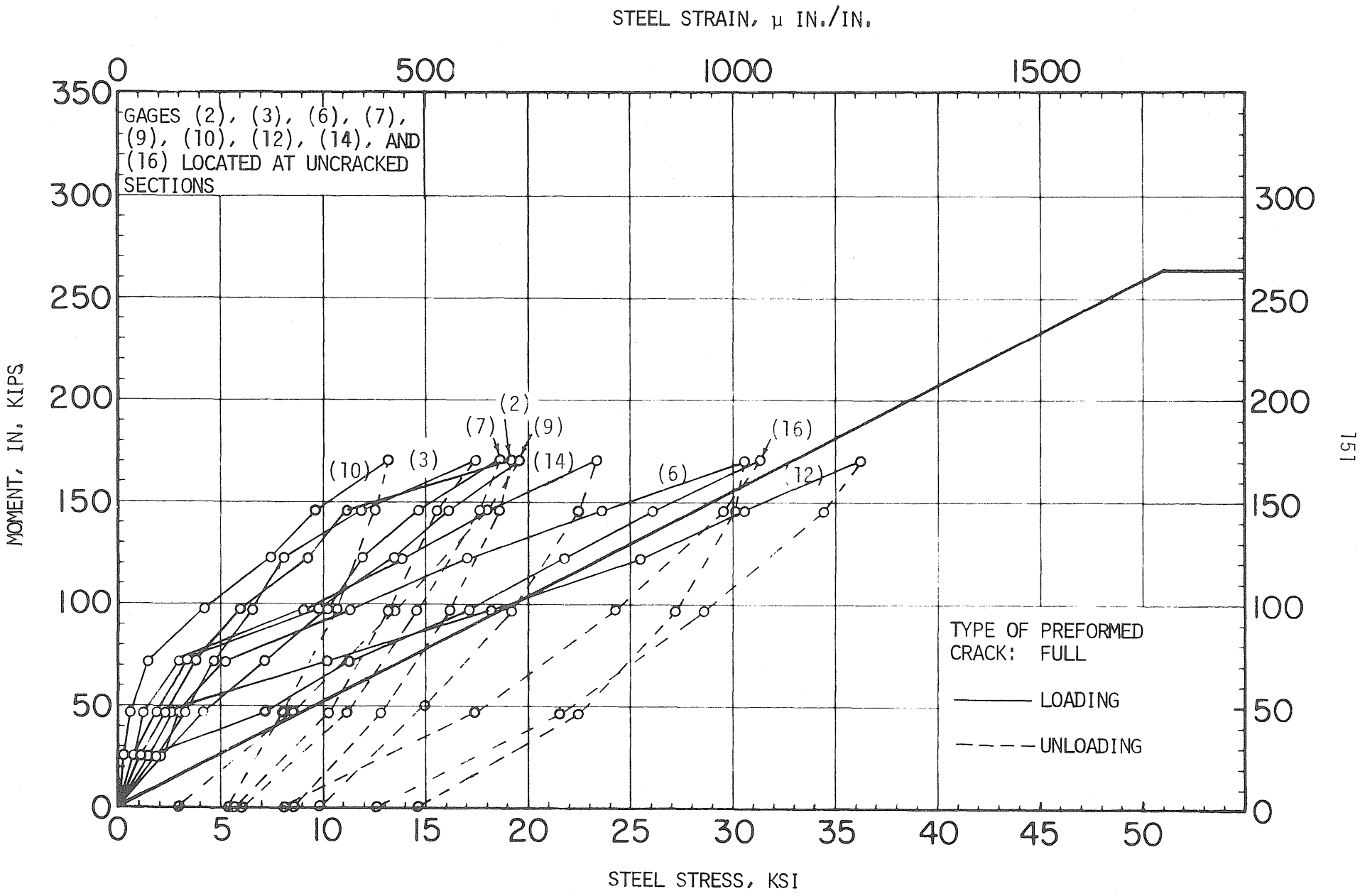

FIG. C21 MOMENT VS. STRESS OR STRAIN FOR BEAM SPECIMEN BW12

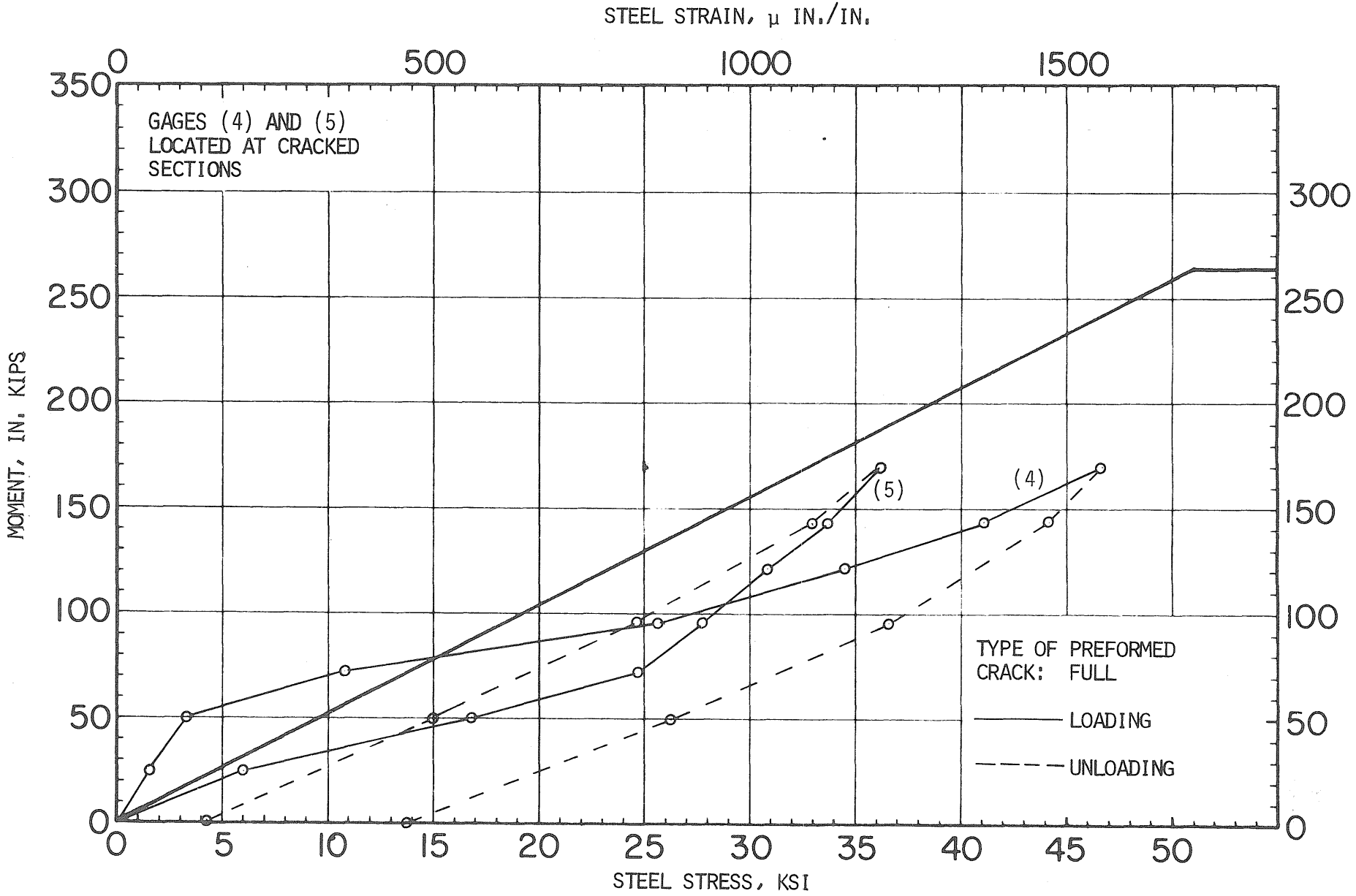

FIG. C22 MOMENT VS. STRESS OR STRAIN FOR BEAM SPECIMEN BW12

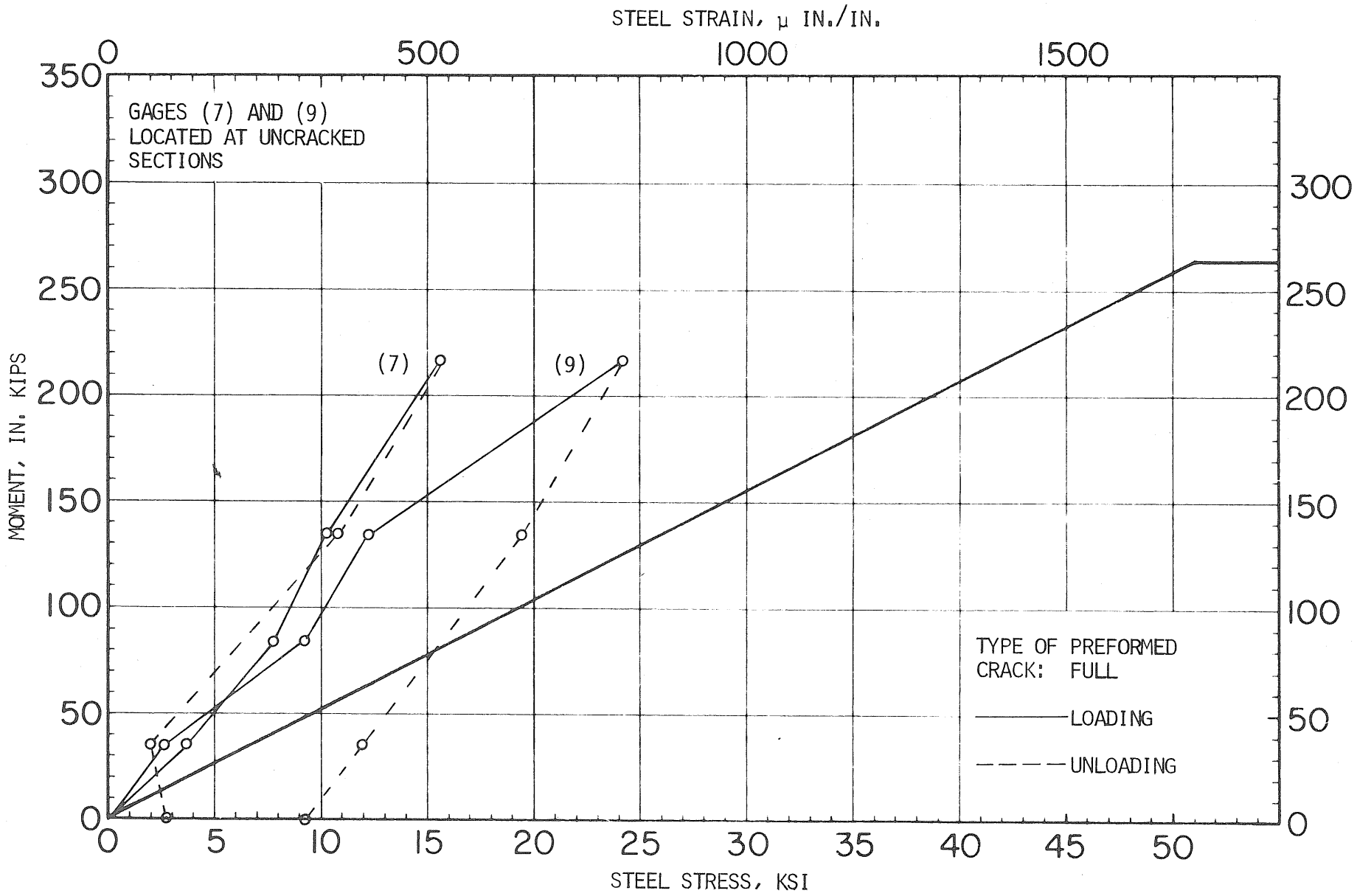

FIG. C23 MOMENT VS. STRESS OR STRAIN FOR BEAM SPECIMEN BW13A

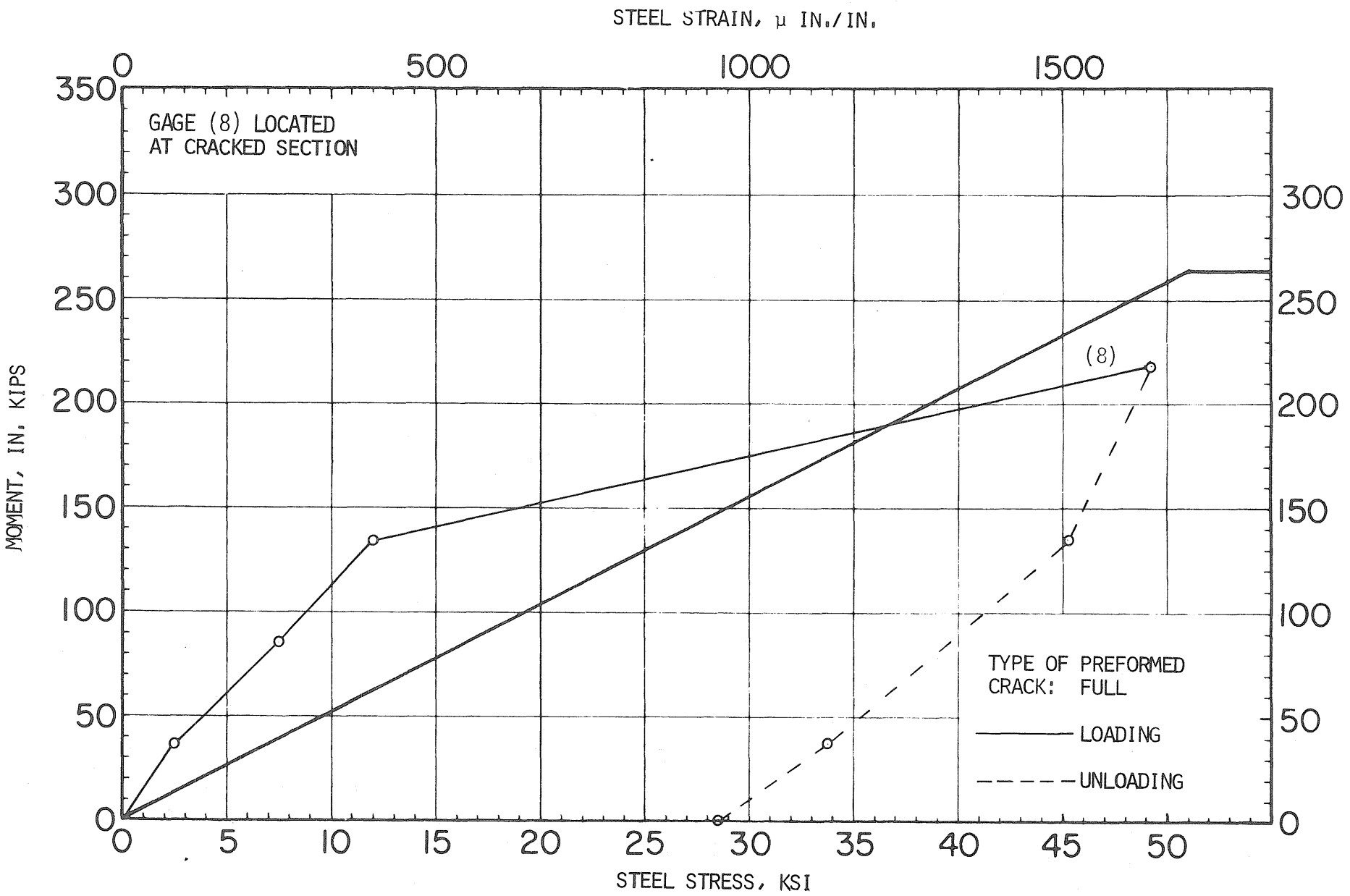

FIG. C24 MOMENT VS. STRESS OR STRAIN FOR BEAM SPECIMEN BW13A

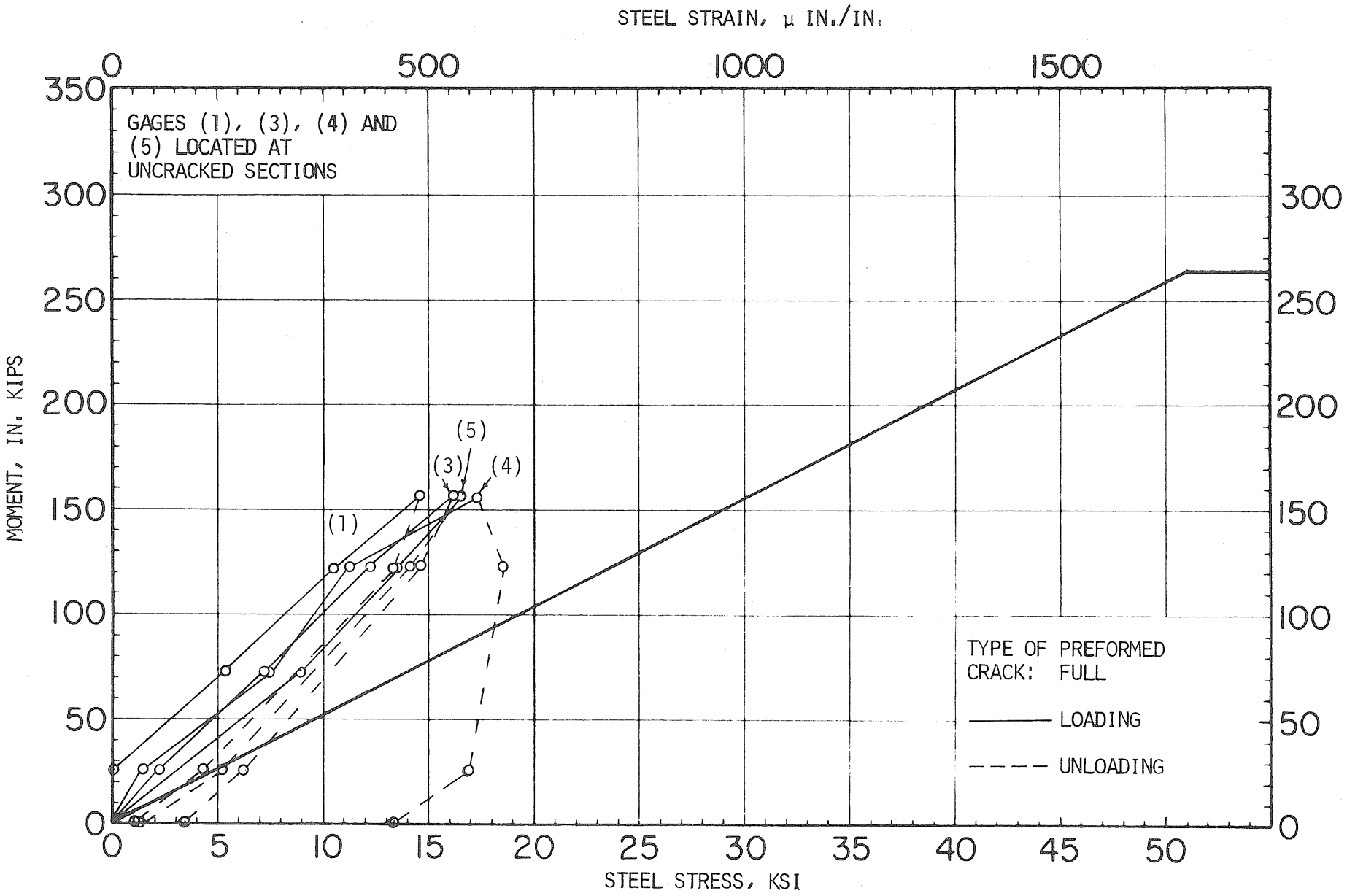

FIG. C25 MOMENT VS. STRESS OR STRAIN FOR BEAM SPECIMEN BW14

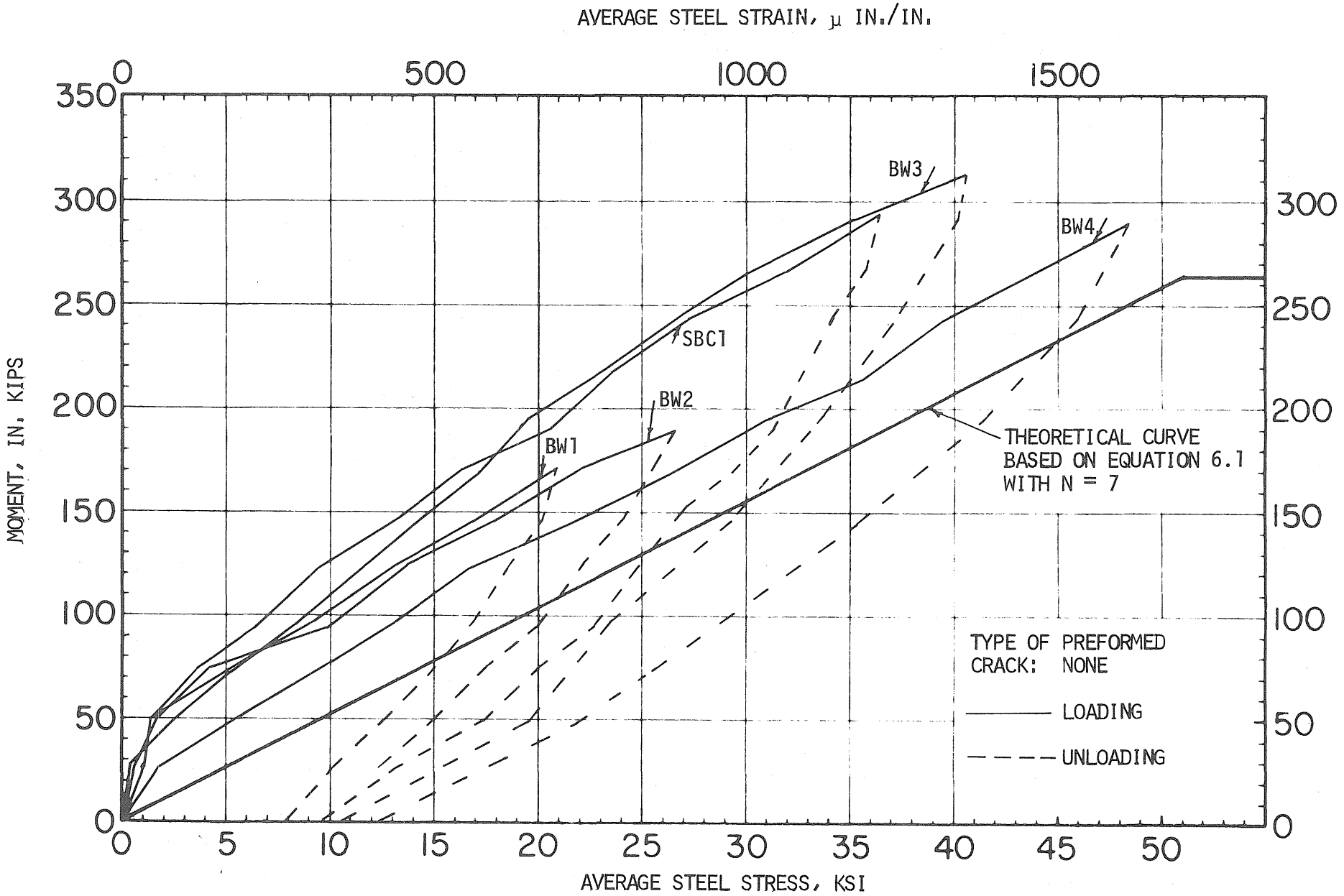

FIG. C26 MOMENT VS. AVERAGE STRESS OR STRAIN AT UNCRACKED SECTIONS, NO PREFORMED CRACK

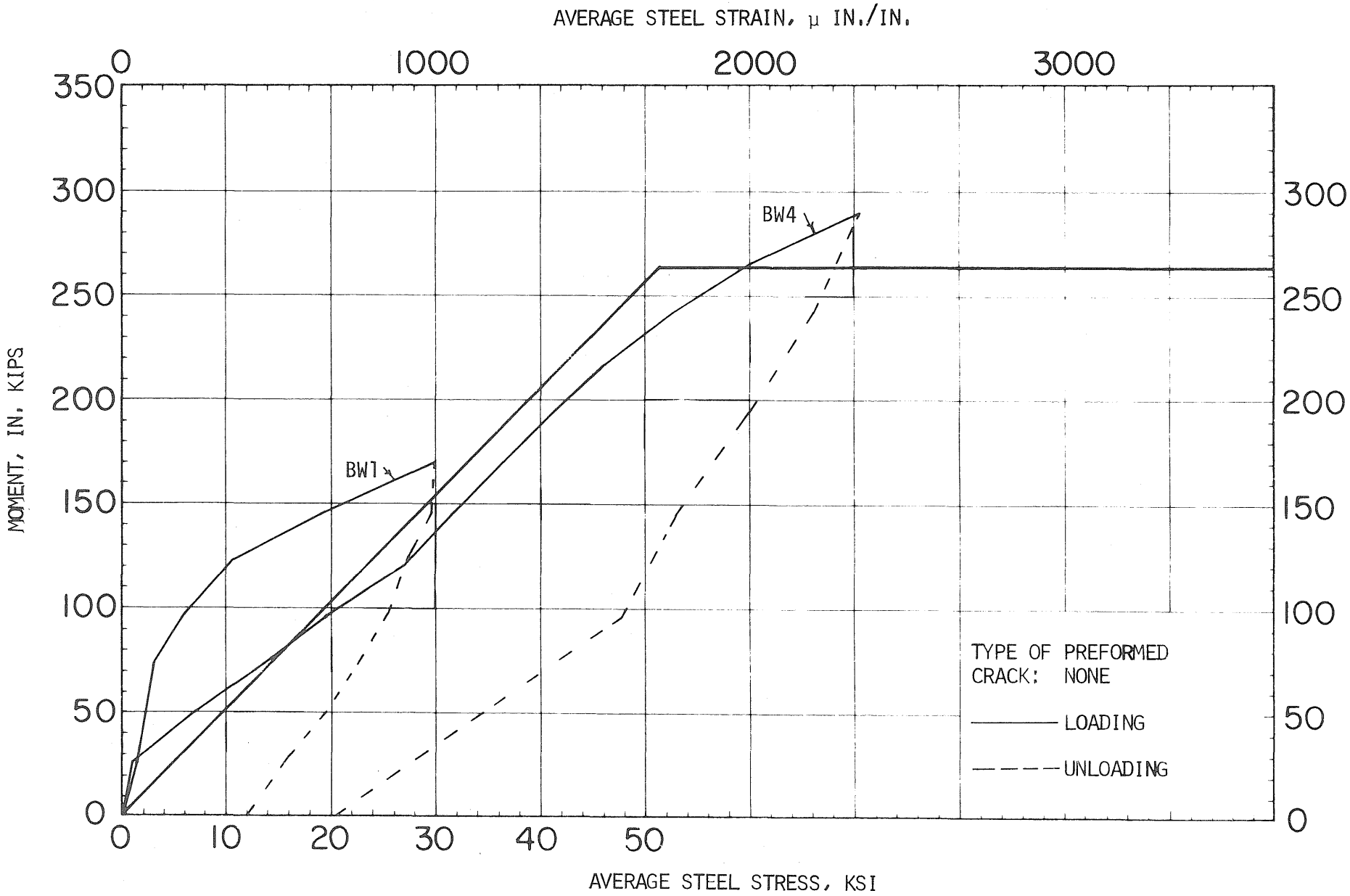

FIG. C27 MOMENT VS. AVERAGE STRESS OR STRAIN AT CRACKED SECTIONS, NO PREFORMED CRACK

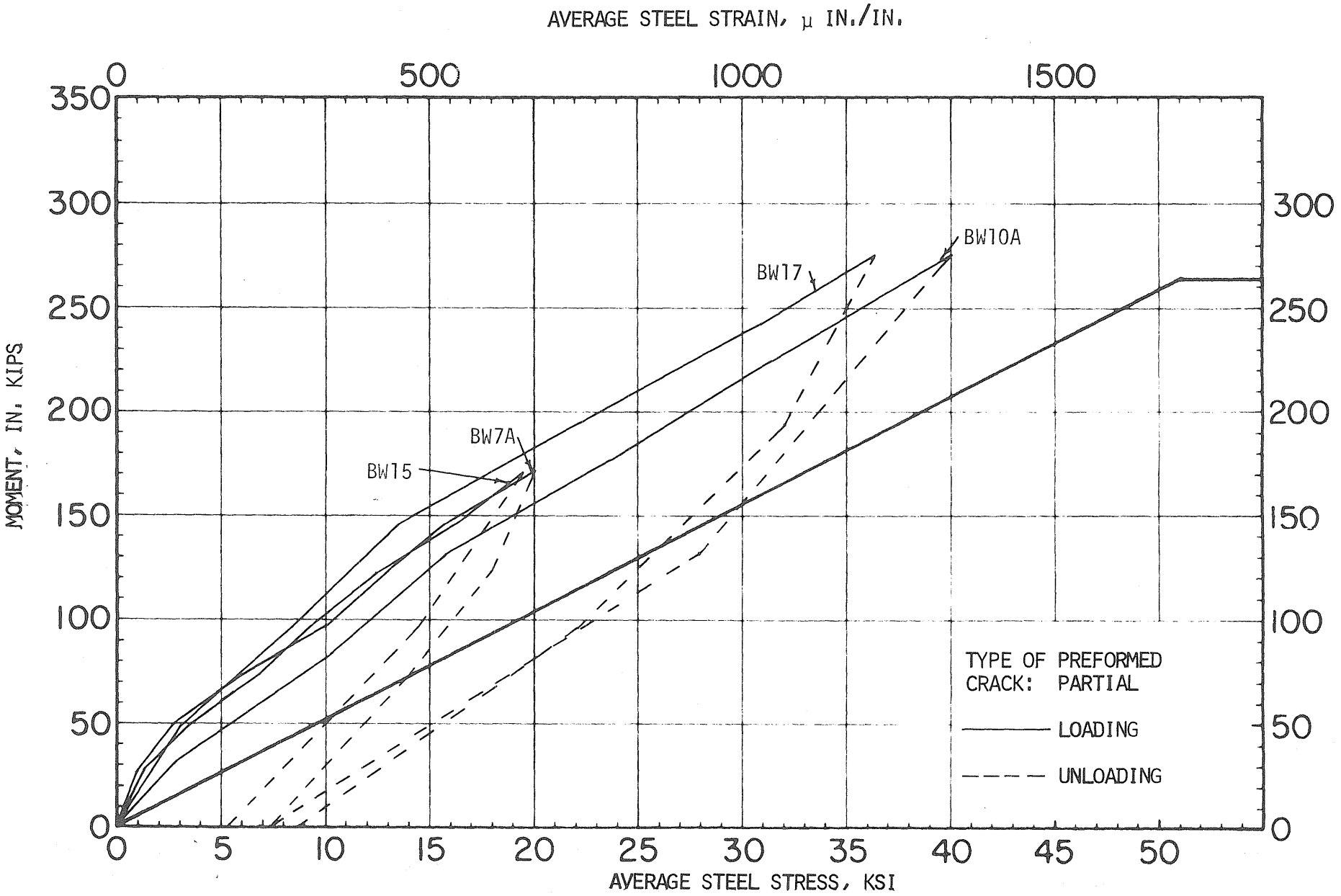

FIG. C28 MOMENT VS. AVERAGE STRESS OR STRAIN AT UNCRACKED SECTIONS, PARTIAL PREFORMED CRACK

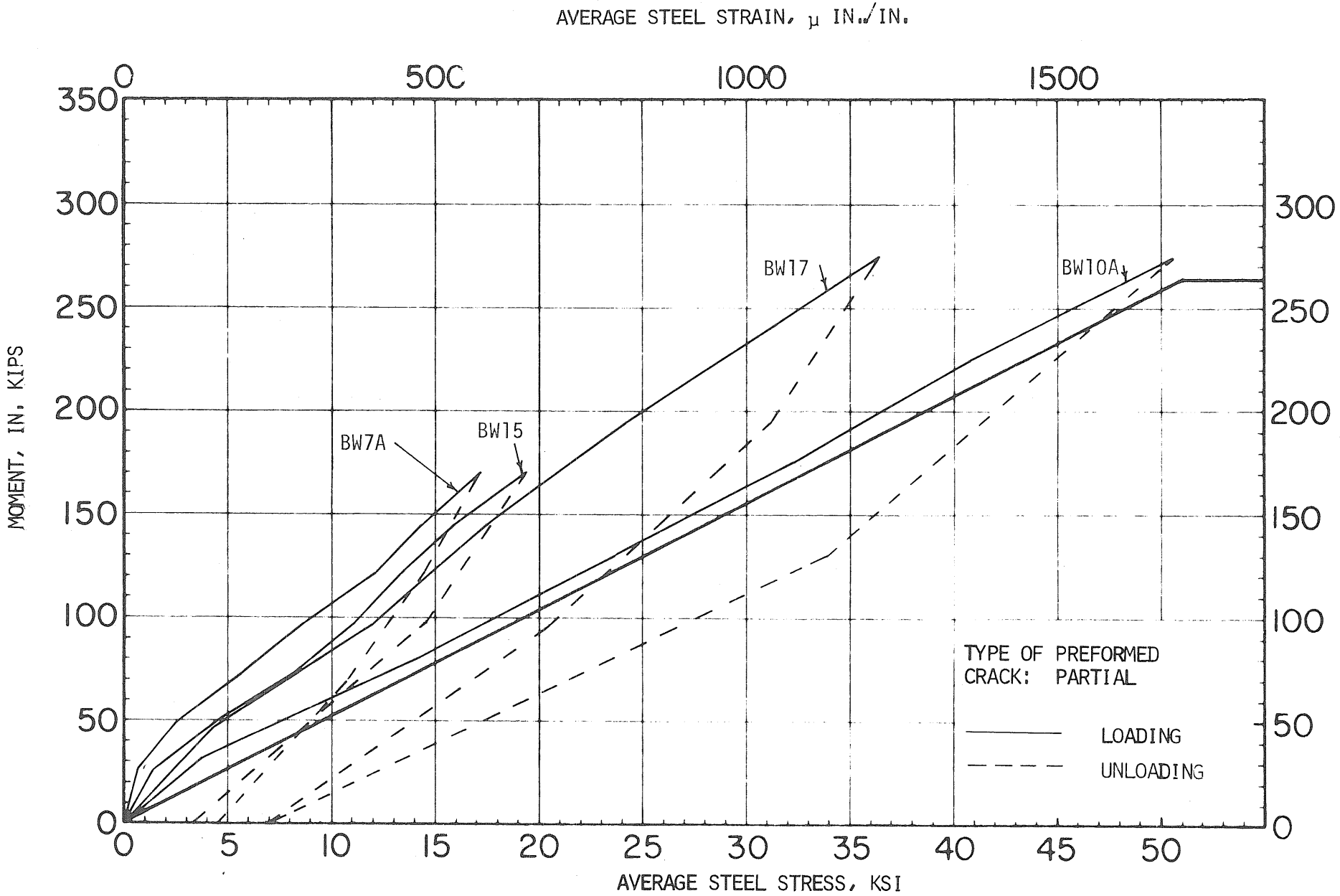

FIG. C29 MOMENT VS. AVERAGE STRESS OR STRAIN AT CRACKED SECTIONS, PARTIAL PREFORMED CRACK

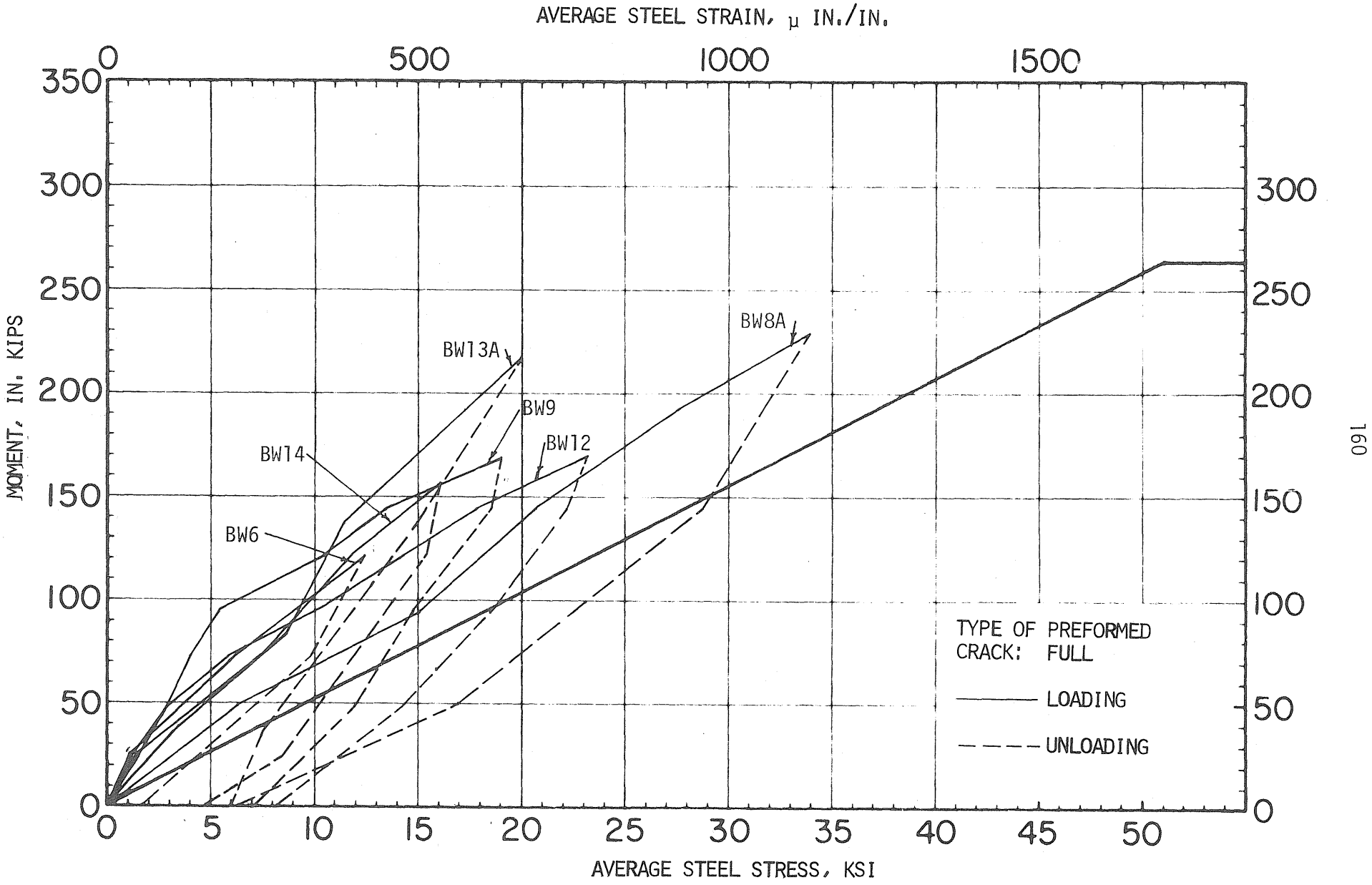

FIG. C30 MOMENT VS. AVERAGE STRESS OR STRAIN AT UNCRACKED SECTIONS, FULL PREFORMED CRACK

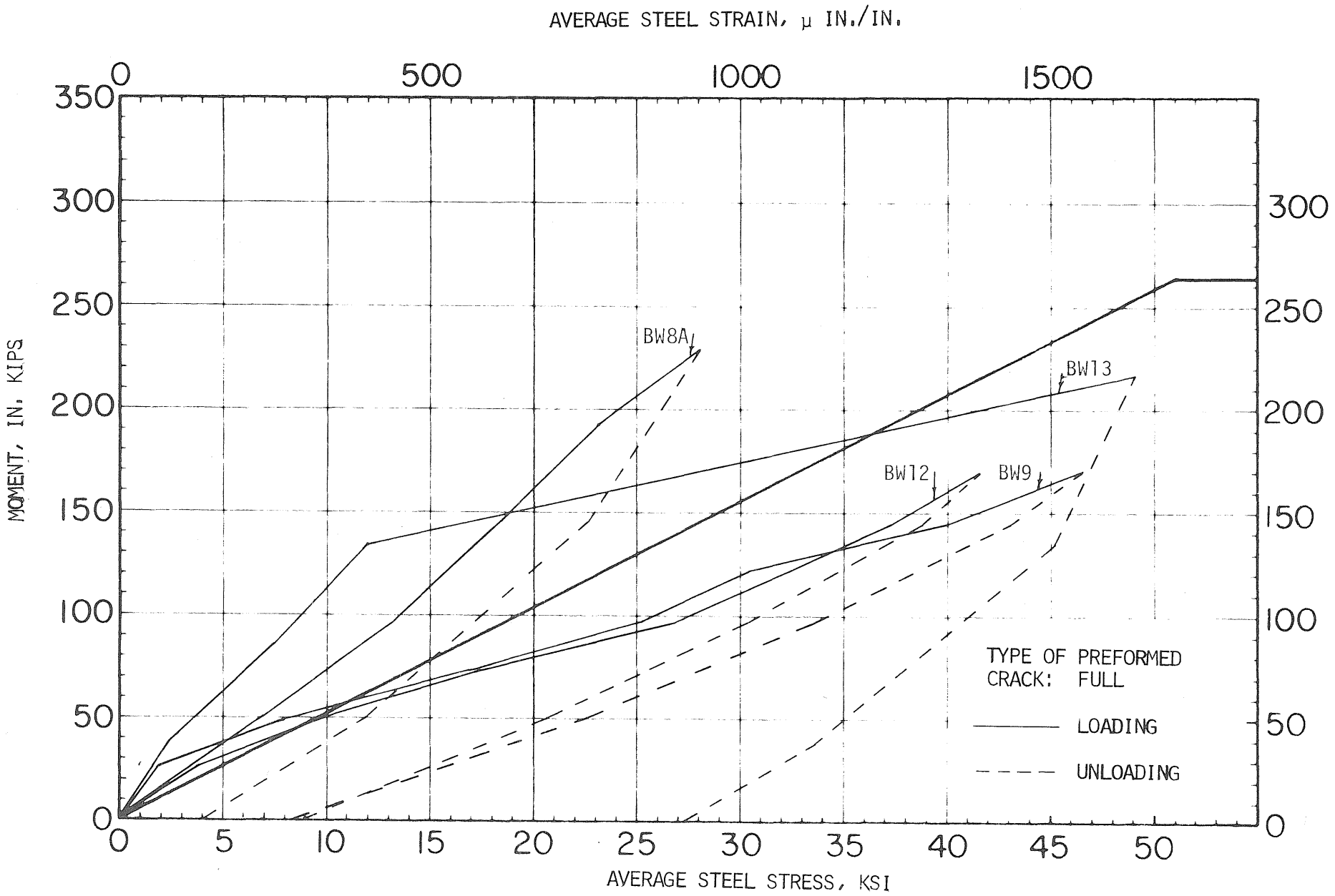

FIG. C31 MOMENT VS. AVERAGE STRESS OR STRAIN AT CRACKED SECTIONS, FULL PREFORMED CRACK